POLYPHOSPHATE IS A NOVEL MODULATOR OF COAGULATION AND INFLAMMATION AND IS A THERAPEUTIC TARGET

BY

RICHARD TRAVERS

DISSERTATION
Submitted in partial fulfillment of the requirements
for the degree of Doctor of Philosophy in Biochemistry
in the Graduate College of the
University of Illinois at Urbana-Champaign, 2015

Urbana, Illinois

Doctoral Committee:

Professor James H. Morrissey, Chair
Professor David Kranz
Associate Professor Rutilio Fratti
Assistant Professor Auinash Kalsotra

ABSTRACT

While the basic outline of the enzymes and reactions that make up the traditional blood coagulation cascade has been understood for many years, appreciation of the complexity of these interactions has greatly increased in recent times. This has resulted in unofficial “revisions” of the coagulation cascade to include new amplification pathways and interactions between the standard coagulation cascade enzymes as well as novel and extensive connections between the immune system and the coagulation cascade. One exciting new area of research in hemostasis and thrombosis focuses on how inorganic polyphosphate (polyP) can mediate many of these novel amplification steps and many of the connections between coagulation and inflammation. Additionally, the multiple procoagulant and proinflammatory roles for polyP discovered in both mice and humans suggest that it may be an attractive therapeutic target for disorders of coagulation and inflammation.

The discovery that polyP is stored in platelet dense granules and is secreted during platelet activation has resulted in a recent burst of interest in the role of this ancient molecule in human biology; however, many standard biochemical techniques are not amenable to working with an inorganic polymer like polyP. To increase our ability to visualize polyP accumulation under both physiological and pathological conditions such as inflammation or thrombosis, I first developed a method for visualizing polyP based upon using a recombinant polyP binding protein as a modified “primary antibody” to specifically label polyP using immunofluorescent staining in cells and tissues. These techniques continue to provide us with more information about the role of polyP in normal human physiology and under pathological conditions like inflammation and thrombosis.

In order to determine if we could target polyP-mediated pathology as an effective method of treatment for inflammation and thrombosis, I have also developed a method of testing polyP inhibitors from high-throughput *in vitro* screening all the way to *in vivo* mouse models. First generation polyP inhibitors based on polycationic substances such as polyethylenimine, polyamidoamine (PAMAM)

dendrimers and polymyxin B, while attenuating thrombosis, all had significant toxicity *in vivo*, likely due to the presence of multiple primary amines responsible for their polyP binding ability. In collaboration with the Kizhakkedathu lab at the University of British Columbia in Vancouver, Canada, I next examined a novel class of non-toxic polycationic compounds, initially designed as Universal Heparin Reversal Agents (UHRAs). I first worked with them to help evaluate the UHRA compounds in clinically relevant mouse models showing that the UHRA compounds can effectively reverse the bleeding side effects associated with a wide variety of heparins currently in clinical use. Next, they worked with me to screen the entire UHRA library for potential polyP inhibitors that shared the non-toxic nature of the UHRA compounds developed to reverse heparin anticoagulation. Several UHRA compounds strongly inhibited polyP procoagulant activity *in vitro* and four were selected for further examination in mouse models of thrombosis and hemostasis. Compounds UHRA 9 and UHRA 10 significantly reduced arterial thrombosis in mice. In mouse tail bleeding tests, administration of UHRA 9 or UHRA 10 was associated with significantly less bleeding compared to therapeutically equivalent doses of heparin. Furthermore, in collaboration with the Esmon Laboratory at the Oklahoma Medical Research Foundation, I have begun to characterize the polyP binding abilities of a family of anti-polyP antibodies discovered in an autoimmune strain of mice. PolyP inhibitors like the UHRA compounds or anti-polyP antibodies offer a new platform for developing novel antithrombotic and anti-inflammatory agents that target anionic polymers like polyP with reduced toxicity and bleeding side effects compared to conventional anticoagulant therapeutics.

ACKNOWLEDGEMENTS

First, I would like to thank my advisor, Dr. Jim Morrissey, for his support and advice throughout my time in his lab. The quality of his scientific knowledge and advice enhanced and enriched my own science and learning during my PhD studies. I hope that someday when I manage a lab I will be able to create an environment as welcoming, intellectually-stimulating, and exciting as Jim provided me and my lab mates. I would like to thank all of my committee members along with present and former lab mates as well for their intelligent discussions and help with all aspects of my PhD career so far. I would also like to thank my collaborators in the Kizhakkedathu Lab for sharing the UHRA compounds with us and for research support in developing the UHRAs as anti-polyphosphate therapeutics. Similarly, I would like to thank the Esmon lab for supplying us with mouse monoclonal antibodies that recognize polyphosphate. For financial support, I would like to thank the National Heart, Lung, and Blood Institute of the National Institutes of Health as well as the American Heart Association.

This research would also not have been possible without the endless support of my family and friends. My parents, Richard and Janet Travers, nurtured and encouraged my love of science since my earliest years. They provided me with all of the opportunities and resources I needed to be successful and taught me through their own actions the value of hard work and dedication in life. I could never repay them for everything they have given me, but I am extremely glad and grateful that they can share in my accomplishments. Finally, I would like to thank my wife Candice, who moved out to the Midwest with me from the East Coast to allow me to follow my ambitions of becoming a physician-scientist. Her love and support have made these years a fun and enriching part of our lives.

TABLE OF CONTENTS

CHAPTER 1: GENERAL INTRODUCTION TO BLOOD COAGULATION AND ANTICOAGULANTS[a]

Introduction

Blood is a liquid that circulates under pressure through the vasculature. Following vascular injury, any escaping blood must rapidly be converted into a gel ("clot") to plug the hole and minimize further blood loss. The plasma portion of blood contains a collection of soluble proteins that act together in a cascade of enzyme activation events, culminating in the formation of a fibrin clot. This review addresses the mechanisms by which the blood clotting cascade is initiated in both hemostasis and pathologic thrombosis. Hemostasis is the normal process by which the clotting cascade seals up vascular damage to limit blood loss following injury. Thrombosis is a group of pathologic conditions in which the clotting cascade is triggered inside the lumen of a blood vessel, leading to the formation of a blood clot (known, in this case, as a "thrombus") that can impede the flow of blood within a vessel. Severe thrombosis can block the flow of blood to a tissue, leading to ischemia and tissue death.

Two major pathways exist for triggering the blood clotting cascade, known as the tissue factor pathway and the contact pathway. The tissue factor pathway is named for the protein that triggers it—a cell-surface, integral-membrane protein known as tissue factor (TF).[1] This way of triggering blood clotting is also sometimes called the Extrinsic Pathway, because it requires that plasma come into contact with something "extrinsic"—i.e., TF—to trigger it. The TF pathway is the mechanism of triggering blood clotting that functions in normal hemostasis, and probably also in many types of thrombosis. Thus, when cells expressing TF are exposed to blood, this event immediately triggers the clotting cascade. This pathway is discussed in much greater detail below.

[a] This chapter has been adapted from a review article originally published online in the journal Critical Reviews in Biochemistry and Molecular Biology, and used in accordance with the publisher's copyright privileges for publication in a dissertation thesis. Full Citation: Smith SA, Travers RJ, Morrissey JH. How it all starts: Initiation of the clotting cascade. Critical Reviews in Biochemistry and Molecular Biology. Published online, DOI: 10.3109/10409238.2015.1050550

The contact pathway of triggering blood clotting has also been termed the "intrinsic" pathway, since it can be triggered without adding a source of TF to the blood or plasma. This pathway is actually triggered when plasma comes into contact with certain types of artificial surfaces. Glass test tubes, diatomaceous earth (celite) and finely ground clay are especially good activators of the contact.[2] While this pathway does not contribute to normal hemostasis, it is thought to participate in thrombotic diseases.[3]

The extrinsic, or TF pathway

The plasma clotting cascade consists of a series of reactions involving the activation of zymogens (inert precursors of enzymes) via limited proteolysis. The resulting enzymes are catalytically active serine proteases, yet they have low inherent enzymatic activity as isolated proteins. Binding of a typical clotting protease to a specific protein cofactor on a suitable membrane surface markedly potentiates the protease's activity, often by as much as five orders of magnitude or more. The protein cofactors of the blood clotting cascade also generally circulate in the plasma as inert procofactors that must be converted into active cofactors via limited proteolysis. Most blood clotting proteins (both zymogens and procofactors) are represented by Roman numerals, with a lower case "a" appended to the numeral once the protein has been proteolytically converted to the active form. For example, the first serine protease in the extrinsic or TF pathway of blood clotting is coagulation factor VIIa (fVIIa), which circulates in plasma largely in the inactive, zymogen form (fVII).

The enzyme that actually triggers the TF pathway of blood clotting thus consists of two subunits: the catalytic subunit is the trypsin-like serine protease, fVIIa, and the positively-acting regulatory subunit ("protein cofactor") is the cell-surface protein, TF. The complex between TF and fVIIa (TF:VIIa) is anchored to the cell surface, because TF is an integral membrane protein.[1] Free fVIIa is a very weak enzyme, but the TF:VIIa complex is an extremely potent activator of coagulation. Once formed, the

TF:VIIa complex activates two downstream substrates in the coagulation cascade via limited proteolysis: factor IX (fIX) is converted to fIXa, and fX is converted to fXa. Both of these active enzymes must assemble on suitable membrane surfaces together with their own protein cofactors (fVIIIa in the case of fIXa; or fVa in the case of fXa) in order to propagate the clotting cascade. This ultimately leads to a large burst of thrombin, the last serine protease in the clotting cascade. Thrombin efficiently processes fibrinogen into fibrin via limited proteolysis, which in turn spontaneously assembles into a fibrin clot. Thrombin is also a potent activator of platelets, further contributing to the formation of a protective hemostatic plug (in normal hemostasis) or a thrombus (in pathologic activation of clotting).

TF

TF, also sometimes known as thromboplastin (perhaps more correctly, tissue thromboplastin), coagulation factor III, or CD142, is a glycosylated, integral-membrane protein of about 46 kDa, consisting of a single polypeptide chain of 261 or 263 amino acids (the two forms are nearly equal in expression).[4-6] Membrane anchoring of TF via its single membrane-spanning domain is essential for full procoagulant activity.[7] TF is unusual among the protein cofactors of the plasma clotting cascade in that it is an integral membrane protein, and also that it is does not require proteolysis for activity.

TF is abundant in adventitial cells surrounding all blood vessels larger than capillaries, in keratinocytes in the skin, and in a variety of epithelial layers such as organ capsules.[8-10] This pattern of expression is consistent with the role of TF as a protective "hemostatic envelope" surrounding the vasculature, organ structures, and the organism in its entirety.[8] Further, there is especially abundant TF at anatomic sites where hemorrhage is likely to result in disastrous consequences, such as kidney and brain.[8, 10] TF expression is quite low in skeletal muscle and synovial tissues.[8, 10] Interestingly, these are two anatomic sites of spontaneous bleeding in hemophilic patients (who lack either fVIII or fIX). A plausible explanation for bleeding at these sites is that activation of fIX by the TF:VIIa complex provides

an additional amplification step, compared with direct activation of fX. This may explain why hemophilic patients do not tend to bleed excessively from superficial cuts in the skin (which has high levels of TF, allowing for direct, abundant activation of fX by TF:VIIa). On the other hand, sites such as skeletal muscle and joints, where TF levels are low, may require the additional amplification of the clot-initiating signal gained from activating fIX by TF:VIIa. The newly-generated fIXa then assembles with fVIIIa to generate larger quantities of fXa than could be generated directly by low levels of TF:VIIa alone.

In cross-sections of normal blood vessels, TF is readily detectable only in the adventitial cells that make up the outermost layers of the vessel wall.[8-10] Circulating blood cells, as well as the endothelial cells that line the blood vessels, do not usually express TF (as detected by antibody staining). However, certain inflammatory mediators[11, 12] or hypoxia[13] can stimulate cultured peripheral blood monocytes and endothelial cells to express significant amounts of TF. Other blood cell types such as neutrophils, eosinophils and platelets have been reported to express TF under some circumstances,[14-17] although this is somewhat controversial.[18] Induced expression of TF in the vasculature by inflammatory mediators may play important roles in thrombotic diseases.

Urine and plasma may contain low levels of TF antigen, although the source of this "blood-borne" TF is a matter of some controversy.[17] An alternatively-spliced, soluble form of TF has been described,[19] and microparticles shed from activated leucocytes likely contribute to blood-borne TF.[20]

FVII/VIIa

Zymogen fVII is a glycosylated protein of approximately 50 kDa, consisting of a single polypeptide chain of 406 amino acids.[21-23] FVII is synthesized in the liver and circulates in plasma at a concentration of about 10 nM.[24] When initially synthesized inside the endoplasmic reticulum of hepatocytes, fVII contains a signal peptide and a propeptide (removed intracellularly) that mediate, respectively, secretion and a specific type of post-translational modification (γ-carboxylation) of all the

glutamate residues within about 45 amino acids of the N-terminus of the mature protein. Like other related vitamin-K dependent coagulation proteins, fVII contains an N-terminal γ-carboxyglutamate–rich domain (GLA domain). The fVII GLA domain contains ten γ-carboxyglutamate (Gla) residues that are essential for the clotting activity of this protein. The GLA domain confers reversible, Ca^{2+}-dependent binding of fVII to membranes containing negatively charged phospholipids such as phosphatidylserine or phosphatidic acid.[25, 26]

FVII, like all the coagulation serine proteases, circulates in the plasma chiefly as an inert zymogen. Unlike most other plasma serine proteases, however, fVII also circulates in its active enzymatic form (fVIIa). Zymogen fVII is converted to its enzymatic form, fVIIa, by proteolysis of a single peptide bond, resulting in two disulfide-linked polypeptide chains. The light chain, approximately 20 kDa, has 152 amino acids and contains the GLA domain and two epidermal growth factor (EGF)-like domains. The heavy chain, approximately 30 kDa, has 254 amino acids and contains the trypsin-like serine protease domain.

The active forms of most coagulation serine proteases have extremely short plasma half-lives (measured in seconds to minutes) because plasma contains high concentrations of protease inhibitors. However, free fVIIa is not susceptible to most plasma protease inhibitors.[27] It consequently circulates with a half-life of approximately 2 hours, similar to the approximately 5-hour half-life of zymogen fVII.[28] Approximately 1% of the fVII in plasma circulates in the activated form in normal humans.[29]

The precise source of circulating fVIIa *in vivo* is not clear. Proteases that are able to activate fVII in vitro include fIXa, fXa, fXIIa, thrombin, plasmin, fVII–activating protease, and the TF:VIIa complex.[21, 25, 30-37] Interestingly, patients deficient in fIX (hemophilia B) have approximately a tenfold reduction in plasma fVIIa levels.[38] This suggests that fIX (presumably, as fIXa) contributes substantially to activation of fVII in vivo. FVIIa concentrations increase during the post-prandial period, in a fIX-dependent manner,

especially after fatty meals.[39, 40] This suggests that generation of circulating fVIIa may involve both fIXa and lipoproteins.

The TF:VIIa complex in hemostasis

TF binds either fVII or fVIIa with high affinity, resulting in a 1:1 complex on the cell surface. Once fVII binds to TF, it is rapidly converted to fVIIa by limited proteolysis.[32] There are consequently two ways to form the TF:VIIa complex: through direct capture of fVIIa by TF, or by capture of fVII and subsequent conversion to fVIIa.

Free fVIIa activates its substrates (fVII, fIX, or fX) extremely slowly, but assembling the TF:VIIa complex on a suitable phospholipid membrane enhances the activity of fVIIa by at least five orders of magnitude.[41-43] Negatively charged phospholipids, most particularly phosphatidylserine, are required for binding of the substrates, fIX or fX, to the phospholipid surface. Quiescent, intact cells expressing TF on their surfaces have much lower procoagulant activity than do damaged or activated cells.[44] TF on a quiescent cell is not fully active until the membrane properties of the cell are altered.[45, 46] This process, sometimes called decryption of "encrypted" cell-surface TF, is incompletely understood. "Decryption" of TF is, at least in part, due to exposure of negatively charged phospholipids on the outer leaflet of the plasma membrane, resulting in expression of efficient binding sites for the substrates of the TF:VIIa complex. Additional proposed mechanisms for encryption/decryption of cell-surface TF include: association with caveolae where lipid composition is altered;[47, 48] dimerization or oligomerization of TF with reduced enzymatic activity;[49] and reduction or oxidation of a specific disulfide bond in TF that is required for cofactor function.[50, 51]

Regulation of the TF:VIIa complex

The TF:VIIa complex is primarily inhibited by the plasma serine protease inhibitor, tissue factor pathway inhibitor (TFPI), which has two isoforms in humans: TFPIα (32 kDa) and TFPIβ (22 kDa).[52] TFPI is a Kunitz-type inhibitor, with the Kunitz-2 domain mediating binding and inhibition of fXa, and the Kunitz-1 domain required for inhibition of fVIIa in the TF:VIIa complex.[53] The majority of TFPI in vivo is associated with the microvascular endothelium,[54] but a small amount of TFPI circulates in the plasma at a concentration of around ~1.6 nM. Most (~80%) circulating TFPI is lipoprotein-bound.[55-57] TFPI is also expressed by megakaryocytes, stored in platelets, and secreted upon platelet activation.[55, 58] A substantial fraction of the TFPI produced by endothelial cells remains at the cell surface, associates with caveolae, and is released by phosphatidylinositol-specific phospholipase C. Thrombin and shear increase the expression and release of TFPI *in vitro,*[59-66] and the administration of heparin causes a rapid increase in the circulating levels of total TFPI in plasma *in vivo.*[67-70]

TFPI regulates coagulation via direct inhibition of fXa, and via fXa-dependent feedback-inhibition of TF:VIIa. The TFPIβ isoform is a weaker inhibitor of fXa than is TFPIα.[71] Protein S substantially enhances the inhibition of fXa by TFPIα.[72] Heparin and other polyanions accelerate fXa inhibition by TFPIα in a template-dependent manner.[73, 74] FXa-dependent inhibition of TF:VIIa by TFPI involves the formation of a quaternary complex consisting of TFPI, fVIIa, TF, and fXa. TFPI-mediated regulation of coagulation is critically important, as evidenced by the effects of disruption of this protein in mouse models, where TFPI-deficient mice die *in utero* from a consumptive coagulopathy,[75] but can be rescued by concomitant fVII or TF deficiency.[76, 77] Antithrombin, in the presence of heparin, is also able to inhibit the TF:VIIa complex.[78, 79]

TF:VIIa in disease

While the TF:VIIa complex is the crucial trigger for hemostatic responses in vivo, excessive initiation of coagulation via the extrinsic pathway can lead to thrombosis, consumptive coagulopathy, or

inflammation. Increased complex formation can be the result of loss of vascular wall integrity, increased TF expression, or increased levels (or activity) of fVII/fVIIa.

Atherosclerotic plaques contain significant levels of TF, generally associated with monocytes/foam cells and smooth muscle cells.[9, 80-83] TF antigen may also be found in the acellular core of atheromas, most likely from necrotic cells. Plaque TF is functional and can bind fVIIa.[82, 83] In atherosclerosis, the blood is separated from TF by only a thin monolayer of endothelial cells. Myocardial infarction is thought to be triggered by rupture of an atherosclerotic plaque in a coronary artery,[84] with the consequent exposure of TF to fVII/fVIIa within the blood. If this coagulation activation is extensive enough to form an occlusive thrombosis within the coronary vessel, myocardial infarction ensues.
TF expression can also be increased with malignancy, potentially leading to cancer-associated thrombosis (also known as Trousseau syndrome).[85] The neoplastic cell itself can express TF, or tumor TF can be associated with infiltrating activated monocytes or stromal cells.

During sepsis, TF is expressed on monocytes, but is also expressed by endothelial cells in some areas, such as the splenic microvasculature.[86] In primate models, coagulopathies associated with sepsis and septic shock are mediated by TF, and TF:VIIa contributes directly to mortality in sepsis.[87, 88]

Epidemiologic studies have indicated that elevated plasma fVII may be a risk factor for thrombotic disease.[89-91] Elevated plasma fVII coagulant activity (fVII:C) or elevated levels of circulating fVIIa have also been described with angina pectoris, transient ischemic attacks, diabetes, uremia, and peripheral vascular disease.[92-101] In contrast, some studies have failed to find a relationship between fVII levels and thrombotic disease.[102, 103] Population studies have reported that fVII levels are unrelated to the degree of carotid artery thickness or other manifestations of vascular disease.[104-108] Results have been mixed with regard to a potential correlation between fVIIa levels and the risk of thrombotic disease.[109-111]

The contact pathway

The contact pathway of coagulation is initiated by activation of factor XII (fXII) in a process that also involves high-molecular-weight kininogen (HK) and plasma prekallikrein (PK). Contact of blood with an artificial surface leads to a change in the conformation of fXII, resulting in the generation of small amounts of active factor XII (fXIIa).[112, 113] This enzyme then activates PK to kallikrein. Further reciprocal activation of fXII by kallikrein, and PK by fXIIa, results in a positive feedback loop.[114] The fXIIa that is generated then activates its downstream substrate, fXI, to fXIa. Limited proteolysis of fIX to fIXa by fXIa then allows for formation of the "intrinsic tenase" complex (i.e., the cell-surface complex of fIXa and fVIIIa), which in turn activates fX to fXa. The final common pathway of blood clotting then leads to thrombin generation and a blood clot.

Despite its important role in clot formation *in vitro*, contact activation appears to have no contribution to hemostasis *in vivo*. This conclusion comes from the fact that mice and humans lacking fXII have no bleeding tendencies.[115] Rather, one of the functions of the contact pathway *in vivo* appears to be the generation of bradykinin, a vital inflammatory mediator that is produced when kallikrein cleaves HK. This small peptide is the ligand for the kinin B2 receptor on endothelial cells. Binding of bradykinin to its receptor results in vasodilation, increased vascular permeability, pain, and neutrophil chemotaxis. Components of the contact system also contribute to fibrinolysis, and inhibit thrombin-induced platelet activation, angiogenesis, and adhesive interactions .[115]

FXII/XIIa

FXII is an approximately 80 kDa protein consisting of a single polypeptide chain of 596 amino acids.[115] It is synthesized in the liver and circulates in plasma at a concentration of around 375 nM. FXII is activated via limited proteolysis by kallikrein, plasmin, and fXIIa (autoactivation), resulting in a two-chain

molecule (αfXIIa) consisting of a 353 amino acid heavy chain and a 243 amino acid light chain, which contains the serine protease domain.

PK/kallikrein

PK is also made in the liver. Prekallikrein contains 609 amino acids, but due to variable glycosylation may have a molecular weight of either 85kDa and/or 88 kDa.[116] It circulates in plasma at a concentration of around 490 nM, with 75% bound to HK.[116] Prekallikrein is activated via limited proteolysis by fXIIa, resulting in a two-chain enzyme (kallikrein) consisting of a 371 amino acid heavy chain and a 248 amino acid light chain, which contains the serine protease domain.

HK

HK is a 120 kDa protein with a plasma concentration of about 670 nM. Granulocytes, platelets and endothelial cells contain HK, but plasma HK is most likely synthesized in the liver. HK binds to cell surfaces in a zinc-dependent manner. The major contribution of HK to the contact pathway is facilitation of substrate presentation to fXIIa.[3] HK is required for efficient formation of kallikrein in surface-activated plasma.[117]

Activators of the contact pathway in vitro *and* ex vivo

Exposure of blood to an artificial surface invariably results in some activation of fXII to fXIIa. In fact, fXII activation is the mechanism by which clotting is initiated when blood is collected into glass tubes. Because activation of fXII is not calcium dependent, collection of blood into common anticoagulants that are metal-ion chelators (e.g., EDTA or citrate) does not block the formation of fXIIa. For typical clotting tests, however, this is not a problem since only low levels of fXIIa are generated in

blood collection tubes in the absence of an added contact activator, and these low levels of fXIIa are continuously inhibited by the protease inhibitors in plasma.

Activation of fXII initiates clotting in the commonly used diagnostic plasma clotting test known as the activated partial thromboplastin time (aPTT). In this test, plasma fXII, PK, and HK assemble onto artificial surfaces such as finely dispersed kaolin, diatomaceous earth (celite), or ellagic acid. The fXIIa is generated via fXII autoactivation and via kallikrein-mediated reciprocal activation of fXII. The generated fXIIa initiates the coagulation cascade via activation of its downstream substrate fXI. Note that, despite having a markedly prolonged aPTT, individuals with fXII deficiency have no tendency for either spontaneous or trauma-induced bleeding.[115]

Ex vivo activation of the contact pathway also occurs during hemodialysis, cardiopulmonary bypass, and extracorporeal membrane oxygenation (ECMO), where blood comes into contact with artificial surfaces. Anticoagulant therapy (e.g., with citrate or heparin) is required to maintain blood flow through the extracorporeal circuit, because fXIIa generation results in cleavage of downstream enzymes. Note that neither of these anticoagulants prevents contact activation, but rather inhibits the activity of downstream coagulation enzymes. Recently, a blocking antibody to fXIIa has shown utility in stopping unwanted blood clotting during extracorporeal membrane oxygenation without the usual bleeding risk associated with conventional anticoagulants.[118]

Activators of the contact pathway in vivo

Several candidate activators of the contact pathway have been proposed, but the precise (patho)physiologic activators in vivo have not been definitively identified. Suggested naturally occurring activators include specific proteins on mammalian cell surfaces,[119] extracellular nucleic acids,[120] inorganic polyphosphate (polyP),[121] misfolded proteins,[122] glycosaminoglycans,[123, 124] and bacterial surface proteins.[125, 126]

Contact activation occurs on the surface of endothelial cells in vitro in a zinc-dependent manner.[127] Endothelial cell binding sites for HK and fXII that have been identified include the C1q receptor, cytokeratin 1, and the urokinase plasminogen activator receptor.[128]

Nucleic acids are released from cells due to apoptosis, necrosis, or extrusion of nuclear material by activated neutrophils—a process termed neutrophil extracellular traps, or NETs.[129] Extracellular nucleic acids can bind to either fXII or fXI, and in vitro studies indicate that they are capable of enhancing fXII activation.[120, 130] The potency of nucleic acids as contact activators *in vitro* is somewhat weak, being some two orders of magnitude lower than that of kaolin on a weight basis.[120] Nevertheless, this mechanism for triggering blood clotting may be quite significant, as animal models employing administration of either exogenous RNA or RNase support a possible role for RNA as a contact activator *in vivo*.[120]

PolyP

Inorganic polyP is an intensely anionic, linear polymer of orthophosphate units linked by high-energy phosphoanhydride bonds. PolyP is widespread in biology, with polymer sizes ranging from a few phosphates up to hundreds or even thousands of phosphates in length, depending on the organism and type of cell.[131, 132] PolyP has mostly been studied in prokaryotes and unicellular eukaryotes, but roles for polyP in mammalian systems are rapidly emerging. Microorganisms store polyP in granules,[133] which typically contain very long-chain polyP, ranging in length from hundreds to thousands of phosphate units.[134] Mammalian cellular compartments that contain polyP include platelet dense granules,[135] a subset of mast cell granules,[136] lysosomes,[137] mitochondria, and nuclei.[138] Upon activation, platelets and mast cells release polyP of about 60-100 units in length.[135, 136] Tissue extracts from mammalian heart, liver, lung and kidneys contain heterogeneous polyP of 50 to 800 phosphate units long, while brain polyP is longer, at about 800 phosphates long.[138]

PolyP binds with high affinity to certain proteins of the contact pathway of blood clotting,[139-141] and is a very strong activator of the contact pathway in vitro in both plasma and purified protein systems.[121, 139] Contact activation by polyP is profoundly dependent on polymer length, with optimal activity requiring very long polyP polymers[141] which, on a weight basis, have potencies greater than that of the artificial activator, kaolin. Platelet-derived polyP, which is much shorter in length, is able to weakly activate contact factors, but is markedly less potent than long-chain polyP.[141] PolyP activates the contact pathway *in vivo* in mouse models as evidenced by development of cutaneous vascular leakage that is bradykinin- and fXII-dependent.[121, 142]

Misfolded protein

Aggregated amyloid β peptide (Aβ) is known to activate fXII *in vitro*,[143] and patients with Alzheimer's disease have evidence indicating increased in vivo generation of fXIIa, particularly in the central nervous system.[144, 145] Amorphous aggregates of Aβ and large amyloid fibrils are also both present in patients with systemic amyloidosis, who also experience increased in vivo activation of both fXII and PK.[122] The generation of kallikrein by misfolded protein aggregates is dependent on fXII, but does not result in increased activation of fXI. Interestingly, the activation of the contact pathway by misfolded proteins does not appear to be procoagulant, suggesting that kallikrein-kinin pathway is regulated differently than the intrinsic pathway of coagulation *in vivo*.[122]

Glycosaminoglycans

Heparin has been long known to be capable of supporting autoactivation of fXII *in vitro*.[146, 147] Heparin released from allergen-activated mast cells initiates fXIIa-mediated activation of plasma PK to kallikrein, but without activating fXI.[123] More recent evidence suggests that glycosaminoglycans can contribute to pathologic activation of the contact system *in vivo*. In particular, contamination of

pharmaceutical heparin with an over-sulfated chondroitin sulfate led to serious adverse effects in patients receiving heparin therapy, from excessive contact activation.[148] Activation of fXII and kallikrein, and cleavage of HK, all occur in patients with anaphylaxis, and are accompanied by increased levels of heparin.[149]

Regulation of the contact pathway

The plasma protease inhibitor, C1-inhibitor, is a crucial regulator of the contact pathway, inhibiting fXIIa, kallikrein, and fXIa, as well as several members of the complement cascade. Inhibitory activity is potently enhanced by the binding of glycosaminoglycans. C1-inhibitor is a member of the serpin superfamily.[150] It is a heavily glycosylated protein of 478 amino acids, with an apparent molecular weight of about 104 kDa and a normal circulating plasma concentration of approximately 1.8 μM. Since C1-inhibitor is an acute phase protein, the plasma concentration can be markedly higher with inflammatory conditions.[150]

The contact pathway in disease

Activation of the contact pathway *in vivo* leads to release of the vasoactive peptide bradykinin. The importance of this pathway is clearly indicated by the clinical manifestations in patients with hereditary angioedema. These individuals experience intermittent episodes of edema and pain due to dysregulation of the contact pathway, usually caused by deficiency of C1 inhibitor.[151] Contact activation also occurs in sepsis and other infectious causes of systemic inflammatory response syndrome,[152, 153] in which continued generation of fXIIa and kallikrein can deplete zymogen levels.[154]

Although the contact pathway is not required for normal hemostasis, recent evidence indicates that it contributes to thrombotic disorders. Deficiency of fXII is protective against thrombus formation in both arteries and veins in animal models,[155, 156] and increased plasma fXII, fXI, or kallikrein activity is

associated with atherosclerosis[66] or myocardial infarction.[157, 158] Individuals with severe fXI deficiency have reduced risk of stroke.[159] In animal models of thrombosis, fXII deficiency decreases formation of arterial thrombi[160] and protects the animals from ischemic brain injury.[161] Activation of the contact pathway *in vivo* via intravenous administration of RNA,[120] or polyP[121] triggers pulmonary embolism in animal models. And finally, inhibitors of polyP are antithrombotic in arterial and venous thrombosis models in mice, with reduced bleeding side-effects compared to heparin.[142, 162, 163]

Recent advances in anticoagulant therapies

As our understanding of the myriad processes involved in the initiation of coagulation in mammalian blood continues to grow, so does our understanding of the complex relationship between hemostasis and pathological thrombosis. Under the original assumption that these processes were inseparable, it made sense to target the most important enzymes in the final common pathway of blood coagulation.

Heparin-based anticoagulants are one of the oldest clinically used anticoagulant agents. The main anticoagulant effects of heparins are mediated by a template effect that enhances the binding of the natural anticoagulant protein antithrombin to fXa or thrombin.[164] It's short half-life in plasma and strongly anticoagulant nature (due to binding some of the most central coagulation proteases) has made unfractionated heparin. Unfortunately, only a small subset of the heparin molecules within a given dose are active,[165] and the binding of heparin to many different proteins can result in complexes that induce severe immune responses,[166] the most well-known of which is heparin induced thrombocytopenia.[167] There have been recent advances in developing low-molecular weight heparins either by size fractionation or chemical synthesis that have less immunological complications than unfractionated heparin,[69, 168] but these molecules still carry extensive bleeding risk, and also are unable to be reversed

by protamine, the only FDA approved heparin reversal agent for use to treat heparin-induced bleeding during surgery, treatment for acute coronary syndromes (i.e. heart attack), or dialysis.[169]

Warfarin is one of the most common anticoagulants proscribed today for prophylactic treatment of patients at risk for venous thromboembolism.[170, 171] It acts by disrupting the formation of the GLA domains of factors VII, IX, X, and prothrombin, which impairs their ability to bind to procoagulant membrane surfaces and is essential to their function. One of the drawbacks to warfarin therapy however is that the anticoagulant state of the patient must be closely monitored, and issues of patient compliance and monitoring can cause wide variation in the real world risks and efficacies of warfarin anticoagulation.[172] Recently, a new class of orally bioavailable small molecule inhibitors of either fXa or thrombin have emerged as potentially safer methods for prophylactic anticoagulation, but their cost effectiveness and efficacy are still being compared in clinical trials.[173]

Classical anticoagulant drugs are some of the most widely prescribed medications today, even with the knowledge that they necessitate straddling a sharp line between too much anticoagulation (risk of bleeding) and too little anticoagulation (risk of thrombosis).[174] Recent advances in our understanding of the role of the contact pathway in thrombosis has led to the intriguing possibility that drugs that inhibit initiation of the contact pathway may be effective antithrombotics with little or no bleeding side effects.

For example, a novel human monoclonal antibody targeting the active site of fXIIa developed via phage display has recently been shown to inhibit venous and arterial thrombosis during both experimental injury and extracorporeal circulation (ECMO) in animal models.[118] This antibody was just as effective as heparin without the concurrent risk of bleeding, and the fact that it specifically targets fXIIa rather than both the activated and zymogen forms of this enzyme means that it can be effective at much lower doses than inhibitors that bind to the zymogen and inhibit activation. Another exciting anticoagulant therapy based on inhibiting the contact (and thrombin-feedback) pathway relies on using

antisense oligonucleotides to inhibit the biosynthesis of fXI. This method has shown to be safe and effective in rabbits,[175] primates,[176] and even humans.[177] These oligonucleotides specifically target fXI mRNA and cause its degradation, leading to a dose-dependent decrease in fXI levels and resulting in decreased risk of thrombosis with less risk of bleeding compared to conventional therapeutics.

Concluding remarks

Inhibition of the contact pathway as a method of anticoagulation not only carries less risk of bleeding than current therapeutics, it also has the potential to reduce the often damaging connections (mediated by the fXIIa/kallikrein/bradykinin pathway) between coagulation and inflammation in human disease. Such novel anticoagulation approaches therefore have the potential to expand the health benefits of antithrombotic therapy to a much wider set of patients (who would otherwise be at severe risk of bleeding from conventional therapeutics) in a safer and more effective manner than is currently possible. Though research in human blood coagulation has a long and successful history, novel research in the mechanisms of thrombosis and hemostasis continues to reveal surprising and exciting insights into human biology that have the potential to save lives.

CHAPTER 2: POLYPHOSPHATE ACTS AS A NOVEL PROCOAGULANT AND PROINFLAMMATORY MEDIATOR[b]

General introduction to polyphosphate

PolyP is a highly anionic, linear polymer of orthophosphate residues held together by high-energy phosphoanhydride bonds. It is an ancient molecule found in all three domains of life, but whose functions have largely been investigated in microorganisms.[134] PolyP is often stored inside cells in complex with high concentrations of Ca^{2+}, Na^{+}, Zn^{2+}, and other cations in small, spherical, acidic, electron-dense subcellular compartments called acidocalcisomes.[178] These polyP-rich compartments have also been known over the years as volutin granules, metachromatic granules, or polyP bodies.[178] PolyP chains found in these granules can be anywhere from dozens to many hundreds or even thousands of phosphate units long.[179] The discovery that the dense granules of human platelets are actually a form of acidocalcisome and contain high concentrations of polyP (with chain lengths of 60-100 phosphates long)[135] has sparked an increasing interest in the role of this ancient molecule in human biology.

The largest body of literature concerning polyP deals with its role in the physiology of prokaryotes and unicellular eukaryotes. In bacteria and yeast, polyP is synthesized in a reversible enzymatic reaction from ATP,[134] and is degraded by endopolyphosphatases (which cleave in the middle of polyP chains) and/or exopolyphosphatases (which release phosphates processively from the ends of polyP chains).[180] A number of functions for polyP have been identified in microbes, including roles in metabolism and survival of nutrient deprivation,[181, 182] protection from heavy metal toxicity,[183, 184] and acting as a molecular chaperone for protein folding.[185] PolyP has also been shown to be essential for pathogenicity of certain infectious microorganisms through varied mechansims.[186-188]

[b] This chapter has been adapted from a review article originally published in the educational supplement to the 20th Annual Congress of the European Hematology Association, and used in accordance with the publisher's copyright privileges for publication in a dissertation thesis. Full Citation: Travers RJ, Smith SA, Morrissey JH. Novel concepts for coagulation activation. Hematology Education. 2015; 9(1):57-61.

Compared with our knowledge of polyP in the microbial world, much less is known about roles of polyP in higher organisms, although this is now changing. Early studies in rats and mice showed that polyP of varying sizes can be found in varying concentrations and chain lengths in almost all tissues and subcellular fractions in mammals.[138] Roles for polyP in mammalian cells have been identified in energy metabolism during respiration in mitochondria,[189] bone mineralization by human osteoblast-like cells,[190] and apoptosis of human plasma cells.[191] PolyP has also been shown to have important procoagulant and proinflammatory effects in mice and humans. While we are gaining a better understanding of some of the roles of polyP in mammalian cells *in vivo*, a detailed understanding of the mechanisms of the production and degradation of polyP in mammals has not yet been elucidated. The first hints about the mechanism of production of polyP production in mice were recently revealed however, when it was shown that knocking out the enzyme inositol hexakisphosphate kinase 1 severely decreases polyP levels in platelets, suggesting a link between biosynthesis of highly phosphorylated inositol derivatives and polyP production and/or storage.[192]

PolyP is a novel procoagulant mediator

The blood clotting cascade can be triggered via two pathways: the tissue factor pathway, and the contact pathway. The tissue factor pathway is essential for normal hemostasis, and also plays roles in a variety of thrombotic diseases.[193] The contact pathway, however, has long been a mystery in the world of hematology, since the best-known activators of the pathway are non-physiologic substances like glass, clay (kaolin), or diatomaceous earth.[3] Furthermore, the contact pathway is dispensable for hemostasis, since humans or mice that completely lack factor XII have no bleeding tendency.[194] Recently however, physiologic anionic polymers such as long-chain polyP,[141] DNA in neutrophil extracellular traps (NETs)[195] and extracellular RNA[120] have been shown to trigger the contact pathway by promoting the activation of factor XII and the plasma kallikrein system. Different requirements regulate the abilities of

these anionic polymers to trigger clotting via the contact system, including specific nucleic acid structures for RNA[196] and polymer length for polyP (longer chains are far more effective).[141] In fact, on a weight basis, long-chain polyP is orders of magnitude more potent at activating the contact pathway compared to non-physiologic clotting activators previously used in contact activation studies.[141] Activation of the contact system by long-chain polyP can be strongly proinflammatory, in a manner dependent on factor XII activation and release of bradykinin from high molecular weight kininogen.[121] These studies suggest that pathophysiologically relevant anionic polymers like polyP may contribute to coagulation and inflammation through activation of the contact pathway during conditions like infection or tissue damage.

Another mystery surrounding the contact system is that while the complete absence of factor XII in humans results in no bleeding tendencies,[194] patients with severe factor XI deficiency have clinically significant bleeding diatheses, usually as a result of injury or surgical procedures, and especially in tissues with high fibrinolytic potential such as mucous membranes.[197] A potential explanation for the role of factor XI in normal hemostasis was uncovered when it was shown that thrombin can back-activate factor XI to XIa,[198] but observing meaningful rates for this reaction *in vitro* necessitated supraphysiologic amounts of thrombin and factor XI. The discovery that some coagulation proteins, including thrombin and factor XI, bind to immobilized polyP *in vitro*[140] led in turn to the discovery that platelet polyP causes an approximately 3000-fold increase in the rate of back-activation of factor XI by thrombin, allowing this reaction to occur at physiologically relevant concentrations of thrombin and factor XI.[199] Even more recently, platelet polyP was also shown to enhance the rate of factor V activation to Va by factor XIa,[200] providing another link between polyP, the contact system, and hemostasis.

Some of the earliest studies into the procoagulant nature of polyP revealed that it can serve as a cofactor for the back-activation of factor V to Va by both thrombin and factor Xa, one result of which is essentially complete abrogation of the anticoagulant activity of tissue factor pathway inhibitor (TFPI).[139]

The importance of these amplification reactions can been seen in the fact that adding polyP can correct prolonged clot times in whole blood samples treated with either heparin or direct oral anticoagulants as well as plasma samples from patients with hemophilia A or B.[201] Another consequence of polyP-mediated amplification of coagulation is that clots formed in the presence of polyP are more resistant to fibrinolysis.[139] Subsequent studies have shown that polyP also directly alters the structure of fibrin clots, increasing fiber thickness and strength and making fibrin more difficulty for fibrinolytic enzymes to digest.[141, 202, 203] **Fig. 2.1** illustrates the various ways in which polyP and other anionic polymers have been shown to modulate novel procoagulant activities within the traditional coagulation cascade.

PolyP's role in the connection between inflammation and coagulation

Recent investigations into the connections between coagulation and inflammation have shown that nucleic acids and polyP may play greater roles in pathological coagulation (i.e. thrombosis) than in normal hemostatic processes.[204] Recent advances using real-time fluorescent imaging of clot formation *in vitro* and *in vivo* have revealed that while a dense core of fully activated platelets are necessary for hemostasis, excessive contact factor activation and platelet stimulation from the release of dense granule contents like calcium, ADP, and polyP can cause the propagation of excessive coagulation that eventually leads to thrombosis and vessel occlusion.[205] One example of this is that mice lacking factor XII show no bleeding abnormalities (as expected from their human counterparts) but are protected from venous and arterial thrombosis, suggesting that while the contact system is unimportant for hemostasis, it plays a significant role in thrombosis and inflammation in mice.[160] Our growing understanding of the differences between hemostasis and thrombosis and the role of molecules like polyP in the interplay between the two processes allows for the possibility of exciting new therapies that are able to target thrombosis with decreased bleeding risks compared to conventional anticoagulants.

In addition to its procoagulant activity, exposure to polyP induces NF-κB activation and leukocyte adhesion in endothelial cells, [206] and polyP is secreted from activated mast cells.[136] Furthermore, histones complexed with polyP activate platelets via toll-like receptors 2 and 4, with greater potency than histones or polyP alone.[207] Our growing appreciation of the role of polyP as a mediator between coagulation and inflammation is consistent with the concept of platelets as modulators of both innate and adaptive immunity.[208, 209] Sepsis and disseminated intravascular coagulation, which are the leading causes of death in the intensive care unit,[210] are prime examples of diseases where the connection between widespread platelet activation, inflammation, and coagulation leads to significant mortality. Novel therapeutic strategies targeting the coagulation-inflammation axis therefore have potential usefulness for treating both pathological thrombosis and thrombo-inflammatory disorders.

New diagnostics and therapeutics based on polyP-mediated coagulation and inflammation

Research into the role of polyP in the biology of mammals has been somewhat hindered because in general mammalian cells contain lower total amounts of polyP than prokaryotes and single-celled eukaryotes, and many techniques for identifying and purifying polyP from biological samples are more suited to working with high concentrations of long-chain polyP. One of the main challenges of working with polyP is that its ubiquity and simple structure leave it intractable to many of the standard biochemical assays. While there are numerous (often debated) methods for quantifying polyP from biological samples[211] or staining polyP for fluorescent microscopy,[136] these techniques are often most suited to single cell types with relatively high concentrations of polyP. Adapting these techniques to human tissues is a complex and laborious process, but it promises intriguing insight in polyP's effects on human biology *in vivo*. One of the first examples of this would be an in-depth investigation of the polyP levels of localization in various human tissues. Early reports of the quantification of polyP in various

mammalian tissues have revealed the fact that both long chain and short chain polyP are widespread in mammalian tissues, with the highest levels being found in the brain, heart, and lungs, followed closely by the liver and kidneys.[138] The presence of long chain polyP in the brain is especially intriguing, because intracranial hemorrhage is an extremely deadly condition that has been shown to be dependent on inflammatory processes similar to those that can be enhanced by polyP.[212] As our understanding of the complex mechanisms between polyP, coagulation, and inflammation, we will continue to need more sensitive and accurate methods for studying its presence in tissues and biological samples during normal physiological and pathological processes.

To that end, a method for the sensitive measure of polyP levels and localization in normal human tissues would give us a starting point for examining the role of polyP in prothrombotic or proinflammatory disease states. For example, it is possible that various disease states (in addition to the aforementioned dense-granule storage disorders) could be accompanied by changes in polyP concentration, chain length, or storage. Diagnostics that could quantify polyP in human samples might provide additional information about the disease state of a particular patient. Steadily increasing interest in the role of polyP in mammalian cells and rapidly advancing techniques for chemically modify polyP hold exciting promise for future elucidation of the various roles of this ancient molecule in our modern understanding of mammalian biology.

Polycationic compounds have been shown to be effective in inhibiting the interaction between polyP and coagulation enzymes in vitro, and in mouse models they have shown efficacy as antithrombotics with reduced bleeding side effects compared to heparin.[163] Inhibition of polyP-mediated amplification of coagulation might therefore be a therapeutic target for interrupting thrombosis without the bleeding risk that comes from conventional anticoagulant drugs that inhibit essential enzymes of the classical coagulation cascade.

Current hemostatic agents, especially those designed to treat internal bleeding, are based upon recombinant proteins that are expensive to produce on a large scale and have relatively short shelf lives once reconstituted. PolyP, on the other hand, is already made in industrial quantities cheaply, and is very stable under appropriate storage conditions. PolyP-based hemostatic agents are therefore an intriguing possibility for treating bleeding disorders. Recently, silica nanoparticles functionalized with polyP have been shown to be more effective than polyP alone in enhancing coagulation,[213] providing proof of principle for polyP based hemostatic agents in the future. In particular, injectable polyP-based nanoparticles could provide extremely important therapeutics for incompressible hemorrhage (i.e. internal bleeding), especially if the potential pro-inflammatory effects of polyP could be mitigated by chemical modification or chain-size optimization and/or targeting the nanoparticles directly to the sites of injury.

The discovery of polyP in platelets and its multi-faceted role in coagulation and inflammation contributes to our evolving understanding of the complex role of coagulation enzymes, both within and outside of the mechanisms of normal hemostasis. These discoveries open the door to research into future diagnostics that enhance our understanding of polyP's role in human biology. PolyP is also both a potential drug target and potential therapeutic agent, for treating deadly disorders of bleeding, coagulation, and inflammation.

CHAPTER 3: VISUALIZING POLYPHOSPHATE

INTRODUCTION

As our understanding of the vascular system continues to evolve, it is becoming increasingly clear that there are some important differences between the processes of normal hemostasis and pathological thrombosis.[204] PolyP is a newly discovered link between inflammation and coagulation, acting to accelerate many clotting reactions and providing a surface for the activation of the Factor XII-bradykinin pathway of inflammation.[214] The discovery of the role of platelet polyP in human pathophysiology has led to a recent burst of interest in the possible roles of this ancient molecule in other cells and tissues. Unfortunately, most classical biochemical assays and imaging agents are designed to be used with proteins or nucleic acids, which have distinct structures and are amenable to enzymatic modifications. There have been many attempts to develop assays to purify and image polyP in mammalian cells and tissues, but most of them have either relied on radioactive phosphate and/or used extraction techniques that are not efficient enough for low amounts and small chain lengths of polyP.[138, 211]

Some advances have been made in developing polyP visualization techniques however, including using a purified recombinant polyP-binding domain of *E. coli* exopolyphosphatase (PPXbd) as a surrogate "primary antibody" to visualize polyP in fungi and cells.[136, 215] These studies rely on detection techniques based on antibodies against various recombinant "tags" on the PPXbd to visualize polyP. Ideally, biotinylating the PPXbd protein would provide a simpler and more direct method of visualizing polyP in cells and tissues via streptavidin-conjugated fluorescent dyes. Unfortunately, direct biotinylation of proteins is almost always based on an amine-reactive chemistry, and this method of biotinylation results in a PPXbd protein with a much lower affinity for PPXbd (data not shown), probably due the fact that there are multiple lysines (which are biotinylated via amine reactive chemistry) in the polyP binding pocket of PPXbd which are presumably important for binding to the anionic polymer.[216] In

order to circumvent these issues, I have created a site-specific biotinylated version of PPXbd based upon AviTag technology (Avidity LLC) that retains full polyP binding ability and can be used to immunofluorescently label polyP in a variety of cells and tissues. This study details the validation of polyP-specific staining in cells and tissues via a mixture of biotinylated PPXbd and streptavidin-conjugated dyes and provides some examples of new findings concerning the localization of polyP in mammalian cells and tissues revealed by this sensitive and specific staining technique.

METHODS

Production, purification, and biotinylation of PPXbd

A synthetic gene containing the AviTag biotin acceptor peptide in place of the previous 6xHis tag was cloned into a previously described PPXbd plasmid[215] using *Nco*I and *Xba*I (performed by Epoch Life Sciences). This plasmid was then transfected into BL21-DE3 cells (New England Biolabs). 1.4 mL of an overnight culture of transfected BL21-DE3 cells was added to 1 L of NYZ media and once the OD_{600} reached 0.4-0.6, PPXbd production was induced overnight at 15°C by the addition of 400 μM (final concentration) IPTG. The cells were then pelleted and lysed, and PPXbd was purified on amylose resin according to the manufacturer's instructions (New England Biolabs). Purified PPXbd was then biotinylated at the biotin acceptor peptide sequence with the BirA ligase kit according to the manufacturer's instructions (Avidity LLC).

RBL-2H3 cell staining

RBL-2H3 cells were purchased from ATCC. They were grown in MEM with glutamine, supplemented with 15% fetal bovine serum, 100 IU/mL penicillin/streptomycin, and 1 mM sodium pyruvate at 37 °C with 5% CO_2. All staining procedures took place at during passages 2-6.

Cells were seeded onto sterile 22 mm glass coverslips placed in 6-well plates at a concentration of at $2x10^5$ cells per well and allowed to attach overnight. Adherent cells were washed twice with saline and then fixed with 4% paraformaldehyde in PBS for 30 minutes at room temperature. They were then washed three times with TBS (100 mM Tris-HCl pH 7.4, 150 mM NaCl, 0.05% NaN_3) and permeabilized by incubation with 0.2% triton X-100 in TBS for 30 minutes at room temperature. Next, cells were washed three times with TBS and incubated with recombinant yeast exopolyphosphatase (1 µg/mL diluted in 60 mM Tris-HCl pH 7.4, 6.0 mM $MgCl_2$, 0.05% NaN_3) or buffer alone for one hour at 37 °C. Then, cells were washed 2 times with TBS and endogenous biotin was blocked according to manufactures instructions (Endogenous Biotin Blocking Kit, Thermo Scientific). Cells were washed twice again with TBS and incubated with 5% BSA in TBS plus 0.05% Tween-20 for 30 minutes at room temperature. Finally, cells were incubated with a mixture of 40 µg/mL PPXbd-biotin and 10 µg/mL streptavidin-conjugated Dylight 650 (Thermo Scientific) for 2 hours at room temperature in the dark, then washed and mounted on slides with ProLong Gold Mounting Media (Invitrogen).

Blood vessel staining

Freshly harvested (unfixed) and snap-frozen aortas from C57BL/6J mice cut to 5 µm sections and mounted on positively-charged slides were purchased from Zyagen. The slides were stored at -80 °C until use. For staining, the slides were removed from -80 °C and fixed with 4% paraformaldehyde for 30 minutes at room temperature. They were then permeabilized, digested, and stained according to the same protocol as the RBL-2H3 staining above. The only modification was the use of 10 µg/mL rather than 1 µg/mL exopolyphosphatase in the digestion step to account for the larger tissue size.

RESULTS

Biotinylated PPXbd can be used to detect polyP in mast cell acidocalcisomes

To investigate whether site-specifically biotinylated PPXbd could be used to image polyP in acidocalcisomes within cells known to contain polyP, we used a combination of biotinylated PPXbd and streptavidin-conjugated Dylight 650 in a one-step staining procedure. Images of RBL-2H3 cells stained with biotinylated PPXbd (**Fig 3.1 A,B**) are nearly identical to images of RBL-2H3 cells stained by PPXbd and detected by secondary antibody,[136] and the staining is not present when either the samples are incubated with streptavidin conjugated dye alone (**Fig 3.1 C,D**) or when the samples are pre-digested with a polyP-specific yeast exopolyphosphatase (**Fig 3.1 E,F**).

PPXbd staining reveals substantial polyP in blood vessel adventitia

As a first step in using biotinylated PPXbd to study polyP localization in other potential tissues of interest in the circulatory system, we obtained frozen sections of normal mouse aortas and stained them according to the same protocol as was used to stain polyP granules in the RBL-2H3 cell line. Stained aortas revealed robust polyP staining in the adventitia, which is absent after pretreatment of the samples with exopolyphosphatase (**Fig 3.2**).

DISCUSSION

The recent burst of interest in studying the role of polyP in higher organisms has been hampered by a lack of polyP-specific methodologies. Here we present a novel biotinylated version of the recombinant polyP binding PPXbd protein. This protein is easy to produce in large quantities and the fact that it is site-specifically biotinylated via the AviTag peptide sequence makes it ideal for sensitive, specific, and replicable detection of polyP in cells and tissue samples.

The polyP staining pattern in RBL-2H3 cells stained via pre-mixed biotinylated PPXbd and streptavidin-conjugated fluorescent dye gave an almost identical pattern as previously published PPXbd staining techniques using a multi-layered PPXbd/anti-epitope tag/secondary antibody approach,[136]

suggesting that the biotinylated PPXbd performs just as well as unmodified PPXbd in binding to polyP. The fact that pre-treatment of samples with an exopolyphosphatase completely abolished the staining further suggests that the biotinylated PPXbd specifically stains polyP rather than other anionic polymers like RNA, DNA, or heparin in the concentrations used in these protocols.

This study also reveals the presence of polyP in the adventitia of large arteries, which to our knowledge is the first report of polyP localization in blood vessels. The presence of abundant polyP in mouse aortic adventitia suggests novel exciting roles for polyP in hemostasis and thrombosis. One interesting note is that the pattern of polyP distribution in the adventitia looks remarkably similar to staining for tissue factor in adventitial fibroblasts.[8] The presence of large amount of polyP localized near tissue factor suggests that it is possible that polyP works to accelerate the clotting process during vascular injury. This could help explain why a complete lack of polyP leads to deficiencies in both thrombosis and hemostasis in mice,[192] although the fact that polyP inhibitors seem to target thrombosis much more heavily than hemostasis[163] suggests that the role and mechanism of action of adventitial polyP could be different than platelet polyP. Investigations of the size and concentration of the polyP found in adventitial cells will also be useful in determining the role of this new source of polyP in physiology and in potential pathological conditions such as vascular injury or atherosclerosis.

While this study has been mostly concerned with the validation of polyP staining by biotinylated PPXbd and some new insights in the localization of polyP in the circulatory system, there are obviously many exciting future avenues of research with this technique. One would be an overall survey of normal mouse and human tissues to determine the extent and relative abundance of polyP in various cells, tissues, and organs. Next, there is the question of whether the amount of polyP in cells and tissues changes in states of infection, inflammation, cancer, or any other number of pathological states, which could give us an idea of potential therapeutic roles and/or side effects of polyP-inhibitor based therapeutics.[163] Finally, while the studies mentioned here have focused on the use of biotinylated PPXbd

as a method for staining polyP in cells and tissues, there are many other possible uses for a biotinylated polyP binding protein in research into the role of polyP in biology. For instance, the biotinylated PPXbd could possibly be attached to an agarose resin and used to purify polyP from biological samples, or it could be used with enzyme-conjugated streptavidin in an ELISA style assay to specifically detect polyP captured from biological samples by some other method. As our knowledge of and interest in the role of polyP in biology continues to grow, so too will the "toolbox" of polyP detection, quantification, and modification methods, such as with the novel biotinylated PPXbd protein described here.

CHAPTER 4: INHIBITION OF POLYPHOSPHATE AS A NOVEL STRATEGY FOR PREVENTING THROMBOSIS AND INFLAMMATION[c]

INTRODUCTION

Polyphosphate (polyP) is a linear polymer of inorganic phosphate residues that is widely present in biology.[131] Of particular interest to hematology, polyP accumulates in many infectious microorganisms[134] and is secreted by activated human platelets[135] and mast cells.[136] Work from our laboratory and others has shown that polyP is a potent procoagulant, prothrombotic, and pro-inflammatory molecule,[121, 139, 214] acting at 4 points in the clotting cascade: it triggers clotting via the contact pathway,[139, 141, 217] it accelerates factor V activation,5 [139] it enhances fibrin clot structure,[202, 203] and it accelerates factor XI back-activation by thrombin.[199]

The ability of polyP (especially, long-chain polyP of the type found in microorganisms[141]) to trigger clotting via the contact pathway is interesting in light of an elegant series of studies that have shown that the contact pathway is important for thrombosis but dispensable for hemostasis.[114, 161, 218, 219] We therefore hypothesized that polyP inhibitors might act as novel antithrombotic/anti-inflammatory agents with reduced bleeding side effects. Raising antibodies against polyP is unlikely to be successful because of the ubiquity of polyP and its simple structure. Phosphatases, such as alkaline phosphatase, can digest polyP,[121, 199] but they take time to act and may degrade other phosphate-containing molecules in addition to polyP. In this study, we identify a panel of polyP inhibitors including cationic proteins, polymers, and small molecules. We report their effectiveness as anticoagulants in vitro and as antithrombotic and anti-inflammatory agents *in vivo* using mouse models. We also compare the effectiveness of these polyP inhibitors against the procoagulant activity of RNA[120] and the anticoagulant activity of heparin. This study therefore provides proof of principle for polyP inhibitors as novel

[c] This chapter has been adapted from a research article published in the Journal *Blood* and used in accordance with the publisher's copyright privileges for publication in a dissertation thesis. Full Citation: Smith SA, Choi SH, Collins JN, Travers RJ, Cooley BC, Morrissey JH. Inhibition of polyphosphate as a novel strategy for preventing thrombosis and inflammation. Blood. 2012;120(26):5103-10.

antithrombotic/anti-inflammatory agents that are directed against a unique target in the blood clotting system.

METHODS

Materials

Reagents were from Sigma-Aldrich unless otherwise noted. Long-chain synthetic polyP (marketed by Sigma-Aldrich as "phosphate glass, water insoluble") was differentially solubilized as previously described.[141] Its polymer lengths ranged from ~50-1500 phosphates, with a modal length of 650 phosphates,[141] and its endotoxin content was 1.6 x 10^{-3} units/μg polyP (by Limulus assay; Charles River Laboratories). Biotinylated long-chain polyP was prepared as described.[140] All polyP concentrations in this paper are given in terms of the concentration of phosphate monomers (monomer formula: $NaPO_3$). Other supplies included human platelet factor 4, antithrombin, plasma kallikrein, factor Xa, and α-thrombin (Enzyme Research Laboratories); human factor XI (Haematologic Technologies); pooled normal plasma (George King Bio-Medical); and Sar-Pro-Arg-p-nitroanilide (Bachem). Recombinant polyP-binding domain from *Escherichia coli* exopolyphosphatase (PPXbd) was produced as described.[199] Liposomes made by sonication had 10% phosphatidylserine, 40% phosphatidylethanolamine, and 50% phosphatidylcholine (Avanti Polar Lipids). Recombinant human tissue factor was relipidated as described.[220]

Inhibition of polyP binding to thrombin

Other than the high-throughput screens, thrombin binding to immobilized biotinylated polyP in streptavidin-coated, 96-well microplates was performed essentially as previously described.[140] Briefly, 35nM human thrombin was incubated with candidate inhibitor in 20mM HEPES NaOH, pH 7.4, 50mM

NaCl, 0.1% BSA, 0.05% Tween-20, 0.05% NaN_3 for 1 hour in wells containing biotin-polyP. After washing, thrombin was quantified by cleavage of 400 µM Sar-Pro-Arg-p-nitroanilide (Bachem).

High-throughput screening assay

High-throughput screens were conducted at the High-Throughput Screening Facility (HTSF) at the University of Illinois. High-binding 384-well plates (Corning) were coated overnight at room temperature with 50 µL/well of 10 µg/mL avidin (Invitrogen) in water, then washed twice with 100 µL/well of TBS 50mM Tris-HCl buffer, pH 7.4, 100mM NaCl, 0.05% NaN_3) containing 0.05% Tween-20. Biotinylated polyP was then immobilized on the wells (and, in the process, the wells were simultaneously blocked with BSA) by incubating the wells for 3 hours at room temperature with 50 µL/well of 20 µM biotin-polyP in TBS plus 1% BSA and 0.05% Tween-20. The wells were washed twice with 100 µL/well of 1M LiCl, followed by 2 water washes. Each well then received 60 µL of storage buffer (50mM Tris-HCl buffer, pH 7.4, 0.05% NaN3), and the plates were stored at room temperature until needed. Thrombin-binding assays were performed by removing the storage buffer and dispensing 50 µL/well of 40nM bovine thrombin (BioPharm Laboratories) in 20mM HEPES-NaOH buffer, pH 7.4, 50mM NaCl, 1.4mM $CaCl_2$, 0.5mM $MgCl_2$, 0.05% Tween-20, 0.05% NaN_3, 0.1% BSA. The wells then received 100-nL aliquots of compounds to be tested. (To decrease the number of plates screened, 5-7 compounds were pooled (always within libraries) and added per well, at 100 nL of each compound per well. Final concentrations in test wells were 1 µg/mL of each compound for the Chembridge compounds, or 2 µM of each compound for the NCI/Marvel/HTSF compounds.) Some wells received no compounds, which served as reference wells for the level of thrombin bound in the absence of any inhibitor. The plates were incubated for a minimum of 30 minutes (maximum of 3 hours) at room temperature, after which they were washed thrice. Each well then received 50 µL/well of 0.4mM chromogenic thrombin substrate (Sar-Pro-Arg-pNA) diluted in 20mM HEPES-NaOH buffer, pH 7.4, 0.05% NaN_3. The wells were

incubated for 1.8 hours at room temperature, after which the reaction was quenched with 25 µL/well of 0.1N HCl, and the absorbance at 405 nm was quantified. (Control experiments indicated that the rate of chromogenic substrate hydrolysis remained linear over the 1.8-hour time course, under the conditions tested.)

Compound libraries screened

Detailed descriptions of all 4 of the libraries screened in this study are available at HTSF web site (http://scs.illinois.edu/htsf/compound_collections.html), including comprehensive structural information files for the compounds in each library, readable by the ChemBioFinder program. The libraries screened in this study, which together included ~175,000 compounds, were: (1) ChemBridge MicroFormat Library (~150,000 compounds); (2) HTSF House Library (~4,700 compounds); (3) Marvel Library (~10,000 compounds); and (4) NCI Library, composed of (a) Open Set (~8000 compounds), (b) Diversity Set (~2,000 compounds), and (c) Natural Products and Challenge Set (~300 compounds).

Inhibition of heparin-catalyzed inactivation of factor Xa by antithrombin

Antithrombin (120nM), unfractionated heparin (1.5×10^{-2} units/mL), and candidate inhibitor were incubated at room temperature for 2 minutes with 4.6 nM human factor Xa in 30mM HEPES NaOH, pH 7.4, 100mM NaCl, 0.1% BSA. Factor Xa activity was quantified by hydrolysis of 250 µM Spectrozyme Xa substrate (American Diagnostica) and converted to percent heparin activity by reference to a standard curve.

Plasma clotting assays

Plasma clotting times were quantified at 37°C using a STart4 coagulometer (Diagnostica Stago). Contact pathway tests used final concentrations of 33% plasma, 25 µM liposomes, 41.7mM imidazole,

pH 7.0, and 8.33mM $CaCl_2$. Contact activator, inhibitor, and liposomes were mixed with prewarmed plasma for 3 minutes; then clotting was initiated with $CaCl_2$. Activator concentrations were selected to give 80- to 100-second clotting times: 10 μg/mL long-chain polyP, 10 μg/mL kaolin, 100 μg/mL diatomaceous earth, or 100 μg/mL polyguanylic acid (RNA). Tissue factor clotting tests used 30pM relipidated tissue factor.

Whole blood thromboelastometry

Human blood studies, conducted in accordance with the Declaration of Helsinki, were approved by the University of Illinois Institutional Review Board. Thromboelastometry was performed using ROTEM (Pentapharm) with supplied software (ROTEM Gamma Version 1.1). Non-anticoagulated whole blood was collected via venipuncture (discarding the initial 3 mL) from normal human donors, then immediately transferred to the supplied plastic cups (280 μL per cup) and thoroughly mixed with 20 μL candidate inhibitor in TBS plus either 20 μL 1.7mM long-chain polyP in TBS or tissue factor reagent (Ex-tem, Pentapharm). Final concentrations were 82% whole blood, 0 or 100 μM polyP, and inhibitor as indicated.

In vivo thrombus formation

Animal studies were approved by the Institutional Animal Care and Use Committee of the Medical College of Wisconsin (venous thrombosis) or the University of Illinois (arterial thrombosis). For venous thrombosis, electrolytic injuries were induced on exposed femoral veins of pentobarbital anesthetized C57BL/6 mice, as described.[221] Three to 5 minutes before thrombus induction, rhodamine 6G-labeled platelets (up to 1 x 10^7 per mouse) and Alexa-647–labeled antifibrin antibodies (10-20 μg per mouse) were injected into the jugular vein at volumes up to 100 μL, followed by inhibitor, unfractionated heparin (APP Pharmaceuticals) or vehicle; fluorescence imaging of the thrombus

induction site was then recorded for 60 minutes. Data among groups were analyzed by 1-way ANOVA, with between-group comparisons using P values calculated from posthoc Tukey test. For arterial thrombosis, C57BL/6 male mice (6-8 weeks old) were anesthetized using isoflurane, polyP inhibitors were injected retro-orbitally, the left carotid artery was exposed, and blood flow monitored with a Doppler vascular flow probe (Transonic, 0.5 PSB) connected to a perivascular flow meter (Transonic, TS420). To induce thrombosis, 2 pieces of 1 x 2-mm filter paper (Whatman GB003) saturated with freshly prepared 5% anhydrous $FeCl_3$ in 0.9% saline were applied to the deep and superficial surfaces of the artery. After 5 minutes, the filter papers were removed and the vessel irrigated with saline. Blood flow was monitored from $FeCl_3$ application for 30 minutes or until occlusion, defined as no detectable flow for 1 minute. Flow data were interpreted with LabScribe2 (iWorx Systems).

In vivo vascular leakage

Vascular leakage assays were used to quantify polyP-induced extravasation of Evans blue dye in animal studies approved by the University of Illinois Institutional Animal Care and Use Committee. Wild-type ICR mice (Harlan Laboratories) anesthetized with isoflurane were injected retro-orbitally with 4% Evans blue in saline (1 µL/g body weight). PolyP inhibitors or saline were administered retro-orbitally (contralateral eye). After 40 minutes, 3 dorsal skin locations were injected intradermally with 25 µL of saline (negative control), 100 µM bradykinin (positive control), or 20 mM long-chain polyP. After 30 minutes, animals were killed, skins removed for punch biopsy (12-mm diameter), and Evans blue quantified as described.[121] Data were compared between groups by Mann-Whitney rank-sum test.

RESULTS

High-throughput screening for polyP inhibitors

We previously showed that polyP binds tightly to thrombin,[222] a central protease in blood clotting. We used this interaction to develop a high-throughput screen for polyP inhibitors by first immobilizing biotinylated polyP on avidin-coated multiwell plates, then incubating wells with mixtures of thrombin and potential inhibitors, washing, and quantifying relative amounts of bound thrombin by chromogenic substrate hydrolysis. Candidate inhibitors were identified from high-throughput screening of a library of ~175 000 small molecules as well as a panel of 42 additional cationic compounds, polymers and proteins chosen for their possible association with a polyanion like polyP. For the latter panel (listed in **Table 4.1**), we hypothesized that cationic substances would bind to polyP, thereby competitively inhibiting its interaction with clotting proteins.

Nine of the tested wells from the initial high-throughput screen of ~175 000 compounds exhibited a ~30% decrease in the rate of chromogenic substrate hydrolysis and were therefore flagged as containing potential inhibitors of thrombin-polyP binding. The 46 individual compounds in these 9 wells were retested singly in secondary screens to identify the actual inhibitors responsible for the reduction in thrombin binding. The secondary screens consisted of: (1) a repeat of the thrombin-polyP binding assay; (2) a kallikrein-polyP binding assay in which 100nM human plasma kallikrein (Enzyme Research Laboratories) was substituted for thrombin and H-D-Pro-Phe-Arg-pNA substrate (Bachem) was used to detect bound kallikrein; (3) a test of direct thrombin inhibition, in which the compound was added directly to 1 nM thrombin in solution, and the rate of chromogenic substrate hydrolysis was quantified; and (4) a test of direct kallikrein inhibition, in which the compound was added directly to kallikrein in solution, and the rate of chromogenic substrate hydrolysis was quantified. The purpose of the parallel assays of both thrombin-polyP and kallikrein-polyP binding was to identify compounds that could inhibit the association of polyP with 2 different polyP-binding proteins, the idea being that this would identify compounds with a general ability to inhibit polyP-protein interactions (presumably via the compound binding to polyP). The purpose of the test of direct inhibition of thrombin and kallikrein

was to identify compounds that decreased the measured signal, not by blocking polyP-thrombin or polyP-kallikrein binding, but by inhibiting the enzymatic activity of these proteases, even in the absence of polyP.

Eight of the tested compounds showed reduced signal in one or more of these secondary assays, the results of which are summarized in **Table 4.2**. Four of the compounds (numbered A, B, D, and G) exhibited < 20% inhibition in the thrombin-polyP binding assay and were therefore not promising leads to explore further. The other 4 compounds in Table 2 (numbered C, E, F, and H) exhibited > 90% inhibition in the thrombin-polyP binding assay. Of these latter 4 compounds, 3 (C, E, and F) inhibited the enzymatic activity of free thrombin by > 98%, one of which (C) also inhibited the enzymatic activity of free kallikrein by 97%. Thus, these 3 compounds are direct protease inhibitors and apparently did not decrease the signal in the thrombin-polyP binding assay by actually interfering with thrombin binding to polyP. One of the compounds, surfen (compound H), decreased the signal in the thrombin-polyP binding assay by 95% and the signal in the kallikrein-polyP binding assay by 55%, while having a modest effect on the enzymatic activity of free thrombin. Thus surfen, which is also reported to be a small-molecule antagonist of heparin and heparan sulfate,[223] was chosen for further analysis. It was perhaps surprising that this relatively large screen identified just a single compound (surfen) that inhibited the binding of both thrombin and kallikrein to immobilized polyP under the conditions tested. A possible explanation is that the screen was performed at rather low concentrations of test compounds (typically, 1 μg/mL), so that only very potent inhibitors could be identified. In addition, the libraries used in this study might not include simple polyamines; and in any case, they did not include polymers or proteins. Given the simple, repeating structure of polyP and its highly anionic nature, cationic polymers and proteins might be expected to bind tightly to polyP and thereby abrogate its procoagulant functions. Accordingly, we screened the additional panel of 42 cationic proteins, polymers, and small molecules for ability to inhibit

polyP-thrombin interactions. The majority of the cationic substances in this panel inhibited thrombin binding to polyP, with the results summarized in **Table 4.1**.

In vitro potency of polyP inhibitors

Potencies of prospective polyP inhibitors were determined using thrombin-polyP binding assays (example inhibition curves in Figure 1). IC_{50} values for the 21 most potent inhibitors are plotted in **Fig 2A** on the basis of both mass and molarity. Of these, surfen was identified from the high-throughput screen and the rest came from the panel of 42 cationic compounds, polymers and proteins. On a mass basis, low molecular weight (MW) polyethyleneimine was the most potent (IC_{50}, 10 ng/mL), whereas the recombinant, isolated PPXbd[224] was the least potent (IC_{50}, 8.5 µg/mL). On a molar basis, poly-L-lysine was the most potent (IC_{50}, 0.49 nM), whereas spermidine was the least potent (IC_{50}, 11.7 µM). Four generations of cationic poly(amido amine) (PAMAM) dendrimers, with ethylenediamine cores and terminal NH_2 groups, all inhibited polyP binding to thrombin. We chose 11 of the inhibitors for further scrutiny for the following reasons (with the compound numbers here in parentheses being the same as those in **Fig 4.2A**): low (inhibitor 1) and high (inhibitor 3) MW polyethyleneimine are among the most potent inhibitors; polybrene (inhibitor 2) is commonly included in prothrombin time clotting tests to inactivate heparin; spermine (inhibitor 4) is an endogenous polyamine that might modulate polyP function; polyP interacts with histone H1 (inhibitor 6) to modulate its procoagulant activities23; surfen (inhibitor 7) is a small molecule antagonist of heparin and heparan sulfate;[223] intravenous protamine (inhibitor 8) is used clinically to reverse heparin anticoagulation;[225] polymyxin B (inhibitor 9) is a clinical antibiotic that targets bacterial lipopolysaccharide (but perhaps polyP is an additional target of this drug, and furthermore, Salmonella lacking polyP kinase exhibit increased polymyxin B sensitivity[226]); platelet factor 4 (inhibitor 10) is secreted from activated platelets and

neutralizes heparin;[227] and PPXbd (inhibitor 11) potently blocks polyP-mediated factor XI activation by thrombin.[199] In addition, cationic PAMAM dendrimers have received much recent attention for nanoparticle formation and drug delivery; we focused on generation 1.0 dendrimer (inhibitor 5; structure given in **Fig 4.3**) because lower generation cationic dendrimers are reportedly less toxic than higher generation dendrimers or amine-functionalized linear polymers.[228] Heparin, like polyP, is a highly anionic linear polymer (although unlike polyP, heparin is strongly anticoagulant via binding to antithrombin). Cationic inhibitors of polyP might also bind to anionic glycosaminoglycans and thus exhibit complex *in vivo* activities. On the other hand, heparin and polyP have different anionic groups (sulfates vs phosphates) with different spacing and charge densities, so a given inhibitor might bind preferentially to one or the other polyanion. **Fig 4.2B** compares IC_{50} values of the 11 selected polyP inhibitors, plotted on the y-axis for potency for abrogating factor Xa inactivation by a mixture of heparin and antithrombin, and on the x-axis for abrogating thrombin binding to polyP. Compounds interacting more potently with polyP than heparin lie above the dotted line, with the most potent and specific polyP inhibitors in the upper left. Spermine was 152 times more potent against polyP than against heparin/antithrombin, whereas polymyxin B, histone H1, polybrene, low MW polyethyleneimine, and PPXbd were 4-7 times more potent against polyP than against heparin/antithrombin. On the other hand, platelet factor 4 was 18 times less potent against polyP than against heparin/antithrombin.

Potency and specificity of polyP inhibitors in clotting assays

We next evaluated the ability of these 11 inhibitors to block polyP-initiated clotting of human plasma. We expected at least some of these inhibitors to be considerably less effective in plasma clotting assays compared with assays using purified proteins because plasma has many proteins and substances that might compete for binding to these candidate inhibitors. In addition, to initiate plasma

clotting, polyP must interact with multiple proteins in the contact pathway, which differ in their affinities for polyP.[140, 199] To investigate inhibitor potency in human plasma, we therefore quantified the concentrations of inhibitors necessary to double the clotting time of plasma triggered by long-chain polyP, compared with clotting times triggered by other agents known to activate the contact pathway, including RNA,[120] powdered kaolin, and diatomaceous earth. Cationic polyP inhibitors might also interfere with downstream clotting reactions (for example, by binding to the anionic lipid, phosphatidylserine); accordingly, we quantified the inhibitor concentration necessary to double the plasma clotting time triggered by relipidated tissue factor, the protein that initiates clotting in normal hemostasis.[229] **Fig 4.2C** shows that, although low and high MW polyethyleneimine and protamine (inhibitors 1, 3, and 8) inhibited polyP-induced clotting, they also significantly prolonged the tissue factor clotting time (confirming the reported anticoagulant effect of protamine[230]). The other 8 inhibitors tested did not significantly prolong tissue factor clotting times at concentrations up to 100 μg/mL (**Fig 4.2C**); of these, generation 1.0 PAMAM dendrimer (inhibitor 5) was the most potent inhibitor of polyP-initiated clotting. Over the concentration range tested, PPXbd (inhibitor 11) inhibited clotting triggered by polyP but not by RNA, kaolin, diatomaceous earth, or tissue factor. Spermine (inhibitor 4) was also a highly specific inhibitor of polyP-triggered plasma clotting, although it had some ability to attenuate clotting triggered by diatomaceous earth. However, because spermine is reported to attenuate platelet aggregation (see "Discussion" for details), we chose not to pursue it as a polyP inhibitor in our in vivo experiments in this study.

Efficacy of polyP inhibitors in whole-blood thromboelastometry

Coagulation of whole blood is more complex than plasma clotting, as it includes contributions from blood cells, including platelets. Consequently, we selected 2 polyP inhibitors (generation 1.0 dendrimer and the antibiotic, polymyxin B) to investigate their effects on polyP-triggered coagulation of

whole blood in vitro, by measuring the viscoelastic properties of the developing clot using thromboelastometry. When clotting was initiated by adding long-chain polyP to whole blood, both generation1.0 dendrimer (**Fig 4.4A**) and polymyxin B (**Fig 4.4B**) prolonged clot formation in a concentration-dependent manner. On the other hand, neither inhibitor, over the same concentration ranges, significantly altered the thromboelastometry profiles of whole blood clotting initiated by tissue factor (**Fig 4.4C-D**).

PolyP inhibitors abrogate the procoagulant activity of platelet polyP

We next investigated the ability of polyP inhibitors to diminish the procoagulant effect of platelet polyP because polyP is known to be secreted by activated platelets.[121, 135] In the first approach, we added polyP inhibitors to freshly drawn human blood, from which we prepared platelet-rich plasma. We then activated the platelets using a thrombin receptor agonist peptide (TRAP) and quantified thrombin generation in real time. In parallel experiments, we triggered clotting by adding tissue factor to the platelet-rich plasma instead of TRAP. Both PPXbd (**Fig 4.5A**) and generation 1.0 dendrimer (**Fig 4.5B**) significantly delayed the onset of thrombin generation (lag time) as well as the time to peak thrombin, with only marginal effects on the peak thrombin levels themselves. In contrast, neither polyP inhibitor significantly altered thrombin generation when clotting was triggered with tissue factor. In the second approach, we examined the ability of releasates from activated human platelets to accelerate factor XI activation by thrombin, which we recently showed was entirely the result of the presence of polyP.[199] All 5 of the tested polyP inhibitors abrogated platelet releasate-dependent factor XI activation by thrombin (**Fig 4.6**); IC_{50} values were: low MW polyethyleneimine, 107 ± 1.7 ng/mL; generation 1.0 dendrimer, 360 ± 13 ng/mL; spermine, 17.1 ± 1.4 μg/mL; PPXbd, 91.7 ± 2.5 μg/mL; and polymyxin B, 128 ± 2.8 μg/mL (mean ± SE; n=4).

Efficacy of polyP inhibitors in a mouse models of venous and arterial thrombosis

PolyP contributes to thrombosis in mouse models.[121] We therefore examined polyP inhibitors in a mouse venous thrombosis model driven by electrolytic injury to the femoral vein.[221] Intravenous administration of generation 1.0 dendrimer or polymyxin B inhibited the accumulation of fibrin (F**ig 4.7A**) and platelets (**Fig 4.7B**) in the developing thrombus (as did heparin, provided for comparison). Peak accumulation of these thrombus markers (comparing mean relative intensities 26 minutes after injury) was significantly ($P < .05$) lower for animals treated with dendrimer, polymyxin B, or heparin compared with animals receiving saline. We also examined polyP inhibitors in a mouse arterial thrombosis model driven by $FeCl_3$ application to the carotid artery. Intravenous administration of generation 1.0 dendrimer, low MW polyethyleneimine, or polymyxin B before $FeCl_3$ application reduced or slowed vessel occlusion (**Fig 4.7C**). Log-rank analyses showed that median patency time was significantly prolonged in mice injected with generation 1.0 dendrimer ($P < .01$; $n = 8$), polymyxin B sulfate ($P < .01$; $n = 10$), or low MW polyethyleneimine ($P < .01$; $n=8$) versus mice injected with vehicle ($n = 11$). PolyP inhibitors therefore significantly attenuate both venous and arterial thrombosis.

In vivo anti-inflammatory activity of polyP inhibitors

PolyP injected intradermally in mice induces vascular leakage that is dependent on localized activation of the contact pathway and concomitant bradykinin production.[121] To evaluate whether cationic molecules could inhibit these proinflammatory effects of polyP in vivo, we used a modified Miles vascular leakage assay. Generation 1.0 dendrimer or polymyxin B was administered intravenously to mice along with Evans blue dye. After 40 minutes, polyP or bradykinin was injected intradermally and local vascular leakage detected by extravasation of Evans blue. Generation 1.0 dendrimer significantly abrogated vascular leakage induced by polyP (**Fig 4.7D**; $P < .001$) but not by bradykinin (**Fig 4.7D**; P =

0.504). Results obtained with polymyxin B were highly variable (**Fig 4.7D**) and not statistically significantly different from control animals (P = 0.549).

DISCUSSION

This study demonstrates proof of principle that inhibitors of polyP, including cationic small molecules, polymers, and proteins, can block the procoagulant and pro-inflammatory effects of polyP, both *in vitro* and *in vivo*. Using in vitro clotting assays, the potencies of these inhibitors toward polyP varied considerably, as did their specificities toward polyP compared with heparin, RNA, minerals, or tissue factor. Spermine and PPXbd, in particular, were selective for inhibiting the procoagulant activity of polyP over that of other clotting activators. Spermine was also much more effective at blocking the procoagulant activity of polyP than the anticoagulant activity of heparin/antithrombin. On the other hand, both generation 1.0 dendrimer and polymyxin B, although more potent toward polyP, also significantly reduced the procoagulant activity of RNA and nonphysiologic, mineral-based activators of the contact pathway. Inhibitors such as these may thus have utility as general inhibitors of the contact pathway of blood clotting triggered by anionic polymers and surfaces in vivo. In particular, the generation 1.0 dendrimer was highly effective *in vivo* at reducing severity of venous thrombosis, arterial thrombosis, and polyP-mediated vascular leakage.

The experiments in **Fig 4.5** on real-time thrombin generation in platelet-rich plasma show that both PPXbd and generation 1.0 dendrimer prolonged the lag time to thrombin generation as well as the time to peak thrombin but had no effect on the peak thrombin concentration itself. This nicely reflects our earlier findings on real-time thrombin generation using platelet-poor plasma to which polyP was added. In that study, we reported that polyP shortened the lag time and the time to peak thrombin generation but not effecting the peak thrombin concentration or the endogenous thrombin potential.[139] The fact that we now also report that generation 1.0 dendrimer reduced thrombus size and decreased

fibrin accumulation in murine thrombosis models is consistent with the idea that slowing the kinetics of the thrombin burst can significantly attenuate thrombosis *in vivo*.

Similar to our results in this study with the generation 1.0 dendrimer, Jain et al have very recently reported that a more highly branched cationic PAMAM dendrimer (generation 3.0) inhibited the procoagulant activity of polyP and nucleic acids in vitro, and prevented thrombosis in mice without increasing surgical bleeding.[162] Our finding that spermine, norspermine, and spermidine are potent polyP inhibitors is noteworthy because the naturally occurring polyamines, spermine, spermidine, and putrescine inhibit aggregation of human platelets,[231-237] and systemic administration of polyamines is reported to prevent carotid artery occlusion in a canine thrombosis model.[238] The latter investigators concluded that the antithrombotic activity of polyamines was the result of inhibition of platelet aggregation, although it is tempting to speculate that inhibition of platelet-secreted polyP procoagulant activity may have also contributed to their protective effects. Direct tissue injection of spermine was effective in preventing footpad edema in a rodent model,[239] and spermine administration was neuroprotective in an ischemic brain injury model in rats.[240] Interestingly, brain contains long-chain polyP,[138] and deficiency of contact pathway clotting factors is neuroprotective in mouse models of cerebral artery ischemia-reperfusion.[161] It would therefore be interesting to examine the in vivo utility of polyP inhibitors in brain injury models.

CHAPTER 5: AFFINITY-BASED DESIGN OF A SYNTHETIC UNIVERSAL REVERSAL AGENT FOR HEPARIN ANTICOAGULANTS[d]

INTRODUCTION

Intravenously delivered or injected anticoagulants based on heparin—including unfractionated heparin (UFH), low – molecular weight heparins (LMWHs), and the synthetic heparin pentasaccharide fondaparinux — form one of the most important classes of clinical anticoagulants.[164, 168, 241-244] Heparins are indirect anticoagulants; they bind to antithrombin (AT), a key endogenous anticoagulant, and accelerate the inhibition of activated factor Xa (FXa) and thrombin.[245] UFH was the first heparin approved for clinical use and remains the primary anticoagulant used to treat acute thrombotic events, such as in acute coronary syndrome (ACS), and in procedures requiring extracorporeal circulation (EC), such as cardiopulmonary bypass (CPB) and hemodialysis.[246, 247] Given its biological nature and unpredictable dose requirement in individual patients, UFH infusion must be closely monitored and the dose carefully titrated to achieve the required anticoagulant activity while avoiding bleeding .[165, 248] Nevertheless, bleeding complications have an impact on survival in 1.2 to 3% of patients treated for ACS with UFH. LMWHs have a more predictable dose response and therefore are increasingly used in prophylaxis and treatment of thromboembolic events.[168, 243] Fondaparinux, a selective FXa inhibitor,[249] has superior antithrombotic activity relative to LMWHs[250] and thus can be administered as once – daily subcutaneous injections to treat ACS and venous thromboembolism.[251] The importance of heparins is demonstrated by its combined annual global market of more than U.S. $4 billion.[252]

Neutralization of anticoagulant activity is necessary after major surgical and EC procedures to prevent the risk of fatal hemorrhage.[174, 253, 254] Protamine is the only antidote approved by the U.S. Food and Drug Administration and available to reverse the anticoagulant effects of UFH; thus, protamine is

[d] This chapter has been adapted from a research article published in the Journal *Science Translational Medicine* and used in accordance with the publisher's copyright privileges for publication in a dissertation thesis. Full Citation: Shenoi RA, Kalathottukaren MT, Travers RJ, Lai BF, Creagh AL, Lange D, Yu K, Weinhart M, Chew BH, Du C, Brooks DE, Carter CJ, Morrissey JH, Haynes CA, Kizhakkedathu JN. Affinity-based design of a synthetic universal reversal agent for heparin anticoagulants. *Science translational medicine*. 2014;6(260):260ra150.

used in every CPB procedure[254] despite its reported toxicities and life-threatening complications.[255-258] Furthermore, protamine has an unpredictable dose response and narrow therapeutic window, only partially reverses the activity of LMWHs,[169] and has no antidote activity against fondaparinux.[259] The ineffectiveness of protamine and lack of alternate antidotes for fondaparinux and LMWHs limit their use for treatment of thrombotic events despite their superior bioavailability, safety, and predictability relative to UFH.[251, 260]

These concerns together with the incidence of hemorrhage associated with heparin treatment are motivating the development of improved anticoagulation-reversal strategies. Although several heparin antidotes have been tested, including small molecules, cationic peptides, and cationic polymers, all have experienced only limited or no clinical success.[261-263] Moreover, most of these approaches were ineffective toward LMWHs and fondaparinux, and the cationic molecules exhibit high toxicities at the desired therapeutic dose.[264] In addition, thromboembolic risks associated with recombinant proteins may limit their therapeutic use.[265] Thus, the clinical need for a safe, rapid, predictable, and cost-effective strategy to reliably reverse the anticoagulation activity of heparin-derived therapeutics remains unmet.

Here, we report a unique design strategy based on a multivalent dendritic polymer that led to the development of a fully synthetic universal heparin reversal agent (UHRA) that is safe, economical, and highly effective in reversing the anticoagulant activity of all clinically relevant parenteral anticoagulants. The structural features of the reversal agent were optimized to achieve strong binding to heparins with excellent biocompatibility. Efficacy and safety studies using animal models demonstrated the universal action and superior safety profiles of lead UHRA designs, which outperformed all currently available methods for heparin neutralization.

METHODS

Study design

The aim of the study was to develop a fully synthetic reversal agent for clinically relevant heparin-based anticoagulant drugs and test its efficacy in vitro with human blood samples and *in vivo* using experimental animal models. The *in vitro* experiments were performed with human blood samples collected at the Center for Blood Research, University of British Columbia, using an approved protocol and with written consent from each individual donor. Donors with different blood groups were selected, and the sample sizes were three to five samples (plasma, whole blood, or serum) to perform statistical analysis on the results. Animal experiments were conducted in mice or rats at the Jack Bell Research Centre of the Vancouver General Hospital (Canada), British Columbia Cancer Research Centre (Canada), and University of Illinois (USA) using protocols approved by the respective Institutional Animal Care Committees. Three to five animals per group were selected to perform statistical analysis. The animals were randomly assigned to the study groups on the basis of their body weights, but the experimenter was not blinded to group identity. The animals were housed in special pathogen-free cages and monitored for any signs of mortality and morbidity during the pretreatment and treatment periods.

UHRA synthesis

UHRAs were synthesized in the Kizhakkedathu lab by anionic ring opening polymerization of glycidol and mPEG400-epoxide followed by a post functionalization protocol. Binding interaction of UHRAs with heparins was evaluated using ITC analysis. Neutralization of heparins was studied in human whole blood and plasma using aPTT, TEG, thrombin generation, and chromogenic FXa assays. Blood compatibility of UHRAs and their heparin complexes was examined in human whole blood and plasma using blood coagulation, platelet activation, complement activation, RBC morphology, hemolysis, and thrombin generation assays. *In vivo* heparin neutralization was studied in rats using anti-FXa assay and mouse tail transection model. Dose tolerance of UHRA was assessed in female Balb/C mice by

intravenous administration of escalating doses of UHRA, monitoring the body weights for 29 days, and analyzing the serum LDH levels. Histopathological analysis was performed on mice tissues using H&E staining. Biodistribution and clearance of UHRA and its UFH complex were studied in female Balb/C mice after intravenous injection of tritiated UHRA and measuring the amount of radioactivity in the plasma, organs, urine, and feces by scintillation counting.

Statistical analysis

Unpaired Student's t test or ANOVA analysis followed by Dunnett's test was used for the statistical analysis of the data, and results are presented as either means ± SD or means ± SEM. A P value of ≤ 0.05 was considered significant. The statistical test used and P values are included in the figures and figure legends.

RESULTS

Design and synthesis of the UHRA

Our efforts began with an examination of the principal reasons why protamine does not completely neutralize the anticoagulant activity of LMWHs and fondaparinux while achieving complete neutralization of UFH activity. Because ion pair–based coulombic attraction is thought to be the energetic driver of the protamine-heparin complex,[266] differences in the charge density and molecular weight (MW) among different heparins will alter their protamine binding affinity and consequent neutralization activity. On the basis of these considerations, we hypothesized that neutralization of all the heparins could be achieved by designing new polymeric architectures that present unique cationic heparin binding groups (HBGs) at densities and spacing so as to achieve high binding affinities. To have clinical use, these scaffolds must also show superior safety at the desired therapeutic concentrations, which is a challenge because conventional cationic macromolecules exhibit

considerable toxicity.[264] This is expected, because cationic macromolecules with high charge density have the potential to bind tightly to a wide range of analytes and surfaces presented in the vasculature, including proteins with low isoelectric point (pI), circulating nucleic acids, and cell membranes. The development of an effective antidote therefore requires the presentation of an array of cationic ligands that have an appropriate affinity to negatively charged heparins (heparins have the highest negative charge density of any biological molecule) in a manner that prevents those same ligands from also showing strong affinity for anionic blood components. Our UHRA design involves the assembly of trivalent cationic HBGs with high charge densities (R) on a dendritic polymer scaffold based on hyperbranched polyglycerol (**Fig. 5.1A**). This scaffold was selected on the basis of a property that permitted control of the MW over a wide range and its excellent biocompatibility.[267] The chains were capped with short polyethylene glycol (PEG), and its density and MW were optimized to generate a protective shell (a brush layer) against nonspecific interactions. Recognizing that the PEG shell disfavors binding of any macromolecular analyte to the cluster of R groups on the UHRA core, the density of the PEG shell was varied to achieve biocompatibility while preserving a binding affinity to heparins that is sufficient to realize UHRA. UHRA constructs were produced via a two-step process: (i) synthesis of the polymer scaffold by the polymerization of glycidol and a-methoxy-w-epoxy PEG and (ii) attachment of HBGs by a post functionalization method (that is, introduction of a functional group onto the polymer chains) that involved tosylation of a portion of the hydroxyl groups, amination using a branched amine, and methylation to produce tertiary amine groups. We anticipated that the scaffold MW, multivalent presentation and density of HBGs, and the length of the PEG shield are the key parameters affecting high-affinity heparin binding[268] and biocompatibility; thus, polymer scaffolds of different MWs and sizes (23, 48, and 116 kD) with varying numbers of HBGs were synthesized (**Fig. 5.1B**). The chemical identity, structure, and purity of UHRAs were determined from nuclear magnetic resonance (NMR) spectroscopy, gel permeation chromatography (GPC), and reverse-phase high-

performance liquid chromatography (HPLC) analyses that demonstrated >99% purity (data not shown). The number of HBGs on the UHRAs was calculated from NMR spectra and conductometric titration data, whereas the surface potentials were equated to the zeta potentials (the electrostatic potential near the surface of a particle) measured in 10 mMphosphate-buffered saline (PBS; pH 7.4). All UHRAs were of narrow polydispersity (1.2 to 1.5, a measure of the molecular weight distribution of a polymer), suggesting that they shared homogeneous structures and their low hydrodynamic size (Rh) relative to a linear polymer of equivalent MW was indicative of a relatively dense, compact architecture in solution (**Fig. 5.1B**). With our synthetic scheme, we expected a random distribution of HBGs on the dendritic scaffold.

Investigation of UHRA-heparin binding interactions by isothermal titration calorimetry

As a first step toward understanding the binding requirements of UHRAs for their universal action, we adapted isothermal titration calorimetry (ITC) technique to determine the affinity of the protamine - UFH complex in PBS at 25°C. Protamine binds UFH with an affinity on the order of 10^6 M^{-1}, providing a useful benchmark for the affinity required for UHRAs to neutralize heparin anticoagulant activity. The binding of heparins to a model compound, MPEG-R (**Fig. 5.1A**), which bears a single HBG attached to a short PEG chain, was used to define avidity effects associated with binding of various UHRAs. The raw ITC data and integrated heats for the binding of fondaparinux to MPEG-R and to one of the UHRAs (UHRA-7) are shown in **Fig. 5.2** and **Table 5.1**. The corresponding data for the binding of other UHRAs to heparins are provided in **Table 5.1**. The binding stoichiometry reported was calculated on the basis of the number of bound MPEG-R or UHRA per weight-averaged MW of heparins. As noted in **Table 5.1**, although ITC provided accurate K_a values for MPEG-R binding to various heparins, the binding was too weak to permit accurate determination of the binding enthalpy and entropy, because the errors in both parameters were commensurate with the regressed values. ITC data revealed that

UHRAs exhibited much stronger binding to heparins in comparison to MPEG-R. For instance, the binding affinities for UHRA-7 interaction with UFH, enoxaparin, and fondaparinux were, respectively, four, two, and three orders of magnitude higher than those for the interaction of these heparins with MPEG-R. Using binding stoichiometries as a guide, we found that UFH bound 16 MPEG-R molecules, but only a single molecule of UHRA-6 or UHRA-7. This observation shows that, energetically, each HBG on the UHRAs bounds UFH more tightly than did the HBG on MPEG-R; indeed, classic enthalpy-entropy compensation was observed.[269]

For a given scaffold MW (23 kD), the binding affinity showed a progressive increase that tracked with the increase in HBG density. UHRA-3, which harbors 4 HBGs, exhibited relatively weak binding toward all heparins, whereas stronger binding and higher exothermic enthalpies were observed as the HBG density was increased. Both the HBG density and MW of heparins influenced the binding stoichiometry for a given UHRA. For instance, UHRA-7 bound UFH with 1:1 stoichiometry, but for fondaparinux, the ratio was 0.3:1, indicating the binding of multiple copies of fondaparinux to UHRA-7. On comparing UHRA-4 andUHRA-7 with 5 and 20 HBGs, respectively, on the 23-kDscaffold, the low HBG density (and therefore wide spacing) onUHRA-4 resulted in weaker binding via multiple pairing of ligands on a single scaffold (2.5 UHRA per UFH).The ability of UHRA-7, through its higher density of HBGs, to bind UFH with 1:1 stoichiometry revealed a much greater degree of negative charge neutralization per binding event and a concomitant two-order magnitude increase in binding avidity. These fundamental ITC studies revealed that a relatively high number and multivalent presentation of HBGs on a blocked scaffold of appropriate size lead to strong avidity effects that create an ability of select UHRAs to bind all clinically relevant heparins with an affinity on par with that for the protamine-UFH complex.

In vitro heparin neutralization and optimization of UHRA

We next investigated, in human plasma and whole blood, the influence of UHRA structure on the anticoagulant neutralization of clinically used heparins with various MWs: UFH (15 kD), the LMWH tinzaparin (6.7 kD), semuloparin (2.3 kD), and fondaparinux (1728 daltons). Higher doses of heparins were used to mimic overdose scenarios. The heparin neutralization activity was tested using activated partial thromboplastin time (aPTT), anti-FXa activity, whole-blood thromboelastography (TEG), and thrombin-generation assays. Our initial comparison was based on the MW of UHRAs (116, 48, and 23 kD) (**Fig. 5.3, A and C**). UFH or tinzaparin (2 IU/ml) was added to human plasma and titrated with increasing doses of UHRA or protamine to determine the neutralization activity as measured by clotting time. All three UHRAs demonstrated dose-dependent UFH neutralization, and complete neutralization was achieved at doses of 0.1 mg/ml. The neutralization activity was retained even at higher concentrations (0.25 mg/ml), unlike what is seen with protamine, which showed a paradoxical anticoagulant effect at concentrations greater than 0.05 mg/ml. UHRAs also completely neutralized tinzaparin activity in contrast to protamine, which was only partially effective (**Fig. 5.3C**). We next evaluated the effect, on neutralization potency, of the number of HBGs decorating the 23-kD scaffold (4 to 24 per polymer) and found that neutralization activity increased with an increase in the number of HBGs (**Fig. 5.3, B and D**). UHRA-3 (with 4 HBGs) was not effective at the concentrations studied, suggesting that five or more HBGs per UHRA molecule are required for neutralization. This is in agreement with ITC data that showed a weak binding between heparin and UHRA-3 (**Table 5.1**).With the increase in the number of HBGs per molecule, heparin neutralization activity was enhanced (**Fig. 5.3, B and D**). For instance, UHRA-6, UHRA-7, and UHRA-8, with 16, 20, and 24 HBGs, respectively, neutralized heparins even at a dose of 0.025 mg/ml. However, HBG densities higher than 20 on a 23-kD polymer scaffold resulted in slight in vitro anticoagulant activity at UHRA concentrations higher than 0.1 mg/ml, suggesting that optimization of molecular structure is critical to achieve maximum efficacy without causing adverse effects on blood coagulation. To investigate the influence of UHRA structure on

fondaparinux neutralization, we initially used a whole-blood TEG assay. Fondaparinux binds exclusively to AT with high specificity compared to UFH and LMWHs; therefore, reversal of fondaparinux binding and anticoagulation activity has been challenging. In the TEG assay, we assessed clot characteristics upon titration of fondaparinux added to whole blood (1.2 IU/ml) with various concentrations of UHRA (**Fig. 5.3E**). Unlike with other heparins, not all UHRAs were effective in neutralizing fondaparinux activity; only UHRA-7, with its high number of HBGs on the 23-kDscaffold, restored normal blood clot properties, as measured by TEG analysis (**Fig. 5.3E**). The fondaparinux-reversal activity of UHRA-7 was further assessed in human plasma with a chromogenic anti-FXa assay, which measures the fondaparinux activity remaining in the plasma by indirectly assessing the activity of FXa using chromogenic substrate CBS 52.44 (Rotachrom heparin). We observed concentration-dependent neutralization of fondaparinux activity with more than 90% neutralization at 0.1 mg/ml and a complete neutralization at 0.2 mg/ml (**Fig. 3G**). In contrast, protamine showed only partial neutralization as reported.[259] The other UHRAs did not exhibit any neutralization effect on fondaparinux, although some of them showed similar or higher association constants and enthalpy of binding relative to UHRA-7 in the ITC study (**Table 5.1**). These findings suggest that the MW of and HBG spacing on the UHRA scaffold play a key role for neutralization of fondaparinux but not in the equilibrium binding of the UHRAs to fondaparinux. We also tested the ability of UHRA-7 to neutralize semuloparin, a hemi-synthetic ultralow molecular weight heparin analog that has been studied for treatment of thrombosis in patients undergoing chemotherapy.[270] TEG studies in whole-blood (**Fig. 5.3F**) and anti-FXa assays in plasma (**Fig. 5.3H**) showed complete neutralization of semuloparin activity (0.75 IU/ml) by UHRA-7. Protamine, on the other hand, neutralized only 70% of the activity of semuloparin as assessed by the anti-FXa assay. Thus, by optimizing the molecular properties of UHRA (MW, branched HBG structure, HBG density and their multivalent presentation, and the PEG shield) and the resulting binding affinities, we have developed a synthetic UHRA for all clinically used parenteral heparins.

In vivo efficacy of UHRAs in animals

We next investigated the efficacy of UHRA-7 by intravenous administration in female Sprague-Dawley rats that were randomly distributed in three groups (n = 5): those that were administered (i) heparins alone (UFH or enoxaparin, 25 IU per rat), (ii) heparins followed by UHRA-7 (3 mg/kg), or (iii) heparins followed by protamine (3 mg/kg). The sequence of events in the experimental design is shown in **Fig. 5.4**. At the start of the experiment, blood was drawn from each animal, and then, either UFH or enoxaparin was administered. Five minutes after heparin administration, the control animals were injected with saline and the other two groups were injected with UHRA-7 or protamine, and the anti-FXa activity in the plasma was measured at various time points after antidote injection. UHRA-7 completely and rapidly neutralized the activity of both UFH and enoxaparin, and the antidote effect was maintained throughout the course of the experiment (**Fig. 5.4, A and B**). Although protamine was effective in completely neutralizing UFH (**Fig. 5.4A**), it could reverse only 60% enoxaparin activity (**Fig. 5.4B**). Thus, the data confirmed that the superior heparin reversal activity of UHRA-7 observed *in vitro* can be effectively translated *in vivo*. We next used a mouse tail transection model to study the heparin neutralization activity of UHRA-7 and any bleeding side effects. UHRA-7 alone did not induce any bleeding in mice when administered at equal and higher concentrations (20 and 50 mg/kg) than protamine (**Fig. 5.4, C and D**). Mice injected with either dose of UHRA-7 did not show any significant differences in bleeding time (P = 0.99 and 0.85) or hemoglobin loss (P = 0.99 and 0.98) compared to saline controls, whereas those injected with protamine had increased bleeding times and hemoglobin loss compared to saline-injected mice. In the heparin neutralization study, UHRA-7 arrested the bleeding induced by all the heparins. Treatment with UHRA-7 (10 mg/kg) at 5 min after administration of UFH or LMWHs significantly reduced the bleeding times and hemoglobin loss compared to treatment with heparin alone (Fig. 4, E and F; $P < 0.0001$). UHRA-7 treatment at a dose of 20 mg/kg also arrested the

bleeding induced by fondaparinux (**Fig. 5.4, E and F**). Together, these results revealed that UHRA treatment alone or excess UHRA in circulation after anticoagulant reversal did not appear to cause bleeding and further demonstrated its potential for the treatment of heparin-related bleeding problems.

Biocompatibility evaluation of UHRAs

Biocompatibility is another critical issue to be addressed if UHRA molecules are to be clinically useful. We systematically investigated the influence of UHRA structure on the compounds' interactions with blood components to arrive at the optimal molecule for clinical use. All of the blood compatibility experiments were performed at a final UHRA concentration of 0.5 mg/ml (higher concentrations were selected to differentiate UHRA designs), which is considerably higher than the required doses for heparin neutralization. Protamine and a polymer construct with similar HBG structure but with primary amine groups were used as controls. The influence of UHRA structure on blood coagulation was investigated by TEG in whole blood and by the thrombin generation assay in PRP.[271] TEG is considered to be closer to in vivo conditions than other clinical coagulation assays because all the blood components are present.[272] The TEG traces for UHRAs were almost identical with that of the saline control, demonstrating that unlike protamine, they did not alter the blood coagulation (**Fig. 5.5A**). The influence of the number of HBG groups per UHRA on TEG coagulation time plotted for different human blood donors (n = 5) (**Fig. 5.5B**) showed no significant differences ($P > 0.05$) between UHRA versus the saline control except for UHRA-8 (with 24 HBGs per scaffold), which was associated with a slight increase in the coagulation time. The significantly prolonged coagulation time relative to the saline control for the control polymer and for protamine ($P = 0.0001$ and <0.0001, respectively) revealed that primary amine groups on HBG may not be useful as heparin antidotes in terms of their biocompatibility. Thrombin generation in the presence of UHRA-7 in pooled PRP (n = 3) (**Fig. 5.5F**) demonstrated a similar profile as that of buffer control. These data demonstrate that UHRAs do not have any procoagulant or

anticoagulant activity at the concentrations studied. Next, we investigated the effect of UHRA structure on complement activation in human serum at 37°C. The total complement consumption by UHRA was quantified with antibody-sensitized sheep erythrocytes (**Fig. 5.5C**) and showed that the UHRAs did not activate complement compared to an EDTA control ($P > 0.05$). In contrast, protamine and the control polymer (which both have $–NH_2$ groups) showed 57 and 25% complement consumption, respectively, observations that support the hypothesis that the presence of tertiary amines in HBG is critical. Platelet activation by UHRAs in human PRP, as determined by measuring the expression of platelet activation marker CD62P (**Fig. 5.5D**), was insignificant compared to the saline control ($P > 0.05$), unlike with protamine ($P < 0.0001$), and the numbers of HBGs did not show an appreciable effect on platelet activation. Similarly, UHRAs did not exhibit hemolytic activity (<3% lysis) (**Fig. 5.5E**) even at a concentration of 5 mg/ml in whole blood, unlike protamine, which caused considerable erythrocyte aggregation (**Fig. 5.5E**). All of these data suggest a high level of biocompatibility for UHRA constructs.

Safety of UHRA in vivo

To further investigate the potential clinical use and safety of the UHRA, we assessed the dose tolerance in female Balb/C mice with single-bolus intravenous injections of escalating doses of UHRA. The mice were monitored over a period of 29 days for changes in their body weights or any signs of acute toxicity. Mice injected with UHRA grew normally during the study period without any signs of toxicity or major body weight loss (**Fig. 5.6A**). The maximum administered dose was 50 mg/kg for UHRA-7 (lethal dose was not reached), and there was no visible toxicity effect. The lactate dehydrogenase (LDH) levels in serum, a measure of necrotic or apoptotic cell damage, also showed no change with injection of UHRA (data not shown), and no abnormalities were observed by necropsy analysis of the organs for any of the injected doses of UHRA relative to untreated control mice. The maximum tolerated dose for protamine was 20 mg/kg (**Fig. 5.6B**), and immediate death of mice was observed after

administration of 30 mg/kg (lethal dose). The safety of UHRA in mice was further confirmed by histopathological analysis of tissue sections from liver, kidney, and spleen collected on day 29 after administration of UHRA-7 (50 mg/kg). The organs were harvested, fixed with formalin, sectioned, stained with hematoxylin and eosin (H&E), and viewed under an optical microscope. There was no detectable abnormality in the tissue structure (no tissue damage, including cell necrosis and disintegration) or leukocyte infiltration (inflammation) in these organs from untreated control mice and mice treated with UHRA-7. Histopathological analysis also showed no tissue damage with protamine (20 mg/kg) administration, which suggests that the immediate death of mice observed at higher protamine doses (30 mg/kg) results from other as yet unknown factors. The biodistribution and clearance of UHRA-4 and UHRA-4/UFH complex were examined in female Balb/C mice by administering intravenously tritium-labeledUHRA-4 (20 mg/kg) and its heparin complex. At different time points, the amount of radioactive UHRA in plasma, organs, urine, and feces was measured by scintillation counting.
There was a progressive decrease in the concentration of UHRA and the UHRA/UFH complex in the plasma with time, and the circulation half-life was about 40min (**Fig. 5.6D**). The accumulation of UHRA or UHRA/UFH complex in vital organs was very low—8% of the injected dose in the liver and 2 to 2.5% in the other organs after 48 hours (**Fig. 5.6, E and F**). This is in contrast to the very high liver accumulation (70 to 90%) observed with conventional cationic polymers such as PAMAM (poly(amidoamine)) dendrimers.[273]

DISCUSSION

We have presented a new design strategy for the development of a fully synthetic, predictable, safe, economical, and highly effective UHRA. Our study revealed that optimization of the polymer structure (MW and PEG shield), the number of HBGs, and their multivalent presentation on the dendritic scaffold are critical for achieving effective binding and universal reversal of heparin anticoagulation

action without compromising the biocompatibility of this polymer therapeutic. We also demonstrated enhanced safety and efficacy for these new agents in mice and rats compared to protamine, the current clinical standard for heparin reversal. Our studies also showed that the scaffold design and spacing of HBGs on the scaffold influence the neutralization of all heparins. Thus, the binding constants measured by ITC were not linearly related to the heparin neutralization, especially in the case of fondaparinux. Although UHRAs can still form ion pairs with sulfate groups on fondaparinux, which are essential for selective binding to AT[274] and, thereby, for reversing anticoagulation activity, the geometries of the various UHRA fondaparinux complexes formed differed from those generated with compounds derived from natural heparin. This is consistent with advanced theories of polyelectrolyte complexes,[275] most notably those that include contributions of the complex's density,[276] which predict that the free energy change for complex formation between a polycation and a weakly charged polyanion (such as fondaparinux) does not continue to become more negative (more favorable) with increasing charge neutralization of (that is, ion paring with) the more weakly charged member of the complex. In such systems, steric and complex density (that is, entropy) factors oppose complex formation in a non-monotonic manner with the average number of ion pairs formed. As a result, binding affinity measured by ITC is no longer predicted to show a linear dependence on the degree of charge neutralization.

The fully synthetic nature ofUHRA-7 avoids the potential for contamination from biological sources, and we anticipate that it also will increase the agent's storage stability. The universal heparin reversal action and low production cost of this agent also make it amenable to clinical translation. However, efficacy in non-human primates or pigs, exploration with arterial or venous thrombosis models, and UHRA immunogenicity must be tested before this material could be taken into the clinic for phase 1 trials. It is also not yet clear how the 40-min plasma half-life of UHRA in mice translates to humans, but on the basis of body mass–to–surface area ratio (37 for human and 3 for mouse),[277] one

can expect a 12-fold increase (~8 hours) in humans. Hence, we anticipate that a single dose of UHRA might be sufficient to neutralize the activity of LMWHs and fondaparinux in humans. Nevertheless, our results point toward the use of this fully synthetic UHRA in high-risk surgical procedures and for treatment of anticoagulant-related bleeding problems. The molecule may also be a potential replacement for protamine, which has numerous limitations and adverse effects. In addition to establishing UHRA's considerable therapeutic potential as an anticoagulant-reversal agent, the design strategy reported here may provide new avenues for diagnostic assays and other macromolecular therapeutics, such as scavengers for prothrombotic and inflammatory anionic macromolecules.[142, 163, 278, 279]

CHAPTER 6: NON-TOXIC POLYPHOSPHATE INHIBITORS REDUCE HEMOSTASIS WHILE SPARING HEMOSTASIS[e]

INTRODUCTION

PolyP's role as an accelerant rather than a required component of the final common pathway of the coagulation cascade makes it an attractive therapeutic target for novel antithrombotics with potentially decreased bleeding risk compared to conventional therapies, all of which target essential enzymes within the coagulation cascade.[204]

Cationic polymers such as polyethylenimine and cationic polyamidoamine (PAMAM) dendrimers make attractive candidates for high-affinity polyP inhibitors, and have proven effective in inhibiting thrombosis and inflammation in mice.[142, 162] These polymers are positively charged due the presence of multiple primary amines, which allows them to bind to and inhibit polyP, but this property can also promote binding to proteins and cell surfaces and thus lead to cellular toxicity, platelet activation, and coagulopathy mediated by fibrinogen aggregation.[280, 281] This severely limits the real-world usefulness of the previously identified polyP inhibitors.

Recently Kizhakkedathu and coworkers developed a family of dendritic polymer-based universal heparin reversal agents (UHRA) as synthetic antidotes to all heparin-based anticoagulants.[282] These UHRAs were designed by assembling multifunctional cationic groups into the core of a dendritic polymer, which are then shielded from non-specific interactions with blood components using a protective layer of short-chain polyethylene glycol (PEG), resulting in increased biocompatibility compared to traditional cationic polymers.

While the development and synthesis of UHRA compounds resulted in the identification of important new heparin reversal agents, we also realized that within the UHRA family of compounds we

[e] This chapter has been adapted from a research article published in the Journal *Blood* and used in accordance with the publisher's copyright privileges for publication in a dissertation thesis. Full citation: Travers RJ, Shenoi RA, Kalathottukaren MT, Kizhakkedathu JN, Morrissey JH. Nontoxic polyphosphate inhibitors reduce thrombosis while sparing hemostasis. *Blood*. 2014;124(22):3183-90.

might find polymer structures that could function as non-toxic polyP inhibitors, since heparin is a highly anionic, linear polymer and thus has some similarities with polyP. Their extremely low toxicity, coupled with the ease with which their chemical composition and pharmacological properties can be varied, makes UHRA compounds ideal candidates for testing and developing this novel class of antithrombotic agents targeting polyP. This study reports the successful identification of UHRA compounds with high affinity for polyP *in vitro*, and which interrupt thrombosis *in vivo*.

METHODS

Synthesis of UHRAs

Chemicals and reagents were from Sigma-Aldrich and used without further purification unless mentioned. Glycidol was purified by distillation under reduced pressure before use and stored over molecular sieves at 4 ^{o}C. ^{1}H nuclear magnetic resonance spectra were acquired in deuterium oxide on a Bruker Avance AV-300 spectrometer. Absolute molecular weights of the polymers were determined by Gel Permeation Chromatography (GPC) on a Waters 2695 separation module fitted with a DAWN EOS multiangle laser light scattering (MALLS) detector coupled with Optilab DSP refractive index detector, both from Wyatt Technology. GPC analysis was performed using Waters ultrahydrogel columns (guard, linear and 120) and 0.1 M $NaNO_3$ (10 mM phosphate buffer) as the mobile phase.

In the first step, a HPG-PEG polymer was synthesized as follows: A three-necked round bottomed flask was cooled under vacuum and filled with argon. To this, 1,1,1-tris(hydroxymethyl)propane (TMP, 0.240 g) and potassium methylate (25 wt% solution in methanol, 0.220 mL) were added and stirred for 30 minutes. Methanol was removed under vacuum for 4 hours. The flask was heated to 95°C and glycidol (2.5 mL) was added over a period of 15 hours. After complete addition of monomer, the reaction mixture was stirred for additional 3 hours. mPEG-epoxide400 (9 mL) was added over a period of 12 hours. The reaction mixture was stirred for additional 4 hours. The

polymer was dissolved in methanol, and twice precipitated from diethyl ether. The polymer was dissolved in water and dialyzed against water using MWCO-1000 membrane for 3 days with periodic changes in water.

The HPG-PEG-10kDa precursor polymer (2.4 g) was then dissolved in 25 mL of pyridine. To this, p-toluenesulfonyl chloride (8 g) was added and stirred at room temperature for 24 hours. Pyridine was removed by rotary evaporation; the polymer was dissolved in 0.1 N HCl and dialyzed overnight. The HPG-PEG-tosylate was isolated by freeze drying. The HPG-PEG-tosylate (2.8 g) and tris (2-aminoethylamine) (8 mL) were dissolved in 1,4-dioxane (25 mL) and refluxed for 24 hours. Dioxane was removed under vacuum and the polymer was dissolved in minimum amount of methanol and precipitated twice from diethyl ether. The polymer was then dissolved in water and dialyzed against water using MWCO-1000 membrane for 2 days. The resulting polymer solution was added to a mixture of formaldehyde (6 mL) and formic acid (6 mL) at 0°C. The reaction mixture was refluxed overnight. After cooling to room temperature, the pH of the solution was adjusted to 10 using NaOH and the polymer was extracted with dichloromethane. Dichloromethane was removed under vacuum; the polymer dissolved in distilled water and dialyzed against water using MWCO-1000 membrane with frequent changes in water for 2 days. The number of binding groups in UHRA 10 (by conductometric titration) was calculated to be 11. ^{1}H NMR ($CDCl_3$, 300 MHz): δ ppm 2.27 (-NCH_3), 2.4-2.7 (-N-CH_2-), 3.38 (-OCH_3 from PEG), 3.4-3.95 (main chain protons from HPG and PEG).

The characteristics of the UHRAs are given below. The number of binding groups on UHRAs was determined by conductometric titration.

UHRA 1: HPG-PEG polymer: PEG content: 35 mol%; Polyglycerol: 65 mol%; GPC-MALLS (0.1 M $NaNO_3$): Mn 116000 g/mol; Mw/Mn 1.2. Number of polyP-binding groups per polymer: 33

UHRA 2: HPG-PEG polymer: PEG content: 33 mol%; Polyglycerol: 67 mol%; GPC-MALLS (0.1 M $NaNO_3$): Mn 48000 g/mol; Mw/Mn 1.45. Number of polyP-binding groups per polymer: 18

UHRAs 3 to 8: HPG-PEG polymer: PEG content: 35 mol%; Polyglycerol: 65 mol%; GPC-MALLS (0.1 M $NaNO_3$): Mn 23000 g/mol; Mw/Mn 1.52. The number of polyP-binding groups per polymer was 4, 5, 11, 16, 20 and 24 for UHRAs 3, 4, 5, 6, 7, and 8 respectively.

UHRA 9: HPG-PEG polymer: PEG content: 32 mol%; Polyglycerol: 68 mol%; GPC-MALLS (0.1 M $NaNO_3$): Mn 16000 g/mol; Mw/Mn 1.8. Number of polyP-binding groups per polymer: 16.

UHRA 11: HPG-PEG polymer: PEG content: 34 mol%; Polyglycerol: 66mol%; GPC-MALLS (0.1 M $NaNO_3$): Mn 9400 g/mol; Mw/Mn 1.34. Number of polyP-binding groups per polymer: 8

UHRAs 12, 13 and 14: HPG-PEG polymer: PEG content: 28 mol%; Polyglycerol: 72 mol%; GPC-MALLS (0.1 M $NaNO_3$): Mn 10000 g/mol; Mw/Mn 1.41. Number of polyP-binding groups per polymer was 2, 5 and 7 respectively in UHRA 12, 13 and 14.

UHRAs 15 and 16: HPG-PEG polymer: PEG content: 32 mol%; Polyglycerol: 68 mol%; GPC-MALLS (0.1 M $NaNO_3$): Mn 4900 g/mol; Mw/Mn 1.4.Number of polyP-binding groups per polymer was 2 and 1 respectively in UHRA 15 and UHRA 16.

Isothermal titration calorimetry

Binding studies were performed using a VP-ITC microcalorimeter from Microcal, Inc. (Northampton, MA) with a cell volume of 1.4 mL at 298K. PolyP ($PolyP_{75}$) and UHRA solutions used for

titrations were prepared in 10 mM phosphate buffered saline (0.137 M NaCl, pH 7.4). Samples were filtered using 0.2 µm filters and degassed prior to addition. Injections of 10µl of UHRA (300 µM) solution were performed from a computer controlled microsyringe at an interval of 5 minutes into 5 µM (estimated polymer concentration based on average polymer size of 75 phosphates) polyP solution in the cell. The heats of dilution from titrations of UHRA solution into buffer only (without polyP) were subtracted from the heats obtained from titrations of UHRA solution into polyP solution to obtain net binding heats. All the experiments were carried out in duplicate. Raw ITC data of UHRA binding to polyP was analyzed with Origin software from Microcal, Inc. (Northampton, MA). The one-site binding model was used to fit the isotherms by a nonlinear least- squares analysis.

UHRA biocompatibility studies

UHRA biocompatibility studies were carried out by the Kizhakkedathu lab. Blood from healthy donors was collected by venipuncture under a protocol approved by the University of British Columbia clinical ethical committee and written consent was obtained from each individual donor. Platelet-rich plasma (PRP) was prepared by centrifuging citrated whole blood samples at 150 x g for 10 minutes. Serum was prepared by centrifuging the blood collected in serum tube at 1200 x g for 30 minutes, one hour after blood collection.

Platelet activation was quantified by flow cytometry. Platelet-rich plasma (PRP) was incubated at 37 °C with UHRA, protamine or PEI (final concentration 1 or 2 mg/mL) in phosphate-buffered saline (PBS) for 1 hour. Five microliters of post-incubation platelet/polymer mixture, diluted in PBS buffer, was incubated for 20 minutes in the dark with 5 µL of phycoerythrin (PE)-labeled monoclonal anti-CD62P-PE (Immunotech). The samples were then stopped with 0.3 mL of PBS. The level of platelet activation was analyzed in a BD FACSCanto II flow cytometer (Becton Dickinson), expressed as percentage of platelet

activation marker CD62-PE fluorescence detected in 10,000 total events counted in gated platelets. PRP from three different donors was used for the analysis and each sample was run in duplicate. Complement activation was measured by CH50 sheep erythrocyte complement lysis assay in human serum. UHRA, PEI or protamine (final polymer concentration of 1 or 2 mg/mL) were added to GVB2+ buffer (CompTech) diluted human serum and incubated for 1 hour at 37°C. Samples were then diluted 1:3 in GVB2+ buffer and incubated with an equal volume of ab-sensitized sheep erythrocytes (CompTech) for 1 hour at 37°C. The reaction was stopped by addition of 300 µL cold GVB-EDTA to each sample. Intact Ab-sensitized sheep erythrocytes were collected at 8000 rpm for 3 minutes and supernatants were sampled. Percentage sheep erythrocyte lysis was calculated using average A540 values.

Comparison of fibrinogen aggregation by PAMAM dendrimers and UHRAs

Turbidity assays were adapted from previous reports of dendrimer-induced fibrinogen aggregation.[281] PAMAM dendrimer generations 1-7, or UHRA compounds 8, 9, 10 or 14, were diluted in TBSC (50 mM Tris-HCl pH 7.4, 100 mM NaCl, 2.5 mM $CaCl_2$, 0.02% NaN3) and added to wells of a 96-well plate. An equal volume of 4 mg/mL human fibrinogen (Enzyme Research Laboratories) diluted in TBSC was added (final fibrinogen concentration of 2 mg/mL) immediately before recording the absorbance at 405 nm every 30 seconds for 30 minutes.

Inhibition of thrombin binding to polyP

Streptavidin-coated 96-well plates (Corning) were incubated with 20 µM biotinylated polyP (monomer concentration, prepared as described[140]) diluted in 50 mM Tris-HCl pH 7.4, 1% BSA, 0.05% NaN_3, and 0.05% Tween-20 for 3 hours at room temperature. Wells were then washed with 1 M LiCl and water and incubated with 40 nM bovine α-thrombin (Enzyme Research Laboratories) plus varying

concentrations of UHRA inhibitors in 20 mM Hepes NaOH pH 7.4, 50 mM NaCl, 1.4 mM $CaCl_2$, 0.5 mM $MgCl_2$, 0.1% BSA, 0.05% Tween-20, 0.05% NaN_3 for 1 hour at room temperature. After washing with 20 mM Hepes NaOH pH 7.4, 0.05% Tween-20, 0.05% NaN_3, the amount of thrombin bound to polyP was quantified by monitoring the rate of cleavage of 400 μM Sar-Pro-Arg-p-nitroanilide (Bachem) in 20 mM Hepes NaOH pH 7.4, 0.05% NaN_3 by measuring A_{405} every 30 seconds for 20 minutes at room temperature in a SpectraMax Plate Reader (Molecular Devices).

Plasma clotting assays

Plasma clotting times were quantified at 37°C using a STart4 coagulometer (Diagnostica Stago). All clotting assays used final concentrations in the clotting reactions of 25 μM liposomes (70:30 phosphatidylcholine:phosphatidylserine), 41.7 mM imidazole pH 7.0 and 8.33 mM $CaCl_2$. A 50 μL aliquot of a solution containing activator (polyP or polyguanylic acid), inhibitor and liposomes was pipetted into a prewarmed coagulometer cuvette, after which 50 μL of prewarmed pooled normal plasma (George King Bio-Medical) was added and allowed to incubate for 3 minutes at 37°C. Clotting was then initiated by the addition of 50 μL of prewarmed 25 mM $CaCl_2$. Activator concentrations of 10 μM long-chain polyP or 25 μg/mL polyguanylic acid (RNA) were chosen to give 60-80 second clotting times without inhibitors.

Animals

C57BL/6 mice were obtained from Harlan Laboratories. All animal procedures were approved by the Institutional Animal Care and Use Committee at the University of Illinois at Urbana-Champaign.

$FeCl_3$-induced thrombosis in mouse carotid arteries

Mice were anesthetized using inhaled isoflurane/oxygen mixture, and UHRA compounds diluted in sterile normal saline were injected retro-orbitally. The left carotid artery was exposed via a midline

cervical incision and blunt dissection, and blood flow monitored with a Doppler vascular flow probe (Transonic, 0.5 PSB) connected to a perivascular flow meter (Transonic, TS420). To induce thrombosis, two 1 x 2 mm pieces of filter paper (Whatman GB003) saturated with freshly prepared 5% anhydrous $FeCl_3$ in 0.9% saline were applied to the deep and superficial surfaces of the artery. After 5 minutes, the filter papers were removed and the vessel irrigated with saline. Blood flow was monitored from $FeCl_3$ application for 30 minutes or until occlusion, defined as no detectable flow for one minute. Mice were then euthanatized by cervical dislocation while still under anesthesia. Flow data were interpreted with LabScribe2 (iWorx Systems). Statistical analyses were performed using GraphPad Prism 5.

Laser-induced thrombosis in mouse cremaster arterioles

Mice were anesthetized with intraperitoneal injection of 125 mg/kg ketamine, 12.5 mg/kg xylazine, and 0.25 mg/kg atropine sulfate. Approximately 10 minutes prior to imaging, fluorescent antibodies against platelets and fibrin were injected via the jugular vein along with either UHRA compounds or saline. One antibody recognized the GPIbβ subunit of the murine GPIb-V-IX complex (rat antibody X649, conjugated to DyLight649, Emfret Analytics) and the other recognized fibrin (mouse anti-fibrin antibody clone 59D8; a generous gift from Hartmut Weiler; labeled with an Alexa Fluor 488 protein labeling kit; Invitrogen).

Anesthetized mice were placed on an intravital microscopy tray and the testis and surrounding cremaster muscle were exteriorized and prepared for microscopy by stretching and pinning the tissue onto a custom-made intravital microscopy stage. The cremaster preparation was superfused with 37°C sterile 0.9% saline throughout the experiment. Fluorescent and brightfield images were captured for 2 minutes following injury, using a 532 pulsed-laser system integrated with image capture and analysis software (VIVO Imaging System with Ablate! Photomanipulation Module, Intelligent Imaging

Innovations). Up to 6 injuries were made per mouse with each subsequent injury upstream of previous ones.

Image analysis of fluorescent platelet and fibrin accumulation

Integrated fluorescence intensity was calculated with Slidebook 5.5 (Intelligent Imaging Innovations) as reported.[283] For each injury, a rectangular area was defined upstream of the injury site including both the vessel and the surrounding tissue. The average maximal values for the Cy-5 (X649, platelets) and fluorescein (59D8-Alexa Fluor 488, fibrin) channels were used as the threshold values to create masks for both platelet and fibrin accumulation. In addition, a small rectangular area was defined completely within the vessel upstream of the injury to serve as a background measurement. Integrated fluorescence intensity at each time point was calculated as (Sum Intensity of the Mask – (Background Intensity*Area of the Mask in Pixels)). Statistical analysis was done by plotting the area under the curve (total fluorescence intensity) for each injury in a given condition and comparing the median values using the Mann-Whitney test. All statistical tests were done using GraphPad Prism 5.0.

Mouse tail bleeding assay

Mice were anesthetized with inhaled isoflurane/oxygen mixture and placed on a heated surgical tray. UHRA compound, heparin, or saline alone was injected retro-orbitally and the tail tip was immersed for 5 minutes in a 15 mL plastic test tube filled with 37°C PBS. The distal 2-4 mm of tail was then transected with a razor blade and re-immersed in 37°C PBS for 10 minutes. Bleeding time was measured with a stopwatch for the entire 10 minutes, after which the blood samples were pelleted at 500 x *g* for 10 minutes at room temperature and the pellet resuspended in 5 mL Drabkin's Reagent (Sigma) and incubated at room temperature for 15 minutes. Amount of hemoglobin lost was quantified

by comparing the absorbance of the samples at 540 nm to a standard curve of bovine hemoglobin in Drabkin's reagent.

RESULTS

Synthesis of non-toxic polyP inhibitors

In order to have clinically useful polyP inhibitors we needed less toxic compounds than the cationic polymers and proteins previously used in proof-of-principle studies.[142, 162] To address this problem, I first obtained a library of UHRA compounds developed and synthesized in the Kizhakkedathu Lab at the University of British Columbia in Vancouver, Canada. The inclusion of a "shell" of short-chain PEG moieties in the UHRA compounds, together with the use of tertiary rather than primary amines, is designed to make these compounds much less toxic than previously-studied polyP inhibitors containing multiple primary amines (**Fig 6.1A**).

UHRA compounds inhibit polyP-thrombin binding and polyP-initiated plasma clotting in vitro

I first screened a panel of UHRA compounds for the ability to inhibit thrombin binding to immobilized polyP, a high-throughput method for identifying polyP blockers.[142] UHRA compounds 1-16 were individually screened in this assay. Eleven of the UHRA compounds had IC50 values ≤ 10 nM for inhibiting thrombin binding to polyP, of which we selected four for further testing: UHRAs 8, 9, 10, and 14, which all inhibited thrombin binding to polyP with IC_{50} values in the 5-8 nM range (**Fig 6.1B, Table 6.1**). The binding was also examined using isothermal titration calorimetry in the Kizhakkedathu lab, which yielded similar results (**Fig 6.2, Table 6.2**).

Because the thrombin binding assay is performed in the absence of plasma proteins that might compete for binding to polyP, I also examined the ability of the four selected compounds to inhibit contact activation in a modified aPTT clotting assay initiated by long-chain polyP (>1000 phosphates per

chain) or polyguanylic acid (RNA). All four compounds doubled the polyP-initiated clotting times in the 50-150 nM range, and the RNA-initiated clotting times in the 1-2 μM range (**Table 6.3**).

Biocompatibility of UHRA compounds compared to previously identified polyP inhibitors

To examine whether the unique structure of the UHRA compounds allowed them to inhibit polyP with reduced toxic side effects, the Kizhakkedathu lab investigated the interaction of UHRAs with blood components in comparison to previously reported polyP inhibitors such as polyethylenimine (PEI) and protamine sulfate.[142] Compared to buffer controls, complement activation was undetectable with UHRAs even at 2 mg/mL (**Fig. 6.3A**). PEI and protamine, on the other hand, strongly activated complement. We also studied platelet activation by measuring CD62P expression in platelet-rich plasma. UHRAs exhibited lower levels of platelet activation (10-15%), compared to protamine and PEI, which activated platelets by about 30% and 100% respectively, when tested at the highest dose (**Fig. 6.3B**).

Cationic PAMAM dendrimers have been identified as proof-of-principle polyP blockers,[142, 162] although they are reported to have significant toxicity, including the ability to cause fibrin(ogen) aggregation and induce a state similar to disseminated intravascular coagulation (DIC).[281] Furthermore, the *in vivo* toxicity of amine-terminated PAMAM dendrimers increases with generation[284] which is unfortunate because their effectiveness in blocking polyP also increases with generation.[142, 162] I examined the ability of UHRAs 8, 9, 10 and 14 versus cationic PAMAM dendrimers (generations 1-7) to induce fibrinogen aggregation (**Fig. 6.4**). Even when tested at 1.5 mg/mL, none of the UHRA compounds showed evidence of inducing fibrinogen aggregation. On the other hand, generation 3 to 7 PAMAM dendrimers caused fibrinogen aggregation at doses from 0.2 to 1 mg/mL.

Next, the Kizhakkedathu lab performed *in vivo* toxicity studies which demonstrated that UHRA 10 was well tolerated in mice after intravenous injection, with no adverse effect up to 200 mg/kg (the maximum injected dose), and essentially identical body weights over a 14-day period relative to saline-

injected control mice (**Fig. 6.5A**). In addition, mice injected with 100 or 200 mg/kg UHRA 10 had serum lactate dehydrogenase (LDH) levels within normal limits (**Fig. 6.5B**). No abnormalities were observed in necropsy performed at day 14, with histopathology analyses showing no evidence of tissue damage, necrosis or inflammation (**Fig. 6.5C**), all consistent with the non-toxic nature of the UHRAs.

UHRA compounds are antithrombotic in two mouse models of arterial thrombosis

To test the antithrombotic effectiveness of UHRA compounds *in vivo*, I employed two mouse models of thrombus formation: laser-induced injury to cremaster arterioles and $FeCl_3$-induced injury to carotid arteries. Initially, 40 mg/kg of UHRA 8, 9, 10, or 14 was administered intravenously to mice after which cremaster arterioles were injured (**Fig. 6.6**). UHRAs 9 and 10 significantly reduced the accumulation of both platelets and fibrin, with UHRA 9 resulting in a 73% decrease in median total platelet fluorescent intensity (**Fig. 6.6 C, F, G**; P = 0.0006) and a 99% decrease in median fibrin total fluorescent intensity (**Fig. 6.6C, H, I**; P = 0.0001) compared to saline control. UHRA 10 was similarly effective, resulting in a 63% reduction in total platelet fluorescent intensity (**Fig. 6.6D, F, G**; P = 0.018) and an 88% reduction in fluorescent fibrin accumulation (**Fig. 6.6D, F, G**; P = 0.0009). While UHRA 8 (**Fig 6.6B**) and UHRA 14 (**Fig. 6.6E**) reduced median platelet total fluorescent intensity by 41 and 60% (**Fig. 6.6F, G**) and median fibrin total fluorescent intensity by 66 and 56% (**Fig. 6.6H, I**) respectively, these decreases were not statistically significant compared to saline controls. We then varied the dose of UHRA 10 to establish its range of effectiveness (**Fig. 6.7**). UHRA 10 significantly reduced median total platelet fluorescence at doses of 20 and 40 mg/kg (**Fig. 6.7C, D, F, G**; P = 0.001 and P = 0.018 respectively) with a maximum inhibition of 73% at the 20 mg/kg dose. Median total fibrin fluorescence was significantly inhibited at doses of 40 and 80 mg/kg (**Fig. 6.7D, E, H, I**; P = 0.0009 and P = 0.0013 respectively), with a maximum inhibition of 94% at the 80 mg/kg dose.

I also examined the ability of UHRA 10 to inhibit mouse carotid artery thrombosis induced by topical application of $FeCl_3$ (**Fig. 6.8**), and found that a dose of 100 mg/kg UHRA 10 performed as well as a dose of 200 U/kg unfractionated heparin, as both treatments significantly increased the median patency time (P = 0.0004 for UHRA 10 and P = 0.007 for heparin). A dose of 200 mg/kg UHRA 10 was as effective as 1000 U/kg unfractionated heparin in completely blocking thrombus formation for 30 minutes.

Antithrombotic doses of UHRA 10 cause less bleeding compared to unfractionated heparin

In order to test if UHRA 10 causes less bleeding than heparin, I used a mouse tail bleeding model to compare treatment with 50, 100, and 200 mg/kg doses of UHRA 10 to treatment either with saline alone or with 200 or 1000 U/kg doses of unfractionated heparin (**Fig 6.9**). Mice treated with a 200 U/kg dose of heparin had significantly longer bleeding times compared to saline controls or mice treated with 50 or 100 mg/kg doses of UHRA 10 (P < 0.0001, Figure 6A). As expected, heparin-treated mice also lost significantly more hemoglobin due to bleeding than did saline-treated mice (P = 0.022, Figure 6B), and although mice treated with 50 or 100 mg/kg UHRA 10 lost less hemoglobin (10.8 ± 2.4 and 7.9 ± 1.4 mg respectively) than heparin treated mice (15.7 ± 4.4 mg), the differences were not statistically significant (P = 0.16 and P = 0.11 respectively). Mice treated with the highest dose of UHRA 10 (200 mg/kg) had significantly shorter bleeding times (P = 0.047), but no significant difference in hemoglobin lost (P = 0.55) compared to mice treated with 1000 U/kg heparin (**Fig. 6.9**).

DISCUSSION

PolyP inhibitors have recently emerged as candidates for antithrombotics with a novel mode of action that differs dramatically from that of conventional antithrombotics.[142, 162] We now report the successful application of a new molecular scaffold for developing antithrombotic agents that target

polyP. UHRAs are dendrimer-like compounds engineered to contain multiple positively charged, branched tertiary amines shielded by a protective layer of short-chain PEG groups. In a library of 16 UHRA compounds containing from 1 to 33 R groups (with each R group containing four tertiary amines), I found that their ability to inhibit thrombin/polyP binding was influenced by the number of R groups in the compound, with the most potent inhibitors requiring the presence of ≥ 5 such R groups. I chose four highly potent UHRA compounds (UHRA 8, 9, 10 and 14; ranging from 7 to 24 R groups per molecule) for more detailed studies. These four compounds strongly inhibited clotting of plasma initiated by both long-chain polyP and RNA (another procoagulant polyanion[120]), with a 12- to 24-fold higher potency toward polyP than RNA.

When I then tested the four UHRA compounds in a cremaster arteriole thrombosis model treatment with all four resulted in lower median levels of accumulation of platelets and fibrin compared to saline-treated controls, although the reductions were statistically significant only for UHRA 9 and 10. UHRA 14 has the same MW as UHRA 10 but has a lower charge density (with 7 R groups in the former and 11 in the latter), and indeed, UHRA 14 was a less effective antithrombotic *in vivo* than UHRA 10. Interestingly, UHRA 8, which was consistently the best polyP inhibitor *in vitro*, did not perform as well as UHRA 9 or 10 *in vivo*.

Higher concentrations of UHRA 10 were needed to inhibit thrombus formation in the carotid artery thrombosis model, a finding consistent with previous studies reporting that complete inhibition of arterial thrombosis caused by injury with 5% $FeCl_3$ necessitates antithrombotic therapy at doses high enough to induce bleeding problems.[285] Laser-induced thrombosis in mouse cremaster arterioles on the other hand has been shown to be sensitive to intervention at more clinically relevant levels of antithrombotic therapy.[283, 286]

In previous[282] and current (**Fig. 6.5**) toxicity studies performed in the Kizhakkedathu lab, UHRAs did not show hemolysis and red blood cell aggregation even at 5 mg/mL while protamine and PEI

induced significant hemolysis. UHRAs compounds also did not show any effect on thrombin generation in human platelet rich plasma and furthermore, UHRAs were well tolerated in mice after intravenous injection with no adverse effect up to 200 mg/kg (the maximum injected dose) *in vivo*. Protamine, on the other hand, was only tolerated up to 20 mg/kg. Biodistribution studies using tritiated UHRA (23 kDa) gave a plasma half-life of about 40 minutes with very low accumulation in vital organs (about 8% of the injected dose in the liver and 2% in spleen, kidney, heart and lung after 48 h) and was cleared mainly via kidney.[282] All these data demonstrated the safety of the UHRAs *in vivo* when compared to the conventional cationic polymers.

This low toxicity profile for UHRA compounds makes them more attractive for clinical use than polyP inhibitors such as PEI, protamine, polymyxin B or PAMAM dendrimers.[142, 162] Polymyxin B has well-documented toxicity in humans.[287] Protamine has demonstrated toxicity as well, including anticoagulant effects in the absence of heparin[288, 289] and ability to precipitate fibrinogen at high concentrations.[290] Cationic PAMAM dendrimers also interact with and precipitate fibrinogen in solution,[281] which was confirmed in this study. UHRA compounds showed no signs of these adverse interactions at concentrations of up to 1.5 mg/mL.

The non-toxic and modular nature of UHRA compounds like the ones investigated in this study makes them attractive candidates for the development of clinical antithrombotic agents with a novel mode of action. While we cannot conclusively say that the antithrombotic nature of these compounds is entirely based on their ability to bind to polyP and inhibit its role in thrombus formation *in vivo*, doses of the compound that are well-tolerated in mice were as effective as heparin in inhibiting thrombosis with less bleeding side effects. While heparin and heparin derivatives are some of the most widely used antithrombotics today, they have well-documented drawbacks that extended even beyond the bleeding risks.[291, 292]

Future generations of the compounds might be developed that have more or less specificity for polyP versus other anionic polymers like extracellular nucleic acids, which have also been implicated in pathological thrombosis.[120, 293] This could lead to a variety of antithrombotic therapeutics that could be used to more efficiently treat the different causes of thrombosis in individual patients. An intriguing possibility along these lines could be the use of polyP inhibitors in sepsis and disseminated intravascular coagulation, where not only platelet polyP but also long-chain polyP from infectious microorganisms might play a role in pathological thrombus formation. Microbial (long-chain) polyP is orders of magnitude more effective than platelet polyP at triggering the contact pathway of blood clotting and can induce multiple inflammatory reactions.[121, 141, 202, 207, 294]

CHAPTER 7: CHARACTERIZATION OF ANTIBODIES RECOGNIZING POLYPHOSPHATE

INTRODUCTION

Inorganic polyphosphate (polyP) is a linear polymer of inorganic phosphates linked together via high energy phosphoanhydride bonds and has been found inside living cells of every domain of life, where it performs many functions that are still being discovered to this day.[134] PolyP chains 60-100 phosphate residues long are located within platelet dense granules and are released on platelet activation, where they accelerate the clotting process by acting as a surface "template" for a number of clotting reactions, as well as activating various inflammatory pathways.[214] Interestingly, infectious microbes also contain polyP, and microbial-sized polyP has been shown to enhance blood clotting and induce inflammation as well or better than platelet-sized polyP.[141] Sepsis is a systemic inflammatory condition caused by microbial infection and often accompanied by a condition known as disseminated intravascular coagulation (DIC), characterized by enhanced coagulation and decreased fibrinolysis.[295] Recent *in vitro* and *in vivo* research suggests that polyP could cause many, if not all, of the inflammatory and procoagulant symptoms of sepsis/DIC, which have previously been attributed almost solely to bacterial lipopolysaccharide (LPS). While LPS clearly plays a major role in sepsis/DIC, DIC is still seen in sepsis cases caused by microbes lacking LPS,[296] and the role of polyP has not been studied in this context.

Current treatments for sepsis/DIC include a combination of anticoagulants like heparin and anti-inflammatory proteins such as recombinant human thrombomodulin and carry a high risk of major bleeding side effects.[297] PolyP inhibitors have been shown to reduce arterial thrombosis (presumably by inhibiting endogenous platelet polyP) with less bleeding risk than clinical doses of heparin, with the added potential advantage of being able to inhibit both microbial and platelet polyP mediated inflammation in sepsis/DIC.[163] One disadvantage of these compounds is their short half-life in plasma however,[282] which might lower their effectiveness during extended bacterial infection and inflammation

that occurs during sepsis and DIC. Novel polyP antithrombotics with a longer half-life (such as anti-polyP antibodies) could potentially target polyP clinically to prevent polyP-mediated contribution to the pathological process of a number of potential diseases, including heart attack, ischemic stroke, sepsis, and DIC, in a safe and effective manner.

Monoclonal antibodies have been one of the mainstays of scientific investigation for many years now, along with playing an increasingly important role as pharmaceutical agents for treating a wide variety of diseases.[298-300] Having antibodies that specifically recognize polyP would be an important addition to both the methodology currently available to study polyP related pathology *in vitro* and *in vivo* and an important addition to the current library of clinically relevant polyP inhibitors. Furthermore, the binding of antibodies to their antigens is very well characterized, and investigating the structure of a polyP-specific antibody could yield important insights into the nature of polyP-protein interactions in general. Unfortunately, conventional antibody development techniques (i.e. immunization of an animal host with a combination of the desired antigen and adjuvant) are unlikely result in the production of an anti-polyP antibody due to the ubiquity of polyP in biological organisms.[134]

The NZBWF1/J strain of mice is a hybrid strain of mice that spontaneously develop a severe autoimmune disease, which is worse in females and increases with age.[301] Over-activation of polyclonal B cells in these mice results in the spontaneous generation of a wide variety of auto-self antibodies, including antibodies to anionic polymers like DNA, and they have long served as a model of systemic lupus erythematosus.[301] In this study, we screen a large panel of monoclonal antibodies isolated from unimmunized aged female NZBWF1/J mice for polyP-binding ability. We then investigate the specificity of the most potent antibody for polyP versus other physiologically relevant anionic polymers and compounds, along with the ability of the anti-polyP antibody to inhibit polyP-mediated coagulation and inflammation *in vitro* and *in vivo*.

METHODS

Screening of monoclonal antibodies for polyP-binding

Purified monoclonal IgGs from hybridomas whose supernatants tested positive for polyP binding ability were a generous gift from the Esmon Laboratory at Oklahoma Medical Research Foundation in Oklahoma City, Oklahoma. Antibodies were diluted to 5 µg/mL in 50 mM Tris-HCl pH 8.0, 0.05% NaN_3, and 100 µL was added to the wells of a medium-binding of a 96-well plate (Corning), and incubated for 1 hour at 37 °C. Wells were then washed three times with 200 µL of wash buffer containing 20 mM HEPES pH 7.4, 10 mM EDTA. Next, 100 µL of 1 µM biotinylated polyP (monomer concentration, prepared as described previously[140]) diluted in 20 mM HEPES, 130 mM NaCl, 5 mM EDTA was added to the wells and incubated for 1 hour at 37 °C. The wells were then washed three times again, and blocked for 1 hour at 37 °C with 20 mM HEPES pH7.4, 50 mM NaCl, 1% BSA, 10 mM EDTA. The wells were washed again three times and 100 µL of 0.1 µg/mL streptavidin-HRP (Thermo Scientific) diluted in 20 mM HEPES pH7.4, 50 mM NaCl, 1% BSA 0.1% thimerosal was added to the wells and incubated for 1 hour at 37 °C. Finally, the wells were washed again three times and 100 µL of TMB substrate (Thermo Scientific) was added to the wells. After 15 minutes, the reaction was stopped with the addition of 2 M sulfuric acid and the absorbance was read at 450 nm to determine the amount of polyP bound in each well.

PP2059 antibody competition testing

Streptavidin-coated 96-well plates (Corning) were incubated with 10 µM biotinylated polyP (monomer concentration, prepared as described previously[140]) in 50 mM Tris-HCl pH 7.4, 0.5 mM EDTA, 5% PEG (MW 8,000), 0.05% Tween-20, and 0.05% thimerosal for 3 hours at room temperature and washed twice with 1 M LiCl and once with deionized water. The size of the chain lengths of the biotinylated polyP ranged from 200-2000 phosphates, with the modal size being 1090 phosphates long. Next, 5 µg/mL (final concentration, diluted in 20 mM HEPES pH 7.4, 100 mM NaCl, 0.5 mM EDTA, 0.5%

PEG (MW 8,000), 0.05% Tween-20, and 0.05% thimerosal) of anti-polyP antibody PP2059 was mixed with varying concentrations of unlabeled polyP of defined chain lengths or other competitors (DNA, RNA, and various glycosaminoglycans) and the mixtures were added to the wells containing biotinylated polyP bound to streptavidin. After a one hour incubation at room temperature, the wells were washed three times with 50 mM Tris-HCl pH 7.4, 0.5 mM EDTA, 0.05% Tween-20, 0.05% thimerosal, and a 1:1000 dilution of goat anti-mouse IgG conjugated to HRP (Thermo Scientific) diluted in 20 mM HEPES pH 7.4, 100 mM NaCl, 0.5 mM EDTA, 0.5% PEG (MW 8,000), 0.05% Tween-20, and 0.05% thimerosal was added to the wells. After one hour incubation at room temperature, the wells were washed again and 100 µL of TMB substrate (Thermo Scientific) was added to the wells. The absorbance at 652 nm was measured after 1 minute.

Preparation of Fab fragments from PP2059

Fab fragments of PP2059 were generated with the Mouse IgG_1 Fab and $F(ab')_2$ Preparation Kit (Thermo Scientific). Briefly, 1 mg of antibody was incubated with 25 mM cysteine and 0.25 mL of ficin-immobilized resin in 0.5 mL of digestion buffer for 5 hours at 37 °C with shaking. The resulting digestion was added to a Protein-A agarose column to remove the Fc columns, and the flow-through was concentrated and stored in PBS at 4 °C.

Plasma clotting assays

Long-chain polyP (10 µM final concentration) was pre-incubated with varying concentrations of PP2059 for 10 minutes at 37 °C. 50 µL of polyP/antibody mixture was added to a coagulometer cuvette and mixed with 50 µL of pre-warmed pooled normal plasma for 3 minutes at 37 °C. Clotting was initiated by the addition of 50 µL of 25 mM $CaCl_2$ and clot time was measured by a STart 4 Coagulometer (Diagnostica Stago).

Lipopolysaccharide (LPS) challenge

LPS challenge studies were performed in the Esmon Laboratory under protocols approved by the International Animal Care and Use Committee at the Oklahoma Medical Research Foundation in Oklahoma City, OK. A combined dose of 20 mg/kg PP2059 or control antibody and 10 mg/kg LPS from *Salmonella enterica* serotype typhimurium (Sigma Aldrich) diluted in PBS was injected retro-orbitally into mice anesthetized with inhaled isoflurane. Survival was monitored once a day for 7 days following injection.

Mouse tail bleeding assay

Tail bleeding assays were performed under protocols approved by the Institutional Animal Care and Use Committee (IACUC) of the University of Illinois at Urbana-Champaign in Urbana, IL. Mice were anesthetized with inhaled isoflurane/oxygen mixture and placed on a heated surgical tray. PP2059 (20 mg/kg), unfractionated heparin (200 U/kg), or saline alone was injected retro-orbitally and the tail tip was immersed for 5 minutes in PBS at 37 °C. The distal 2-4 mm of tail was then transected with a razor blade and re-immersed in 37 °C PBS for 10 minutes. Bleeding time was measured with a stopwatch for the entire 10 minutes, after which the blood samples were pelleted and resuspended in 5 mL Drabkin's Reagent (Sigma). The amount of hemoglobin lost was quantified by comparing the absorbance of the samples at 540 nm to a standard curve of bovine hemoglobin in Drabkin's reagent.

RESULTS

Candidate anti-polyP antibodies bind biotinylated polyP to varying degrees

In order to compare the wide range of potential polyP binding antibodies provided by the Esmon Laboratory, we initially compared their ability to bind polyP head-to-head in a biotinylated polyP

capture assay. This initial screen of monoclonal antibodies generated from unimmunized NZBWF1/J mice showed that a wide variation in polyP-binding ability (**Fig. 7.1A**). Due to its superior signal in initial screening and robust expression of the monoclonal by its hybridoma line, PP2059 was chosen for further study.

Analysis of PP2059 binding to polyP in vitro

To analyze the specificity of PP2059 for various sizes of polyP and for other anionic polymers, I pre-incubated 5 µg/mL PP2059 with differently sized fractions of polyP or other competitors and then determined the ability of those competitors to inhibit PP2059 from binding long chain biotinylated polyP immobilized on streptavidin coated 96 well plates. In these competition assays, shorter chain polyP was not able to fully compete with the antibody's preference for binding to longer chain polyP (**Fig. 7.1B**). At their maximal concentrations (25 times higher than the maximal concentration of biotinylated polyP bound to the well on a monomer basis), polyP size fractions were able to reduce PP2059 to approximately 45% (size range 63-270 mer), 35% (size range 266-510mer), 28% (size range 570-852mer), and 9% (size range 1190-1430mer) of the no-inhibitor control values. Additionally, Fab fragments generated from PP2059 could only reduce PP2059 binding to biotinylated polyP to approximately 40% of control values, even when present in a 150 times greater molar concentration than the intact IgG molecule (**Fig. 7.1C**).

In competition assays with other anionic polymers, the highly sulfated glycosaminoglycan (GAG) heparin was able to reduce the amount of polyP binding to approximately 12% of the control value, while the less sulfated GAGs chondroitin sulfate and hyaluronic acid had little effect (**Fig 7.2A**). The highly sulfated polysaccharide Dextran sulfate was the best competitor, and was able to reduce the amount of PP2059 bound to 7% of the control value at the lowest concentration tested (157 ng/mL). Human genomic DNA and total RNA (from HEK-293 cells) were able to reduce PP2059 binding to

approximately 45% of the control value at the maximal concentrations tested (**Fig 7.2A**). Finally, at very high concentrations (up to 500 µg/mL) LPS from *Salmonella enterica* serotype typhimurium (Sigma Aldrich) was shown to reduce the binding of PP2059 to immobilized polyP to approximately 6% of the control value.

Anticoagulant and anti-inflammatory effects of PP2059 in vitro and in vivo

To examine the ability of PP2059 to inhibit long chain polyP in human plasma, I used a modified activated Partial Thromboplastin Time (aPTT) test where contact activation was initiated with 10 µM long chain polyP as opposed to kaolin or other traditional contact activators. In this model, PP2059 pre-incubated with long chain polyP caused a dose dependent increase in clotting time (**Fig 7.3A**). Next, in a mouse model of sepsis involving challenge with a lethal dose of LPS, a 20 mg/kg dose of PP2059 was able to greatly increase 7-day survival compare to an isotype-control antibody in mice challenged with 10 mg/kg LPS (**Fig. 7.3B**). In order to test the effect of therapeutic doses of PP2059 on hemostasis *in vivo*, we tested the effect of an intravenous dose of 20 mg/kg PP2059 on bleeding time and blood loss in a mouse tail clip model. The 20 mg/kg dose did not significantly increase bleeding time or blood loss in the mice, while a dose of 200 U/kg of unfractionated heparin caused significant increases in both bleeding time and blood loss in this model (**Fig 7.3C,D**).

DISCUSSION

This study details the identification and characterization of monoclonal antibodies generated in an autoimmune mouse strain that bind to polyP and other anionic polymers, and have the potential to be anti-inflammatory and anticoagulant therapeutics. Interestingly, it seems that in the antibody with the highest binding ability, PP2059, the polyP-antibody interaction does not follow some of the "normal" rules for interactions between an antibody and antigen. First, we see that smaller sized polyP

molecules cannot compete with longer chains for binding to PP2059, and the inhibition curves seem to plateau at different maximal amounts of inhibition. (**Fig 7.1B**). If the antibody-polyP interaction was solely based upon binding to a set of phosphates within each chain, then we would actually expect the shorter chains to *better* compete with the longer chains for binding to PP2059, since at a given concentration of monomer phosphate, a size fraction with shorter chain lengths will have a higher "chain concentration" than a size fraction with longer ones (i.e. "chain concentration" = (monomer concentration of phosphate) / (average chain length)). This suggests that there are multiple polyP "binding sites" in the antibody, and that they are only fully satisfied by very long chains of polyP. These binding sites also do not seem to be limited solely to the CDR region of the antibodies either, as demonstrated by the fact that individual Fab fragments of the PP2059 antibody cannot fully compete with intact PP2059 IgG for binding to long chain polyP (**Fig 7.1C**). Together, these data suggest that PP2059 binds to chains of polyP either as some kind of structure (long chain polyP folded into something that can only be recognized by the whole IgG molecule) or that there are polyP "binding sites" located on the Fc region IgG as well (i.e. the polyP wraps around the whole IgG molecule). Also, PP2059's differing interactions with various anionic polymers (**Fig. 7.2A**) suggests that anti-polyP antibodies are able to discriminate between polyP and things like DNA, RNA, and GAGs to a certain extent.

This unique binding of PP2059 preferentially to longer- versus shorter-chain polyP and it ability to inhibit the procoagulant effects of long-chain polyP *in vitro* (**Fig. 7.3A**) make it interesting as a potential therapeutic, since it has been shown that longer-chain polyP is much more procoagulant and proinflammatory than shorter-chain polyP.[141] This longer-chain polyP has been shown to be present in many pathogens,[180] and while much of the recent focus on polyP in mammals has centered around the shorter-chain polyP found in platelets, it has also been shown that mammalian tissues, especially including the brain, can contain large amount of longer-chain polyP.[138] While the fact that PP2059 can increase survival during LPS challenge in mice (**Fig 7.3B**) likely has something to do with its ability to bind

directly to LPS (**Fig 7.2C**), it is also possible that LPS challenge (i.e. sepsis) could cause exposure of the host to large amounts of longer-chain polyP from other sources (including directly from pathogens in sepsis induced by polymicrobial infection). This would explain the ability of anti-polyP antibodies to act as novel anti-coagulant and anti-inflammatory therapeutics in prolonging survival during sepsis.

In summary, the discovery of anti-polyP antibodies in NZBWF1/J mice offers a new development in polyP research. Just from initial screenings, we have identified the polyP binding antibody PP2059 that seemingly binds to its antigen in a method different both from "normal" antibody binding schemes and from any previously characterized polyP-protein interaction as far as we know. With the continuing development of new monoclonal antibodies from this mouse line and perhaps modification of previously identified anti-polyP antibodies (i.e. though phage display or yeast display), we hope to find powerful new tools and potential therapeutics to advance the exciting research in polyP's role in mammalian physiology and pathology.

FIGURES AND TABLES

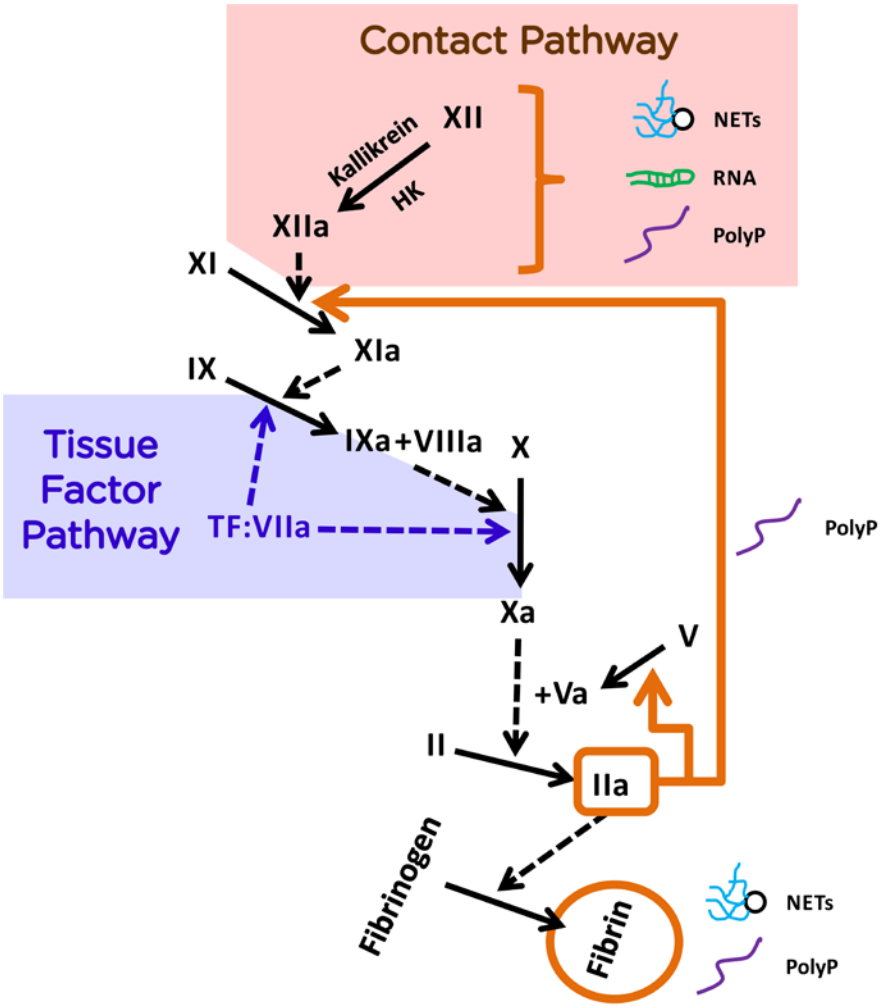

Figure 2.1 Summary of the known ways in which anionic polymers interact with the coagulation cascade. The clotting cascade can be activated by two pathways, both of which are shaded in this image: the Tissue Factor Pathway, which is activated by the complex of factor VIIa and tissue factor (TF); and the Contact Pathway. PolyP, DNA (within NETs), and RNA are novel (patho)physiological activators of the contact pathway of coagulation. PolyP can also enhance certain downstream clotting reactions, including the ability of thrombin (factor IIa) to activate factors V and XI. In addition, both polyP and NETs have been shown to interact with fibrin(ogen) to enhance the strength and stability of the final fibrin clot. Figured prepared by James Morrissey and Richard Travers.

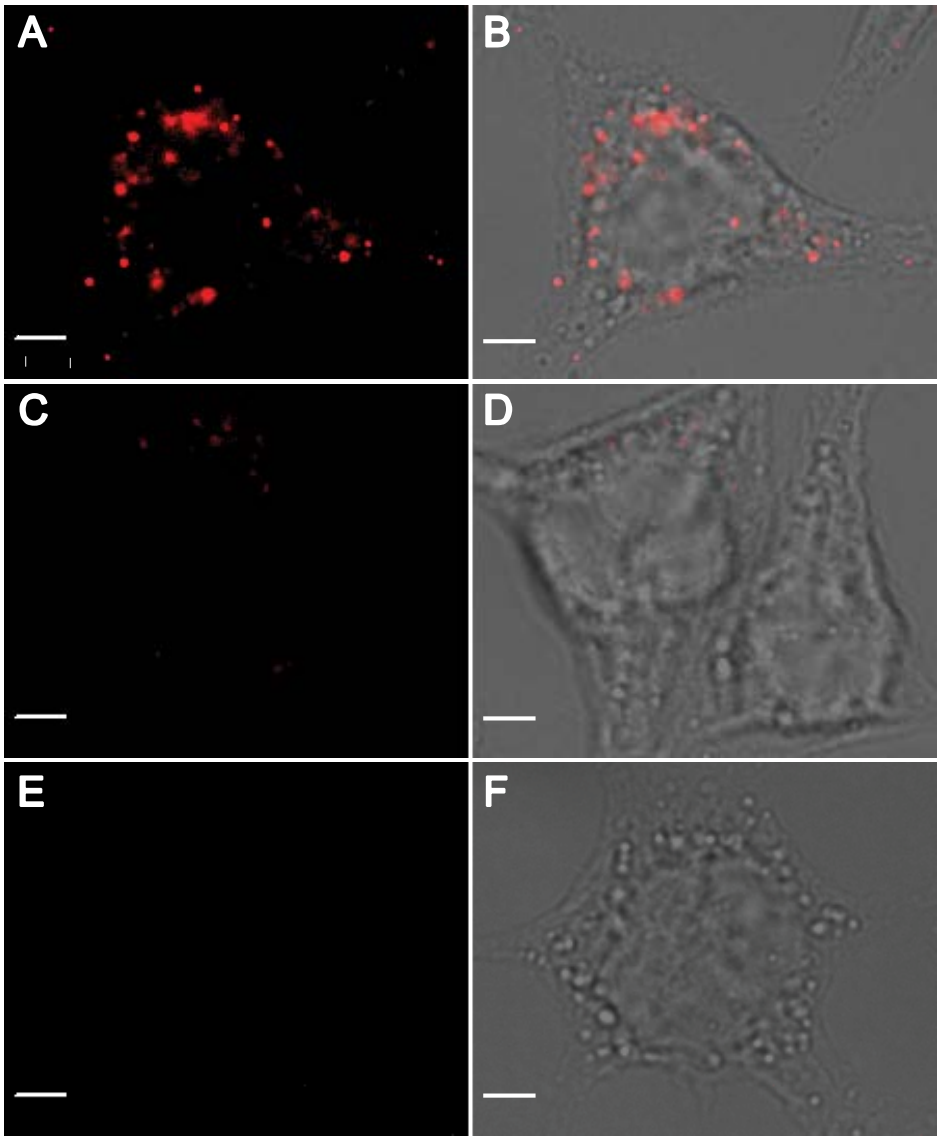

Figure 3.1 Staining of polyP-dense granules in RBL-2H3 cells. (A,B) Fluorescent (A) and overlay of fluorescent on brightfield (B) imaging of RBL-2H3 cells stained with a combination of biotinylated PPXbd and streptavidin conjugated Dylight 650 showing polyP-rich acidocalcisomes. (C,D) Negative controls showed that the granules are not stained if the samples are incubated with streptavidin conjugated dye alone. (E,F) The PPXbd staining disappears if the samples are treated with a yeast exopolyphosphatase after permeabilization but prior to incubation with biotinylated PPXbd and streptavidin conjugated dye. Images are representative of 3 independent experiments, scale bars = 10 µm.

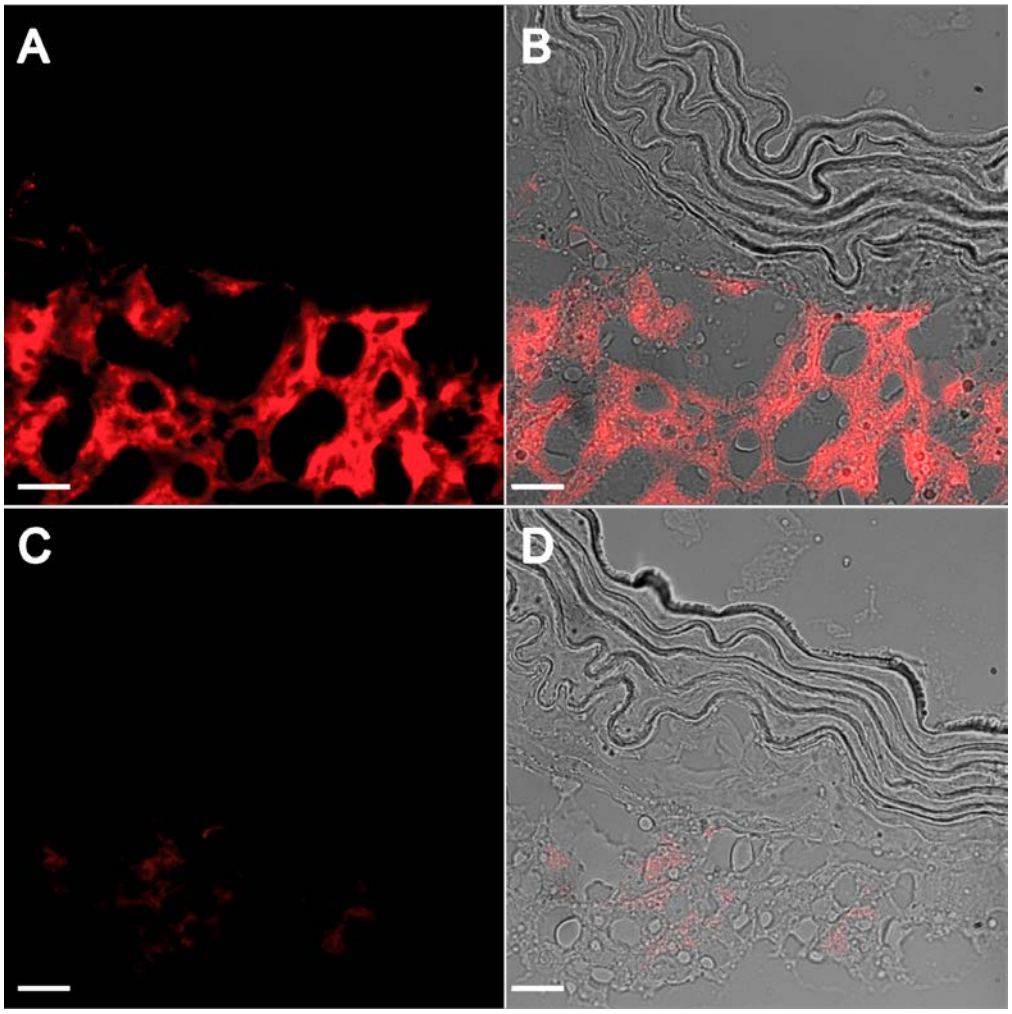

Figure 3.2 PolyP is present in mouse aortic adventitia. (A,B) PPXbd staining reveals abundant polyP staining in the adventitia of a mouse aorta. (C,D) This staining is reduced to background levels after pretreatment of samples with exopolyphosphatase. Images are representative of 3 independent experiments, scale bars = 100 µm.

Table 4.1. Panel of cationic compounds, polymers and proteins

Compound	No.	IC_{50} (or % inhibition)*
Low MW polyethyleneimine	[1]	10 ng/mL
Polybrene	[2]	19 ng/mL
High MW polyethyleneimine	[302]	35 ng/mL
Generation 3.0 Dendrimer		40 ng/mL
Generation 2.0 Dendrimer		47 ng/mL
Norspermine		52 ng/mL
Spermine	[4]	57 ng/mL
Generation 1.0 Dendrimer	[5]	58 ng/mL
Histone H1	[6]	59 ng/mL
Poly-D-lysine		79 ng/mL
Poly-L-arginine		81 ng/mL
Protamine sulfate	[8]	0.11 µg/mL
Poly-L-lysine		0.14 µg/mL
Generation 0.0 Dendrimer		0.14 µg/mL
Heparin		0.27 µg/mL
Polymyxin B	[9]	0.38 µg/mL
Histone H2A/H2B dimer		0.38 µg/mL
Histone H2B		0.46 µg/mL
Histone H3.1/H4 tetramer		0.53 µg/mL
Histone H4		0.84 µg/mL
Colistin		0.91 µg/mL
Histones (mixed)		0.93 µg/mL
Histone H2A		1.3 µg/mL
Spermidine		1.7 µg/mL

Table 4.1 (Continued from page 90)		
Histone H3.1		2.5 µg/mL
Human platelet factor 4	[10]	3.8 µg/mL
PPXbd	[11]	8.5 µg/mL
Lon protease polyP-binding domain		72 µg/mL
1,3-diaminopropane		0.47 mg/mL
Ethylenediamine		0.89 mg/mL
Norspermidine		(62% inhibition at 200 µg/mL)
1,2-bis(3-aminopropylamino)ethane		(53% inhibition at 200 µg/mL)
Kanamycin		(48% inhibition at 200 µg/mL)
DNase I		(36% inhibition at 200 µg/mL)
RNase A		(23% inhibition at 100 µg/mL)
Bacitracin		(12% inhibition at 200 µg/mL)
Methylenediamine		(73% inhibition at 6 mg/mL)
Ammonium chloride		(44% inhibition at 2.7 mg/mL)
Melamine		(0% inhibition at 200 µg/mL)
Cystamine		(0% inhibition at 200 µg/mL)
Histamine		(0% inhibition at 200 µg/mL)
Histidine		(0% inhibition at 200 µg/mL)

Each substance was tested at 200 µg/mL (or indicated concentrations) for inhibition of thrombin binding to immobilized biotin-polyP. Those exhibiting >70% inhibition were retested at varying inhibitor concentrations, from which IC_{50} values were derived (listed here in order of decreasing potency). Numbers in square brackets are the compound numbers used in Figure 2. Data from JN Collins, table preparation by JH Morrissey.

Table 4.2. Secondary screening of eight compounds identified from the high-throughput screen of approximately 175,000 compounds

#	Chemical Name	Library	Concentration tested	Percent inhibition of: Thrombin binding to polyP	Kallikrein binding to polyP	Free thrombin activity	Free kallikrein activity
A.	N-benzyl-2,2,6,6-tetramethyl-4-piperidinamine dihydrochloride	Chembridge	3 µg/mL	0%	0%	36.1%	---*
B.	[(6-nitro-1,3-benzodioxol-5-yl)methylene]malononitrile	Chembridge	10 µg/mL	17.5%	0%	11.1%	2.5%
C.	2-(allylthio)-1-(1,3-benzodioxol-5-ylcarbonyl)-1H-benzimidazole	Chembridge	10 µg/mL	95.1%	81.4%	99.6%	97.4%
D.	N-(2,4-dichlorophenyl)-N'-{5-[(4-nitrophenoxy) methyl]-1,3,4-thiadiazol-2-yl}urea	Chembridge	10 µg/mL	0%	0%	5.3%	1.5%
E.	1-(3,4-dimethoxybenzoyl)-3-(2-furyl)-1H-1,2,4-triazol-5-amine	Chembridge	10 µg/mL	98.6%	18.8%	98.9%	39.3%
F.	5-(benzylthio)-1-butyryl-3-phenyl-1H-1,2,4-triazole	Chembridge	10 µg/mL	92.8%	9.6%	99.5%	12.3%
G.	2-(3- nitrophenyl)-3,1-benzoxazin -4(4H)-one	NCI Open Plate Set	2 µM	2.0%	0%	3.8%	0.6%
H.	Surfen (*bis*-2-methyl-4-amino-quinolyl-6-carbamide)	NCI Diversity Set	2 µM	95.6%	55.3%	32.2%	---*

*not tested

Data from JN Collins, table preparation by JH Morrissey

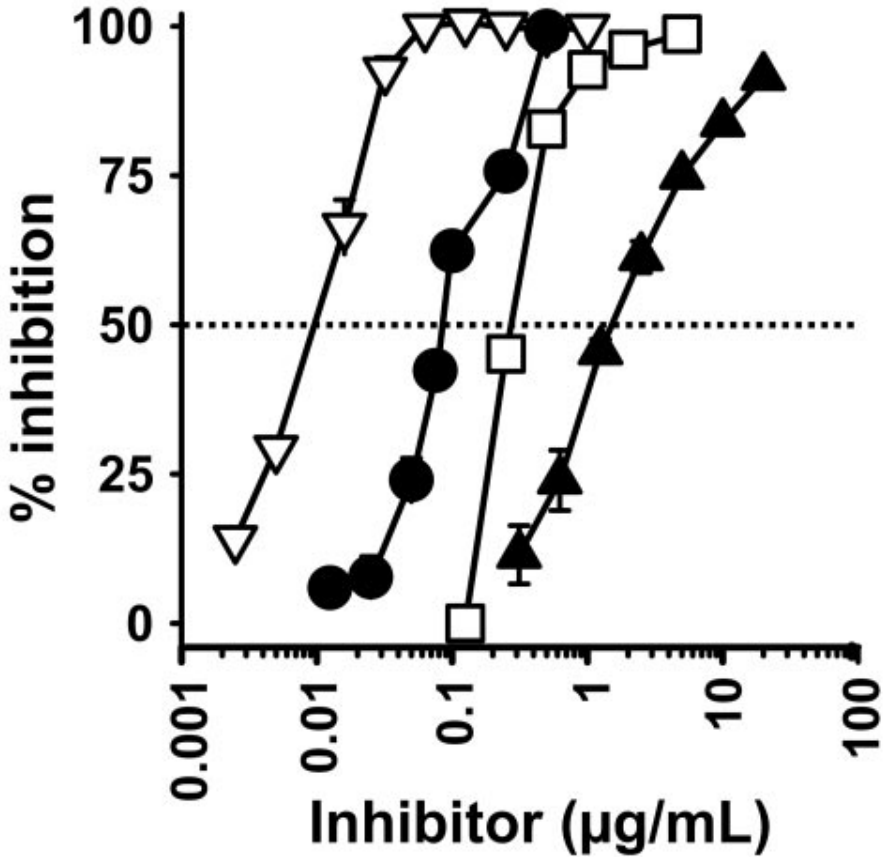

Figure 4.1. Examples of plots of inhibition of thrombin binding to immobilized polyP for 4 selected inhibitors. The percent inhibition of thrombin binding to polyP is plotted for the following inhibitors that encompassed a range of IC_{50} values: low MW polyethyleneimine (open triangles), generation 1.0 PAMAM dendrimer (closed squares), polymyxin B (open squares), and spermidine (closed triangles). The dotted line represents 50% inhibition. Data are mean ± SE (n = 3). Data from JN Collins, figure preparation by SA Smith.

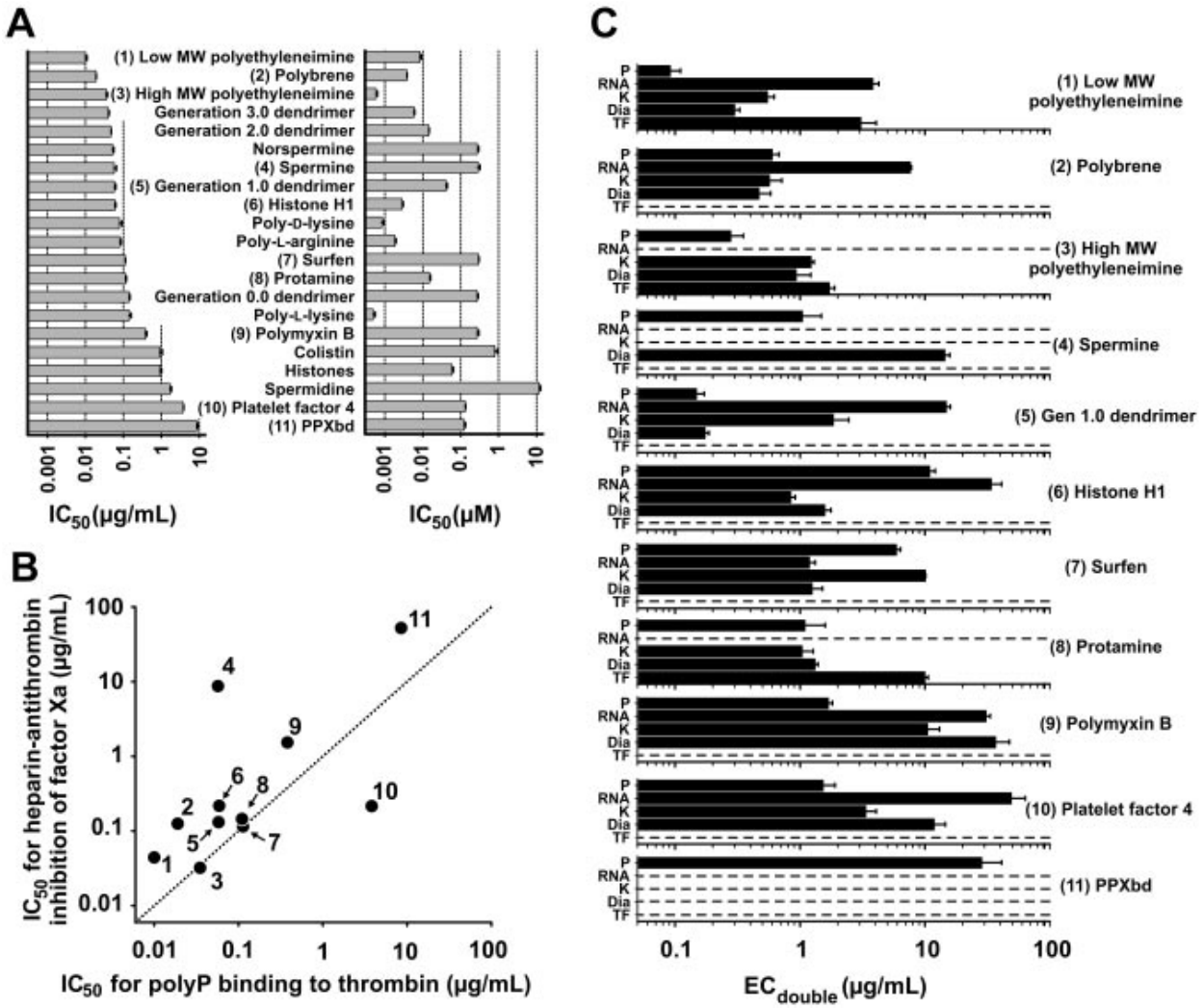

Figure 4.2. Relative potencies of polyP inhibitors. (A) Inhibitor concentrations resulting in 50% reduction of thrombin binding to immobilized polyP (IC50) are plotted for the 21 most potent substances tested, expressed in terms of mass (left) and molarity (right). Inhibitors that were also used in panels B and C are numbered in parentheses. Data are mean ± SE (n = 3). (B) Plot of IC_{50} values of the 11 numbered substances from panel A for inhibition of heparin-mediated inactivation of factor Xa by antithrombin (y-axis) versus inhibition of thrombin binding to immobilized polyP (x-axis). Dotted line represents equivalent potency. Data are mean ± SE (although error bars are within the symbols; n = 3). (C) Effectiveness of polyP inhibitors in prolonging clotting. Clotting of human plasma was initiated by long-chain polyP (P), polyguanylic acid (RNA), kaolin (K), diatomaceous earth (Dia), or tissue factor (TF). Data are mean inhibitor concentrations that doubled the clotting time relative to no inhibitor (EC_{double}) ± SE (n = 4). Horizontal dotted lines indicate that the clotting time with that initiator was either unaffected by the inhibitor or was not prolonged sufficiently to reach a doubling point, even at 100 µg/mL inhibitor. Data from JN Collins, SA Smith, and SH Choi.

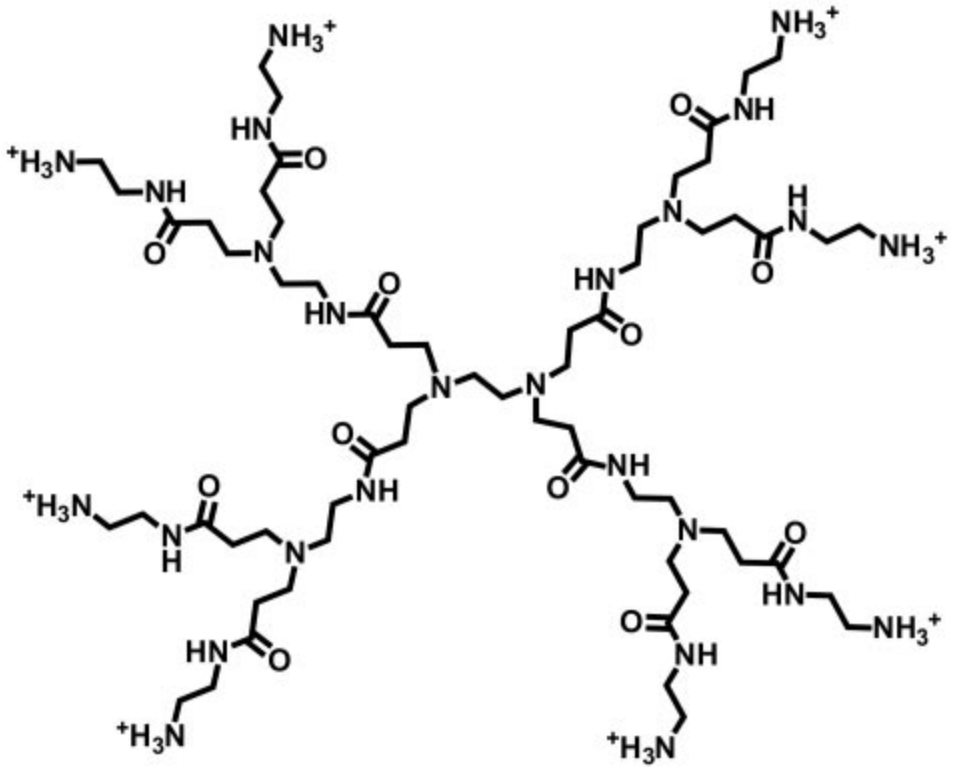

Figure 4.3. Chemical structure of the generation 1.0 cationic PAMAM dendrimer used in this study. Figure by JH Morrissey

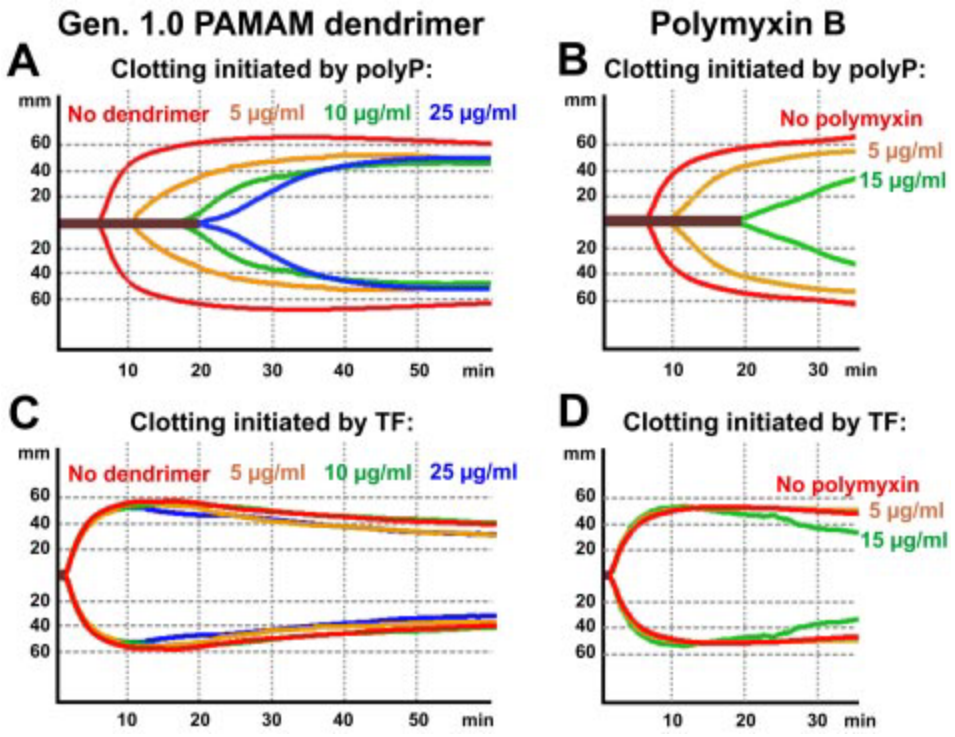

Figure 4.4. Generation 1.0 dendrimer and polymyxin B inhibit clotting of whole human blood initiated by polyP but not by tissue factor. Thromboelastometry (ROTEM) profiles are given for clotting of freshly drawn, nonanticoagulated whole human blood initiated by long-chain polyP (A-B) or tissue factor (C-D), in the presence of generation 1.0 dendrimer (A,C) or polymyxin B (B,D). The x-axis represents time from addition of clotting trigger; and y-axis, amplitude of clot strength. Data and figure by SA Smith

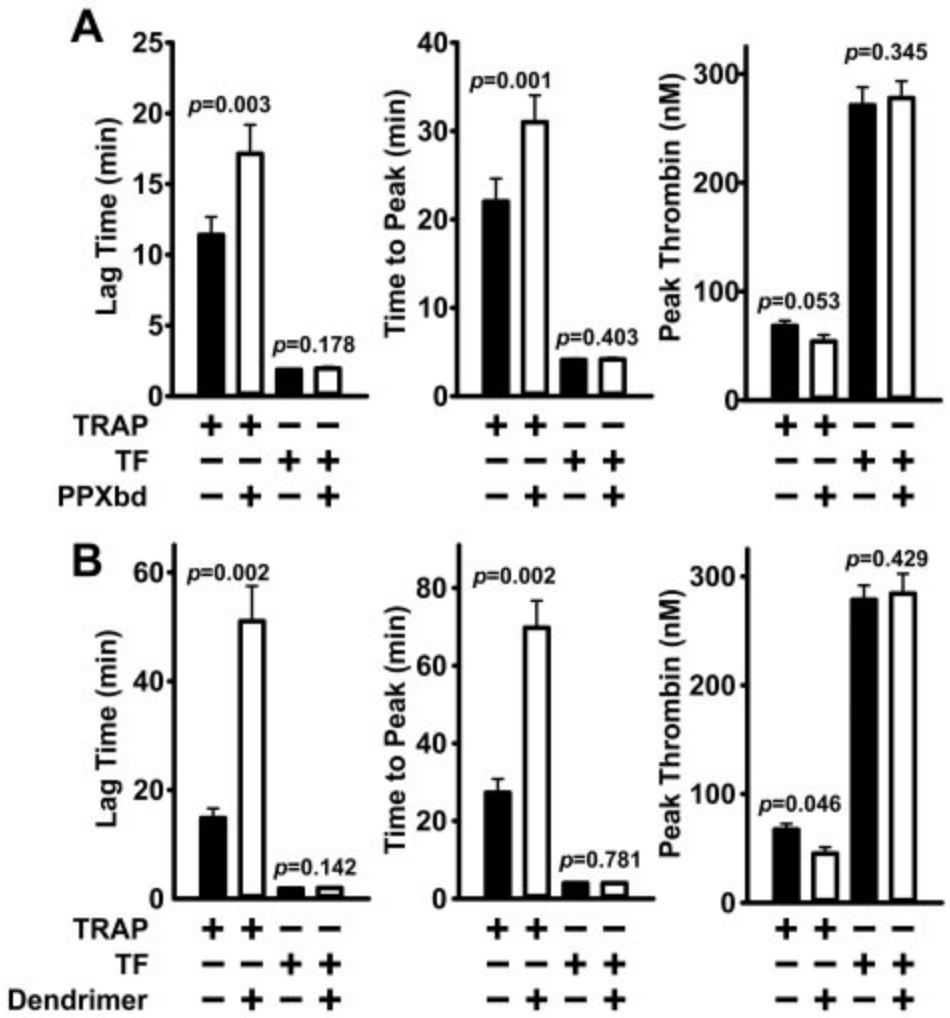

Figure 4.5. Thrombin generation. (A) PPXbd and (B) generation 1.0 dendrimer delay thrombin generation in human plasma containing activated platelets. Real-time thrombin generation in plasma was quantified using calibrated automated thrombogram assays (Thrombinoscope; Diagnostica Stago). PPXbd (500 µg/mL), 20 µg/mL dendrimer, or saline was added to freshly drawn, citrated human blood, from which platelet-rich plasma was prepared and the platelet concentration adjusted to 150,000/µL. To some platelet-rich plasmas, TRAP was added at 10µM to activate platelets. After 5 minutes, FluCa reagent (fluorogenic substrate $CaCl_2$) was added and thrombin generation was quantified. Parallel assays were performed on the same platelet-rich plasmas not pretreated with TRAP, but in which clotting was triggered using FluCa reagent that also contained 5 pM tissue factor (TF). Thrombin generation parameters are plotted as mean ± SE (for 5 donors assayed in triplicate). Indicated P values are from paired t tests with and without inhibitor. Data and figure by SA Smith

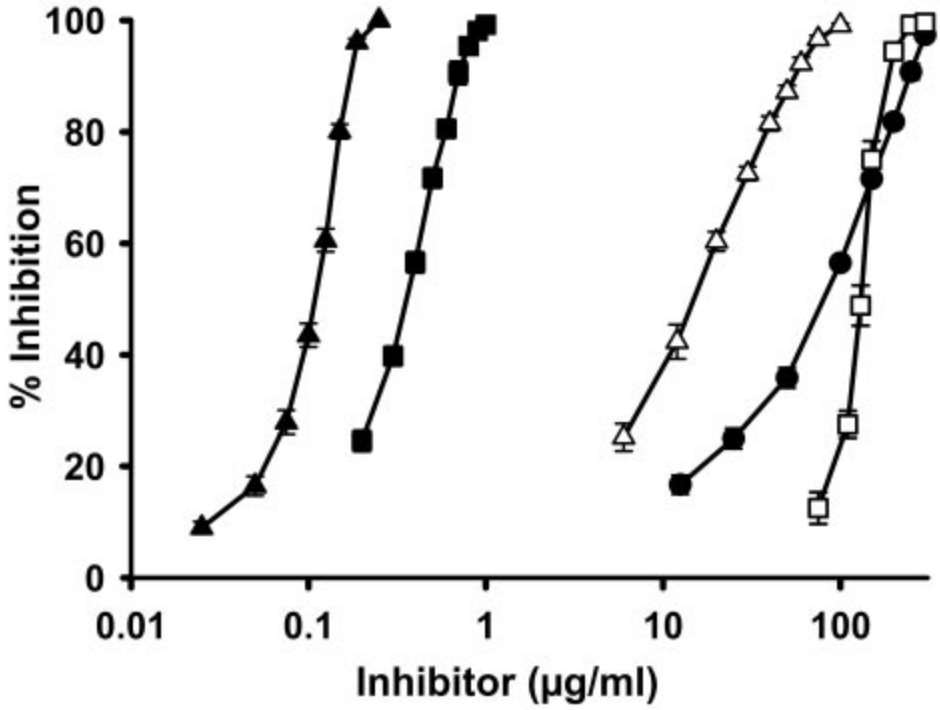

Figure 4.6. PolyP inhibitors reverse the ability of platelet releasates to accelerate factor XI activation by thrombin. Initial rates of activation of 30nM human factor XI by 20nM human α-thrombin were determined in the presence of releasate prepared from TRAP-stimulated human platelets as described, normalized to the rate of factor XI activation without any added polyP inhibitor. Percent inhibition is plotted versus inhibitor concentration for the following: low MW polyethyleneimine (closed triangles); generation 1.0 dendrimer (closed squares); spermine (open triangles); PPXbd (closed circles); or polymyxin B (open squares). Data are mean ± SE (n = 4). IC_{50} values calculated from these curves are given in the text. In the second stage of the assay, factor XIa levels were quantified, as previously described,[199] by monitoring the rate of cleavage of the chromogenic substrate, L-Pyr-Pro-Arg-p-nitroanilide. At the concentrations used, none of the inhibitors altered the rate of hydrolysis of this substrate by factor XIa. Data and figure by SH Choi.

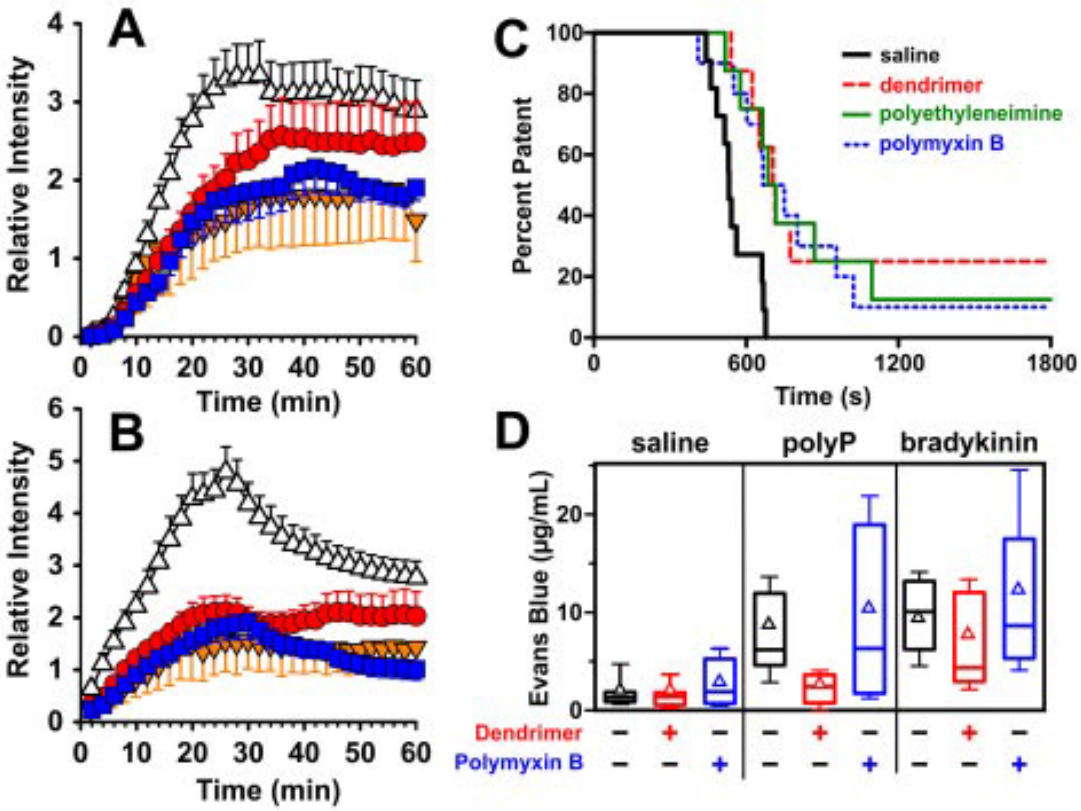

Figure 4.7. In vivo antithrombotic and anti-inflammatory efficacies of polyP inhibitors. (A-B) Murine model of venous thrombosis. Inhibitors were administered intravenously to mice before initiation of electrolytic injury of the femoral vein (time = 0 in the graphs). Data are mean relative intensities for accumulation of fluorescently labeled fibrin-specific antibodies (A) or labeled platelets (B) in the developing thrombus for mice receiving: red circles, 4 µg/g generation 1.0 dendrimer (n = 10); blue squares, 2 µg/g polymyxin B (n = 8); orange inverted triangles, 100 units/kg unfractionated heparin (n = 5); or open triangles, vehicle only (n = 14). Bars represent 1 SE. (C) Murine model of arterial thrombosis, with Kaplan-Meier curves showing percentage of mice with patent arteries. Inhibitors were injected retro-orbitally 10 minutes before ferric chloride injury to the carotid artery. Blood flow was monitored by Doppler, with occlusion defined as no flow for 1 minute. Log-rank analyses indicated that median patency time was significantly longer for mice injected with 8 µg/g generation 1.0 dendrimer ($P < .01$, n = 8), 4 µg/g polymyxin B ($P < .01$, n = 10), or 5 µg/g low MW polyethyleneimine ($P < .01$, n = 8) versus mice injected with vehicle (n = 11). (D) Murine model of polyP-induced vascular leakage. Mice were given separate retro-orbital injections with Evans blue dye and either a polyP inhibitor (48 µg/g generation 1.0 dendrimer or 20 µg/g polymyxin B) or vehicle. After 40 minutes, saline, bradykinin, and polyP were injected intradermally at 3 respective sites on the back. After an additional 30 minutes, mice were killed and dye was extracted from skin biopsies for quantification. Plots show median (central horizontal lines), mean (triangles), 25th-75th percentile (top and bottom of boxes), and 10th-90th percentile (whiskers) concentrations of extracted dye. Dendrimer administration resulted in significantly less dye leakage at the site of polyP injection compared with control animals ($P < .001$). Each group (no inhibitor, dendrimer, and polymyxin B) contained 15 mice. Data for (A,B) from BC Cooley, data and figure for (C) by RJ Travers, data for D from JN Collins, RJ Travers, and SA Smith (who also prepared the figure).

A

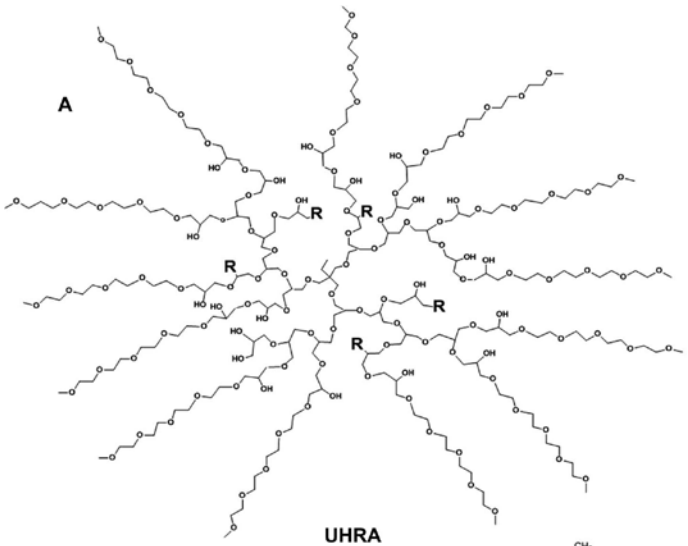

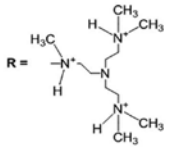

Heparin binding group (HBG)

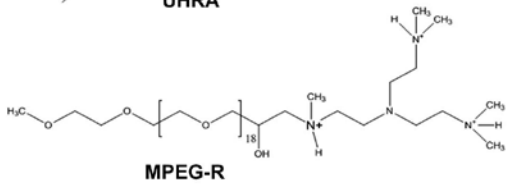

B

Molecular characteristics of synthesized UHRA

UHRA	M_n[a]	M_w/M_n	R_h (nm)	No. of HBGs (R)	Zeta potential (mV)
UHRA-1	116,700	1.2	10	33	8.9 ± 1.6
UHRA-2	48,000	1.45	4	18	14.8 ± 0.9
UHRA-3	23,000	1.52	3	4	10.5 ± 1.9
UHRA-4	23,000	1.52	3	5	12.7 ± 1.1
UHRA-5	23,000	1.52	3	11	15.5 ± 0.4
UHRA-6	23,000	1.52	3	16	17.1 ± 3
UHRA-7	23,000	1.52	3	20	19.8 ± 1.6
UHRA-8	23,000	1.52	3	24	22.7 ± 3

[a] Molecular weight of the scaffold polyner

Figure 5.1. Molecular structure and characteristics of synthetic dendritic polymer – based UHRA. (A) Chemical structures of a representative UHRA, the HBG, and the model compound with a single HBG (MPEG-R). The UHRA structure consists of dendritic polyglycerol core decorated with HBG("R") in a multivalent fashion. The number of HBGs on the scaffold was varied to generate different UHRA constructs. The trivalent cationic nature of the HBG, hexamethylated tris (2-aminoethylamine) (contains four tertiary amine groups), at physiological pH is shown. The heparin binding R group–decorated dendritic polymer core is protected with short PEG chains as an entropic bumper (brush layer) to minimize nonspecific interactions. The whole polymer structure is essential for enhanced heparin binding and biocompatibility. (B) Molecular characteristics of the optimized UHRA constructs. Both the MW and the number of HBGs per dendritic scaffold were varied. Figure and data from Kizhakkedathu lab.

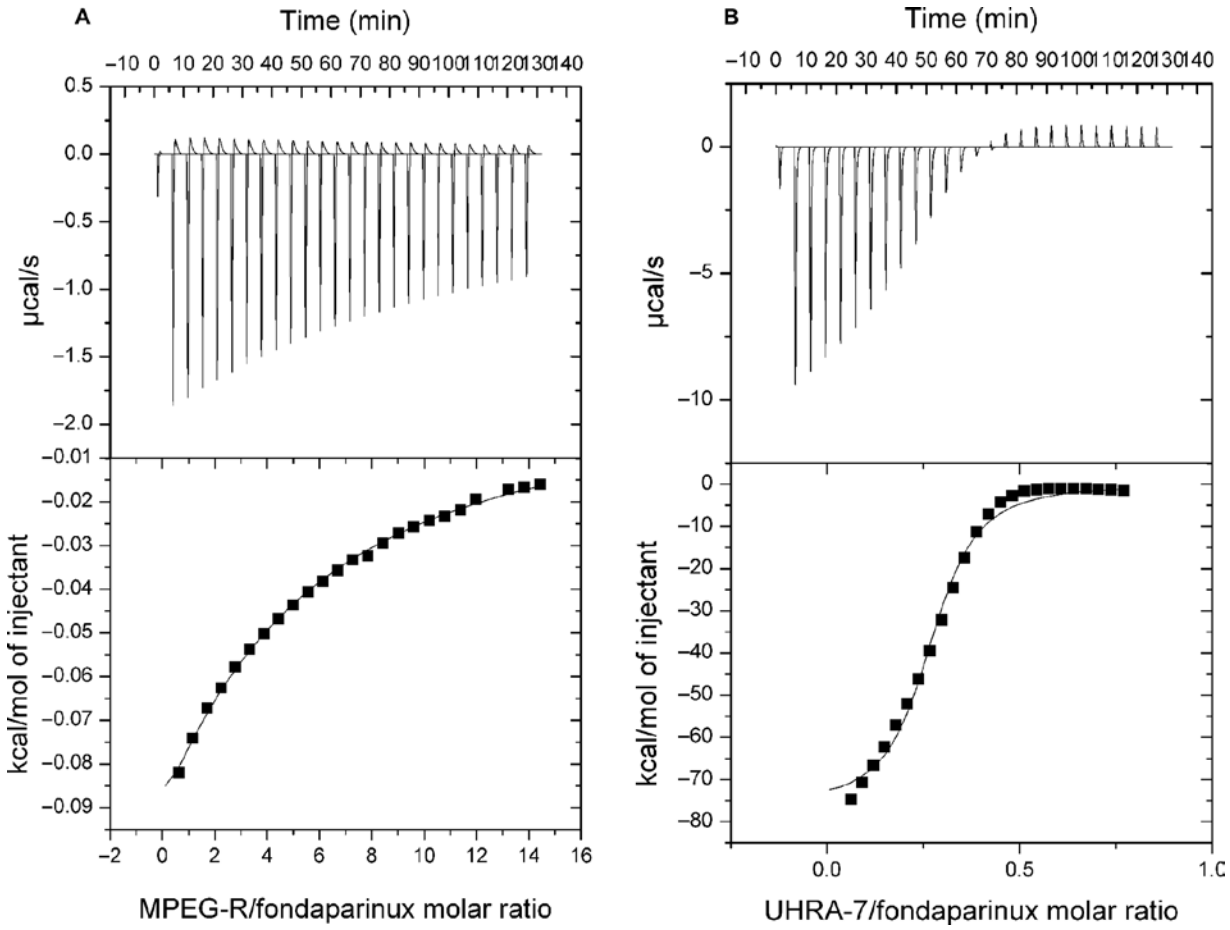

Figure 5.2. Antidote potential of UHRA deduced on the basis of ITC-derived association constants, stoichiometry, and thermodynamic parameters. (A and B) Raw data and the integral heat of binding for the titration of (A) MPEG-R and (B) UHRA-7 (UHRA with 20 HBGs on a 23-kD scaffold) into fondaparinux in 10 mM PBS at pH 7.4. The thermodynamic parameters for these experiments and other UHRAs with heparins are given Table 5.1. Figure and data from Kizhakkedathu lab.

Table 5.1 Thermodynamic parameters for the interaction of UHRA constructs with heparins measured by ITC in PBS at 25^{o}C

Macromolecule	Ligand	N*	K_a (M^{-1})	ΔG (kcal/mol)**	ΔH (kcal/mol)**	TΔS (kcal/mol)**
UFH***	MPEG-R	16.3 ± 0.4	$7 \pm 2 \times 10^{2}$	-3.9 ± 0.2	N/A	N/A
	UHRA-1	0.63 ± 0.01	$9.9 \pm 0.8 \times 10^{5}$	-8.2 ± .05	-130 ± 8	-120 ± 8
	UHRA-3	ND	$<1 \times 10^{4}$	ND	ND	ND
	UHRA-4	2.5 ± 0.1	$1.5 \pm 0.8 \times 10^{4}$	-5.6 ± 0.3	-16 ± 10	-10 ± 10
	UHRA-6	0.98 ± 0.01	$4.4 \pm 0.2 \times 10^{5}$	- 8.0 ± 0.05	-87 ± 3	-80 ± 3
	UHRA-7	1.08 ±0.02	$1.24 \pm 0.07 \times 10^{6}$	-8.3 ± 0.03	-100 ± 6	-95 ± 6
Enoxaparin	MPEG-R	6.20 ± 0.8	$4.0 \pm 2 \times 10^{3}$	-4.6 ± 0.9	N/A	N/A
	UHRA-1	0.17 ±0.01	$3.3 \pm 0.2 \times 10^{5}$	-7.5 ± 0.03	-210 ± 40	-200 ± 40
	UHRA-3	ND	$<1 \times 10^{4}$	ND	ND	ND
	UHRA-6	0.28 ± 0.01	$4.4 \pm 0.2 \times 10^{5}$	-7.7 ± 0.03	-100 ± 4	-97 ± 4
	UHRA-7	0.28 ± 0.01	$5.6 \pm 0.2 \times 10^{5}$	-7.8 ± 0.02	-130 ± 1	-122 ± 1
Fondaparinux	MPEG-R	1.44 ± 0.62	$2.2 \pm 0.2 \times 10^{2}$	-7.8 ± 0.01	N/A	N/A
	UHRA-1	0.42 ± 0.04	$5.0 \pm 0.8 \times 10^{5}$	-3.2 ± 0.8	-110 ± 20	-100 ± 20
	UHRA-3	ND	$<1 \pm 10^{4}$	ND	ND	ND
	UHRA-6	0.38 ± 0.01	$1.0 \pm 0.09 \times 10^{6}$	-8.2 ± 0.3	-47 ± 0.9	-39 ± 0.9
	UHRA-7	0.27 ± 0.01	$7.06 \pm 1.0 \times 10^{5}$	-8.0 ± 0.5	-76 ± 2	-68 ± 2

*N is the number of ligand binding sites per macromolecule
** ΔG, ΔG, andT ΔS are calculated per mole of the ligand
*** Binding affinity (K_a) for UFH-protamine interactions is 10^{-6} M^{-1}
Data from Kizhakkedathu lab.

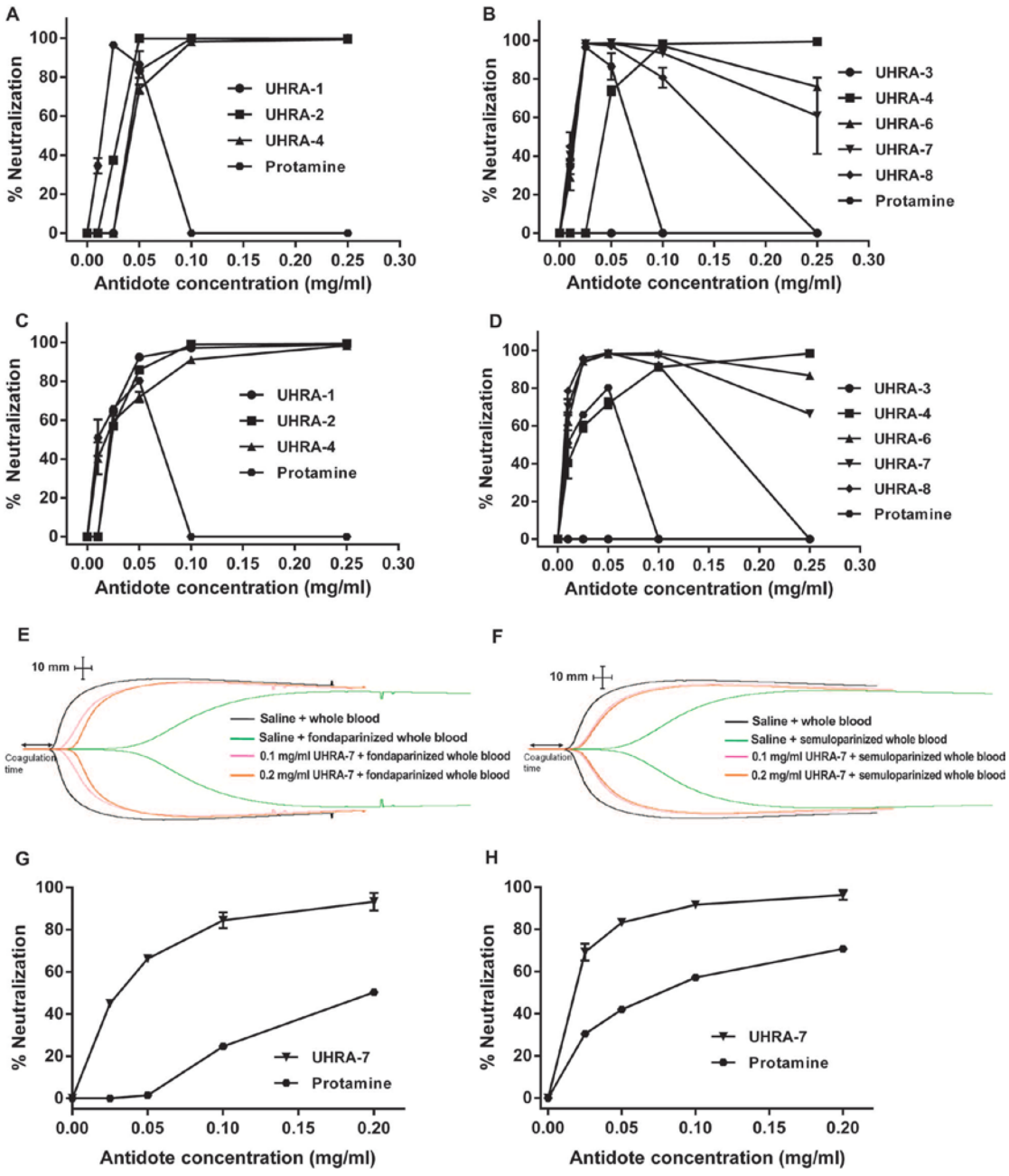

Figure 5.3. Impact of UHRA molecular structure on heparin neutralization in human whole blood and plasma. (A-D) Effect of the (A, C) MW of and (B, D) number of HBGs on UHRAs on neutralization of UFH and tinzaparin (2 IU/ml) measured by aPTT analysis (n = 5 human donors). Sodium citrate - anticoagulated plasma was incubated with heparins and titrated with various concentrations of UHRA or protamine solubilized in PBS. The percentage of heparin neutralization was calculated from the clotting times. The heparin activities were completely neutralized in a dose-dependent manner by UHRAs with five or more HBGs. (E-F) Neutralization of fondaparinux (1.2 IU/ml) and semuloparin (0.75 IU/ml) by UHRA-7 in human whole blood measured by TEG (n = 5 human blood donors; representative graph for one donor is shown). (G-H) Neutralization of fondaparinux (1.2 IU/ml) and semuloparin (0.75 IU/ml) in plasma measured with the chromogenic anti-FXa assay. The measurements were performed in triplicate, and the values reported are means ± SD from two different donors. Figure and data from Kizhakkedathu lab.

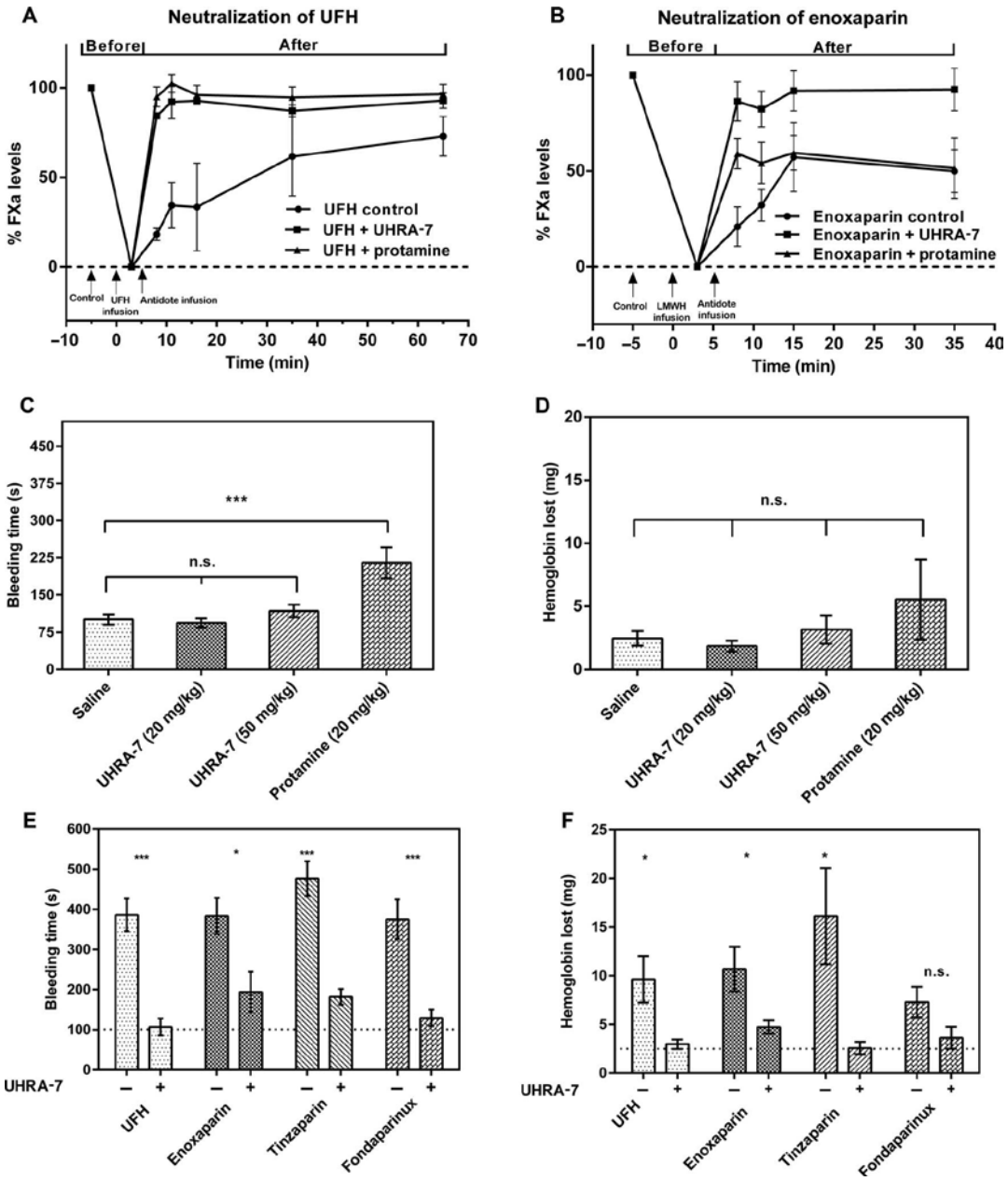

Figure 5.4. In vivo heparin neutralization and attenuation of bleeding side effects by UHRA. (A and B) Neutralization of (A) UFH and (B) enoxaparin by UHRA-7 or protamine in rats. The chronological order of the experiment is at the top of (A) and (B). Rats (n = 5 per group) were injected with 25 IU of heparins (0 min). Blood was collected after intravenous heparin infusion (5 min), and then, UHRA-7 or protamine (3 mg/kg) was injected intravenously. Neutralization was monitored by measuring anti-FXa concentrations in rat plasma. (C and D) Bleeding time and hemoglobin loss were measured in a mouse tail bleeding model after administration of UHRA-7 or protamine. Mice (n = 10 for each group) were treated with UHRA-7 (20 or 50 mg/kg), protamine (20 mg/kg), or saline (control) by retro-orbital administration. Bleeding time was measured for 10 min with a stopwatch, and hemoglobin loss was measured using Drabkin's assay and by measuring the absorbance of the samples at 540 nm. ***P < 0.0005, n.s. (A,B) Figure and data from Kizhakkedathu lab. (C-F) Figure and data from Richard Travers.

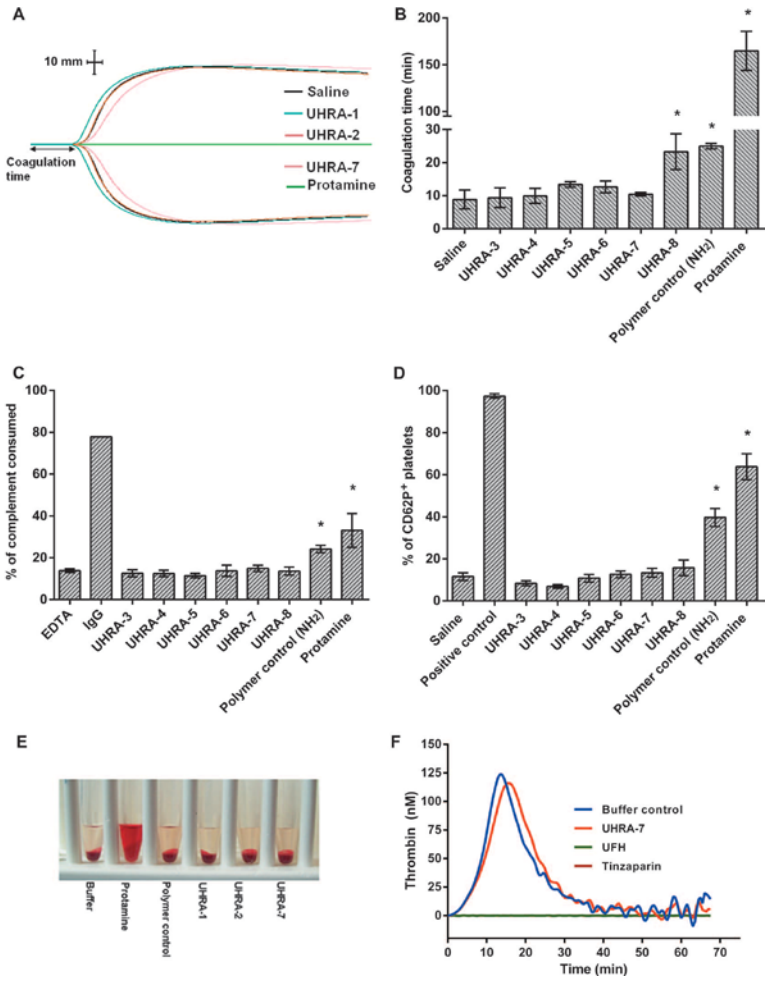

Figure 5.5. Impact of UHRA structure on biocompatibility in vitro. All the studies were performed at 37°C with UHRA (0.5 mg/ml) or protamine unless otherwise specified. Measurements were made in duplicates for five human blood donors, and values are reported as means ± SD (*P < 0.05 indicates a significant difference by unpaired Student's t test). (A) Blood coagulation: whole-blood TEG traces for saline control, UHRAs, and protamine. (B) Effect on TEG coagulation time of the number of HBGs decorating the 23-kD UHRAs. (C) Complement activation: effect on complement activation of the number of HBGs decorating the 23-kD UHRAs. Shown are comparisons between the positive control (immunoglobulin G (IgG)), protamine, and polymer control with primary amine groups (–NH2) versus the tertiary amine groups (–N(CH3)2) on UHRA. Complement activation was determined in human serum using a sheep erythrocyte–based complement consumption assay (described in the Supplementary Materials, Section 4.2.3). (D) Platelet activation: effect of the number of HBGs decorating the 23-kD UHRAs on platelet activation in PRP, measured on the basis of expression of the platelet activation marker CD62P. Positive control (thrombin), normal control (control PRP), protamine, and a polymer control are also shown. (E) Red blood cell (RBC) hemolysis: Images of the RBCs incubated with UHRAs or protamine (5 mg/ml) at 37°C for 1 hour. (F) Thrombin generation was assessed in PRP in the presence of UHRA-7 (0.1 mg/ml) at 37°C (by measuring the fluorescence intensity upon cleavage of a fluorogenic substrate, Z-Gly-Gly-Arg- AMC, by the generated thrombin). PBS and UFH or tinzaparin were used as normal control and positive control, respectively. Figure and data from Kizhakkedathu lab.

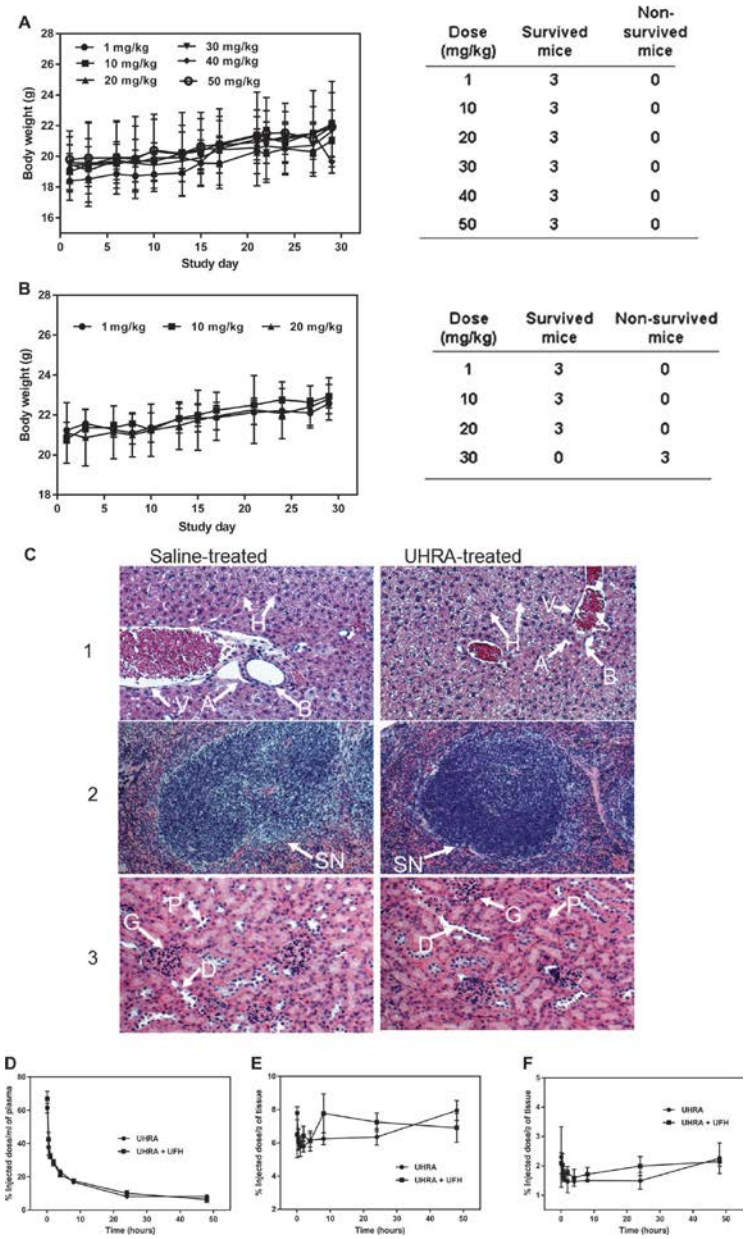

Dose (mg/kg)	Survived mice	Non-survived mice
1	3	0
10	3	0
20	3	0
30	3	0
40	3	0
50	3	0

Dose (mg/kg)	Survived mice	Non-survived mice
1	3	0
10	3	0
20	3	0
30	0	3

Figure 5.6. Measures of safety of the UHRA constructs in a mouse model. (A and B) Dose tolerance for (A) UHRA-7 and (B) protamine was measured by monitoring the body weight of individual mouse for 29 days after intravenous administration of escalating doses in female Balb/C mice (mean ± SD, n = 3). A maximum tolerated dose was not reached with UHRA-7. Mouse survival data are also shown at the right of (A) and (B). (C) Representative micrographs of tissue sections of mouse liver (1), spleen (2), and kidney (3) 29 days after intravenous administration of UHRA-7 (50 mg/kg) in female Balb/C mice. The tissue sections were stained with H&E. A, hepatic artery; V, portal vein; B, bile duct; H, hepatocytes; SN, splenic nodules; G, glomerulus; P, proximal tubule; D, distal tubule. (D to F) Biodistribution in female Balb/C mice after intravenous administration of tritiated UHRA-4 (20 mg/kg) or the UHRA-4–UFH complex. Shown are radioactivity amounts measured by scintillation counting of homogenized mouse (D) plasma, (E) liver, and (F) spleen. Both UHRA-4 and its heparin complex exhibited plasma circulation half-lives of ∼40 min and showed minimal nonspecific tissue accumulation. Data are shown as means ± SD; n = 4 for each group. Figure and data from Kizhakkedathu lab.

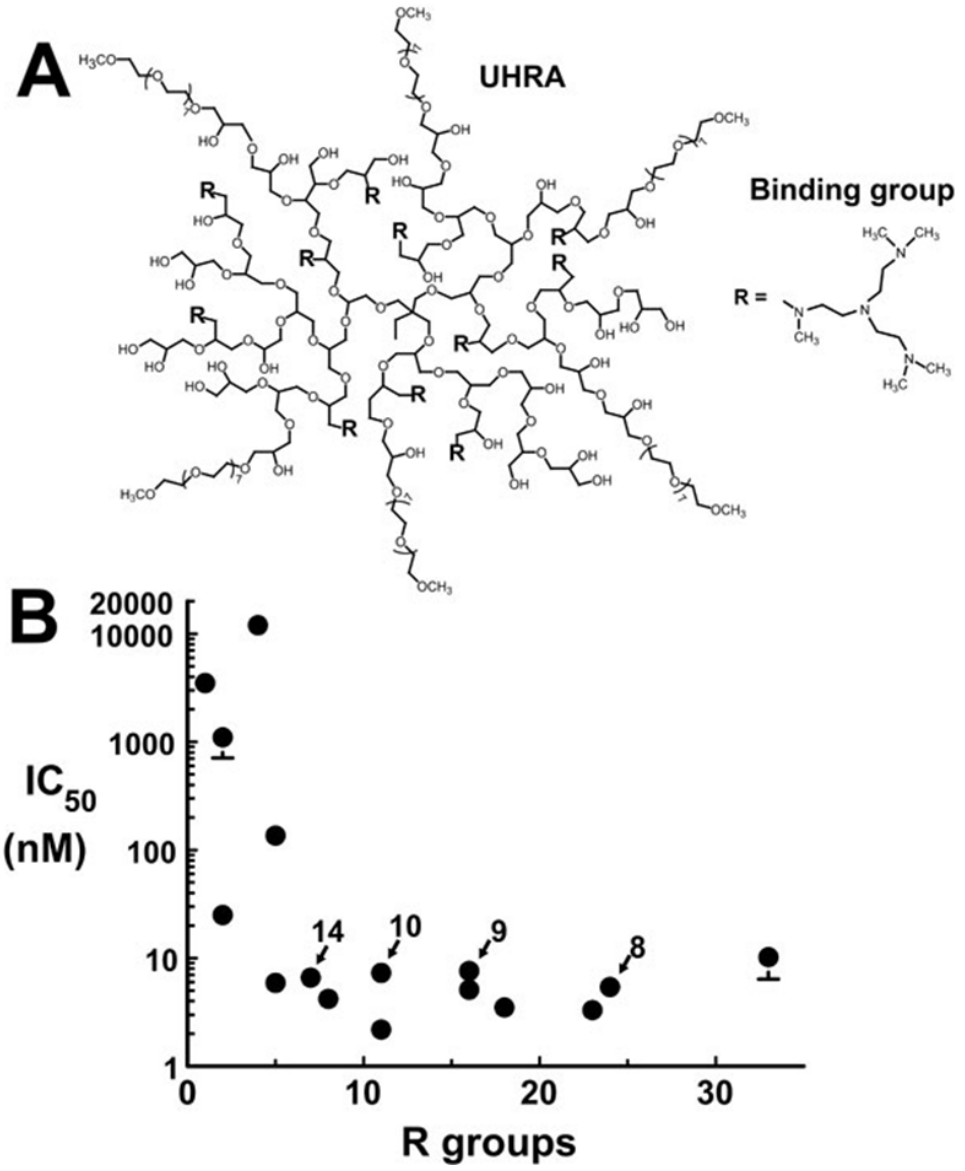

Figure 6.1 Design and structure of UHRA compounds, and efficacy in blocking thrombin binding to polyP. (A) Representative structure of a typical UHRA scaffold (in this case, for UHRA-10), containing a dendritic polyglycerol core bearing the randomly distributed polyP-binding groups (R) and an outer shell of short-chain polyethylene glycols. The molecular weight and number of R groups was varied to generate the other UHRAs. Image adapted from chemical structures provided by the Kizhakkedathu Lab. (B) IC_{50} values for the ability of sixteen UHRA compounds to inhibit thrombin binding to immobilized polyP. Arrows indicate the four compounds selected for further study: UHRA 8 (R=24; 23 kDa), UHRA 9 (R=16; 16 kDa), UHRA 10 (R=11; 10 kDa), and UHRA 14 (R=7; 10 kDa). Data for (B) from Richard Travers, figure prepared by James Morrissey.

Table 6.1. UHRA compounds used in this study

			Inhibition of Thrombin Binding to PolyP	
Compound	**MW (kDa)**	**R Groups**	**IC_{50} (ng/mL)**	**IC_{50} (nM)**
UHRA 1	116	33	1200	10.2
UHRA 2	48	18	166	3.5
UHRA 3	23	4	280000	12000
UHRA 4	23	5	3100	136
UHRA 5	23	11	50.1	2.18
UHRA 6	23	16	117	5.1
UHRA 7	23	20	74	3.3
UHRA 8	23	24	123 ± 18	5.4 ± 0.78
UHRA 9	16	16	122 ± 14	7.6 ± 0.90
UHRA 10	10	11	73 ± 17	7.3 ± 1.7
UHRA 11	9	8	38	4.2
UHRA 12	10	2	11000	1100
UHRA 13	10	5	59	5.9
UHRA 14	10	7	66 ± 11	6.6 ± 1.1
UHRA 15	5	2	124	25
UHRA 16	5	1	18000	3500

UHRA compounds were screened for ability to inhibit thrombin binding to immobilized polyP as described in Methods. "R-groups" refers to the number of binding groups per polymer (see Figure 1 in the text for a general overview of UHRA structure). IC_{50} values (given in concentrations by weight and molarity) indicate the concentration of UHRA needed to yield 50% inhibition of thrombin binding to polyP (n = 1-5, data reported as mean ± SEM for $n > 3$ and mean for $n < 3$). UHRA compounds 8, 9, 10, and 14 (shaded blue) were chosen for further study.

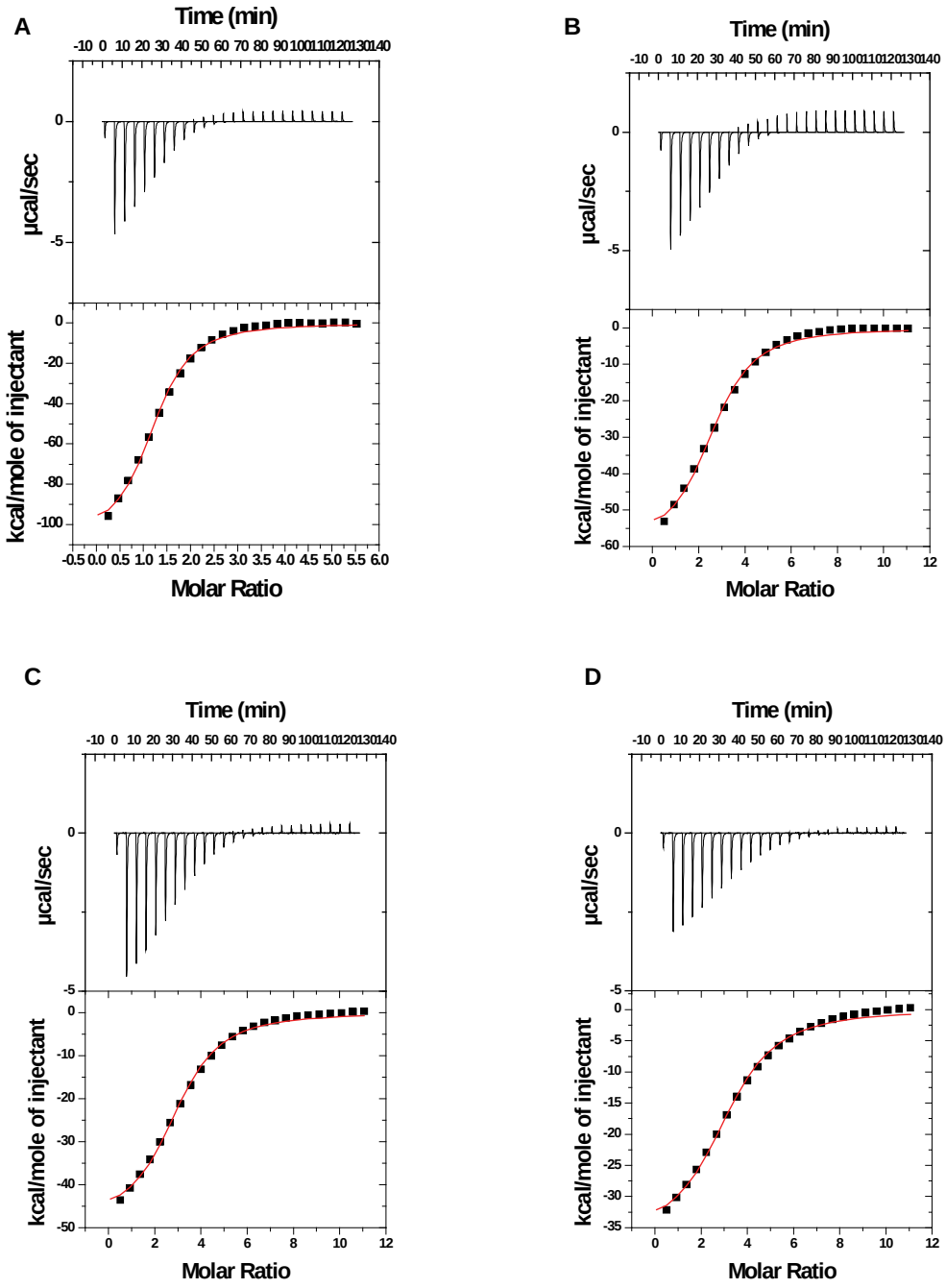

Figure 6.2. Isothermal titration calorimetry analysis for UHRA-polyP binding. (A-D) Raw data and integral heats for the titration of (A) UHRA-8, (B) UHRA-9, (C) UHRA-10, and (D) UHRA-14 into $polyP_{75}$ in 10 mM phosphate buffered saline (PBS) at pH 7.4 and 25°C. One-site binding model was used to obtain fit for all the titration data. Thermodynamic parameter analysis is presented in **Table 6.2**. Figure from Kizhakkedathu lab.

Table 6.2. Thermodynamic parameters for interaction of UHRA with polyP$_{75}$ determined by isothermal titration calorimetry.

Compound	N[a]	K_d (μM)[a]	ΔG (kcal/mol)[b]	ΔH (kcal/mol)[a]	TΔS (kcal/mol)[b]
UHRA 8	1.23	0.727 ± 0.01	-8.34 ± 0.01	-107 ± 0.3	-98.7 ± 0.3
UHRA 9	2.66 ± 0.007	1.71 ± 0.04	-7.83 ± 0.01	-59.5 ± 0.3	-51.7 ± 0.3
UHRA 10	2.98 ± 0.007	1.83	-7.79	-48.9 ± 0.2	-41.1 ± 0.2
UHRA 14	3.22 ± 0.01	2.24 ± 0.05	-7.67 ± 0.01	-36.6 ± 0.3	-28.9 ± 0.3

[a]Obtained from isothermal titration calorimetry experiments
[b]Calculated from the equation $\Delta G = \Delta H - T\Delta S = -RT\ln K_a$

All data were collected in PBS at pH 7.4 and 25^{o}C. Values given represent an average from two independent titrations and standard deviations are indicated in parentheses. N: number of moles of UHRA binding per mole of polyP$_{75}$; K_d: dissociation constant; ΔG: free energy change; ΔH: enthalpy change; TΔS: entropy change. UHRAs exhibited binding affinities in the micromolar range (0.7-2.2 μM) to polyP$_{75}$ (a polyP preparation with median polymer lengths of approximately 75 phosphate units). UHRA-8 (23kDa with 24 binding groups) exhibited the highest binding affinity (K_d= 0.727 μM) among the inhibitors. At the similar inhibitor molecular weight, the greater the number of binding groups per UHRA molecule, the stronger the affinity to polyP (UHRA 10 vs UHRA 14). There was no significant difference in free energy of binding (ΔG) among the polymers; however, the enthalpy of binding (ΔH) increased with an increase in molecular weight as well as the number of binding groups on UHRAs. Data from Kizhakkedathu lab, table preparation by Richard Travers.

Table 6.3 *In vitro* inhibition of polyP activity by selected UHRA compounds

			Thrombin Binding		Plasma Clotting Assay			
			IC_{50}		EC_{double} polyP		EC_{double} RNA	
Compound	**Size (kDa)**	**R Groups**	**nM**	**ng/mL**	**nM**	**µg/mL**	**µM**	**µg/mL**
UHRA 8	23	24	5.4 ± 1.8	124 ± 41	52 ± 15	1.20 ± 0.34	0.62 ± 0.21	14 ± 4.8
UHRA 9	16	16	7.6 ± 2.0	122 ± 32	80 ± 16	1.28 ± 0.26	1.9 ± 0.59	30 ± 9.4
UHRA 10	10	11	7.3 ± 3.7	73 ± 37	132 ± 38	1.32 ± 0.38	2.0 ± 0.58	20 ± 5.8
UHRA 14	10	7	6.6 ± 2.4	66 ± 24	92 ± 13	0.92 ± 0.13	2.2 ± 0.65	22 ± 6.5

Results are: IC_{50} for inhibiting thrombin binding to immobilized polyP (*n*=5); and EC_{double} (concentration needed to double the clotting time) in plasma clotting assays initiated with either 10 µM long-chain polyP (EC_{double} polyP, *n*=3) or 25 µg/mL polyguanylic acid (EC_{double} RNA, *n*=3). Data are reported in terms of both molarity and mass/volume ± SEM.

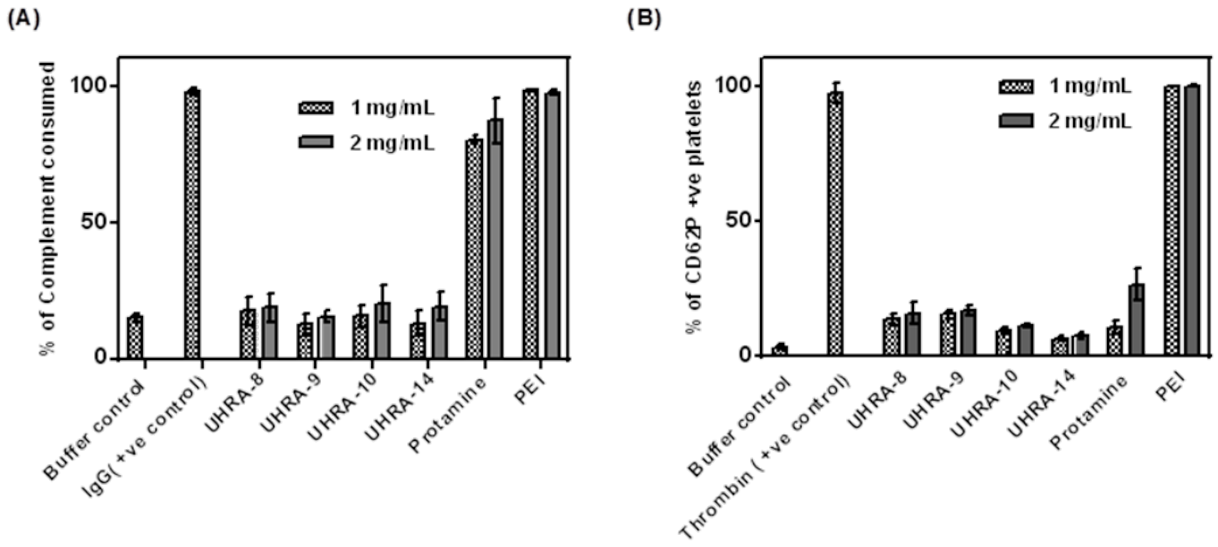

Figure 6.3 Biocompatibility of UHRAs compared to other polyP inhibitors. (A) The ability of UHRA compounds, protamine and PEI (tested at 1 or 2 mg/mL) to activate complement in human serum was measured by sheep erythrocyte complement consumption assay. Heat-aggregated human IgG (1 mg/mL) and PBS were the positive and negative controls, respectively. UHRAs did not activate complement compared to buffer controls, while protamine and PEI showed high levels of complement activation. (B) The ability of UHRA compounds, protamine and PEI (tested at 1 and 2 mg/mL) to activate platelets in human platelet-rich plasma (PRP) was measured by flow cytometry for expression of platelet activation marker CD62P. Bovine thrombin (at 1 IU/mL) was used as the positive control, and PBS alone as the negative control ("buffer control"). UHRAs showed low levels of platelet activation compared to PEI. Data and figure preparation from the Kizhakkedathu lab.

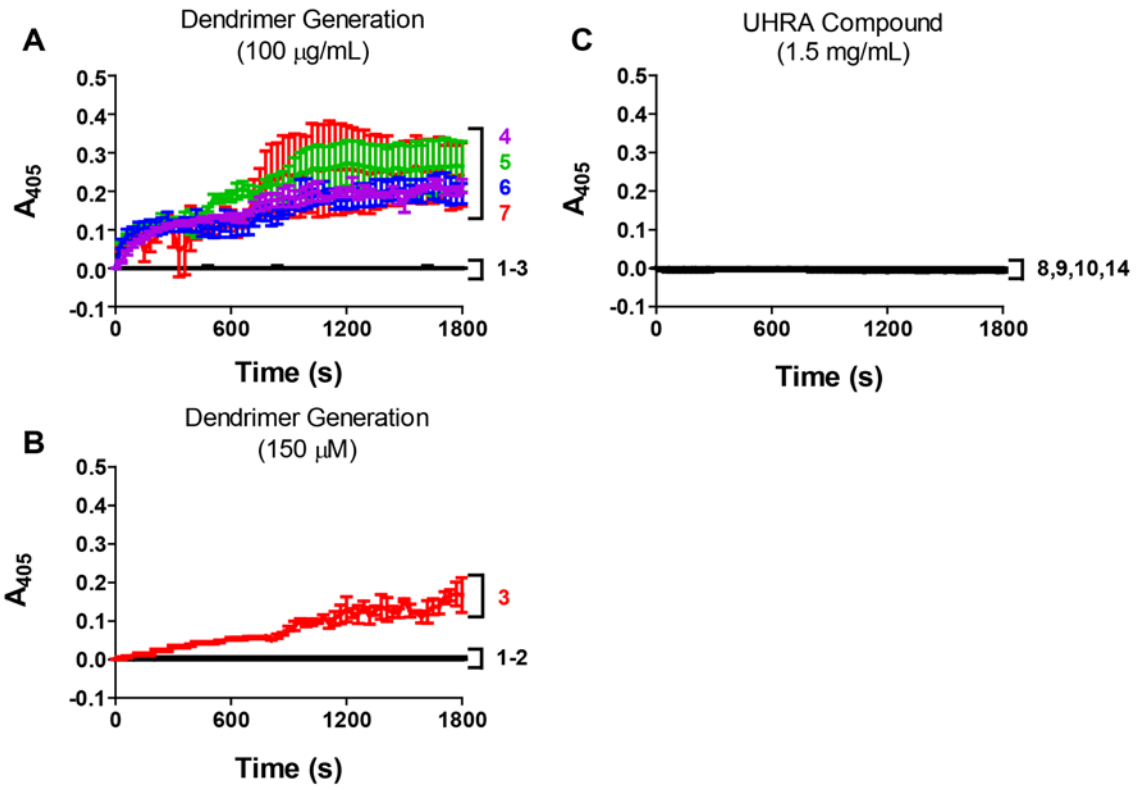

Figure 6.4 PAMAM dendrimers but not UHRA compounds induce fibrinogen aggregation. Turbidity assays were adapted from previous reports of dendrimer-induced fibrinogen aggregation.1 PAMAM dendrimer generations 1-7, or UHRA compounds 8, 9, 10 or 14, were diluted in TBSC (50 mM Tris-HCl pH 7.4, 100 mM NaCl, 2.5 mM $CaCl_2$, 0.02% NaN_3) and added to wells of a 96-well plate. An equal volume of 4 mg/mL human fibrinogen (Enzyme Research Laboratories) diluted in TBSC was added (final fibrinogen concentration of 2 mg/mL) immediately before recording the absorbance at 405 nm every 30 seconds for 30 minutes. Graphs are baseline-subtracted mean ± SEM, n=3 for all experiments. (A) At concentrations of 100 μg/mL, PAMAM dendrimer generations 4-7 all showed increased turbidity, indicating the induction of fibrinogen aggregates. (B) While PAMAM dendrimer generations 1-3 did not show signs of fibrinogen aggregation at 100 μg/mL, when tested at 150 μM (or 0.21, 0.49, and 1.0 mg/mL respectively), generation 3 PAMAM dendrimer also caused detectable turbidity, indicative of fibrinogen aggregation. (C) UHRA compounds showed no detectable fibrinogen aggregation even at concentrations up to 1.5 mg/mL. (Note that 1.5 mg/mL UHRA 8 is 150 μM).

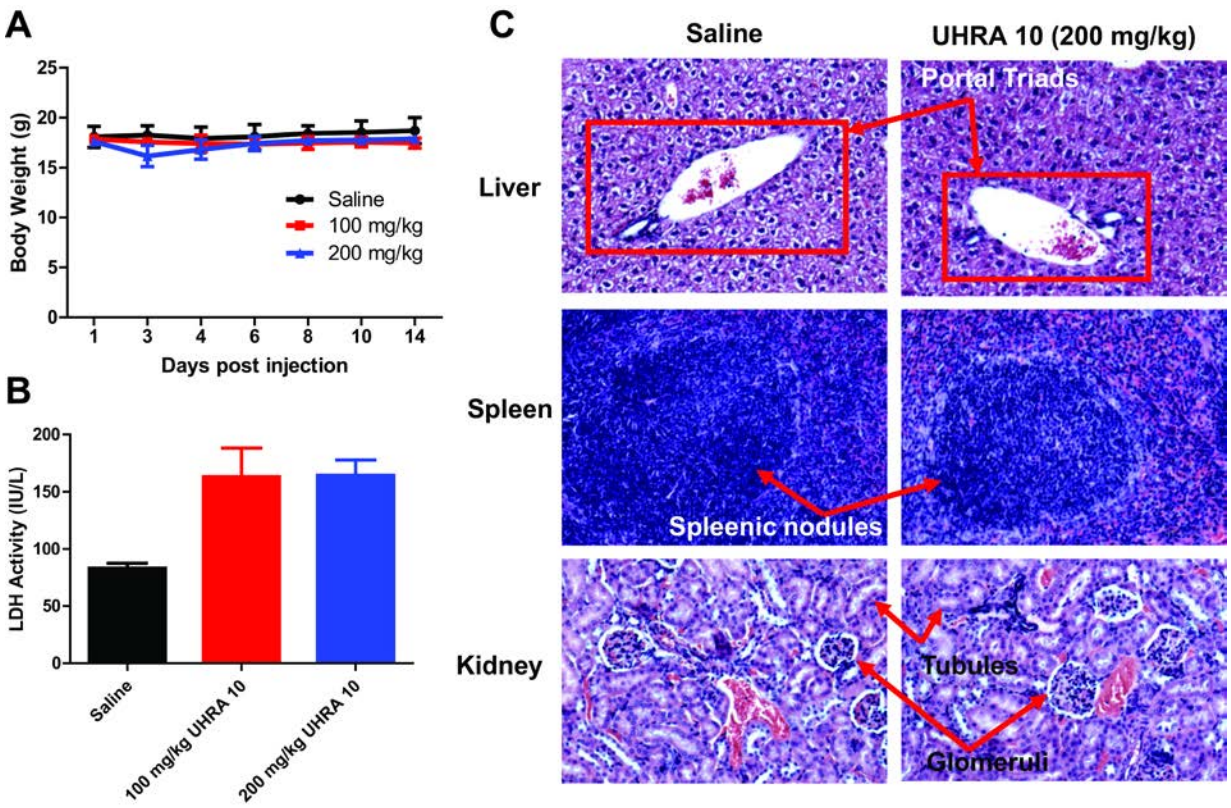

Figure 6.5 Lack of UHRA 10 toxicity *in vivo*. Dose tolerance of UHRA 10 was examined in mice by the administration of 100 mg/kg or 200 mg/kg of UHRA-10 in a protocol approved by the University of British Columbia animal ethics committee (with studies performed at British Columbia Cancer Research Centre's animal facility). Female Balb/C mice (6-8 weeks, 20-26 g) were individually weighed and were divided into groups of for each dose. Each group of mice (n=3) were injected intravenously (via tail vein) with UHRA-10 (100 mg/kg or 200 mg/kg) using a 28 G needle. The injection volume was 200 µL/20 g mouse. After injection, the mice were housed in cages and monitored for signs of acute toxicity over a period of 14 days. Body weights of individual mice were recorded prior to injection and three times per week thereafter. On day 14, mice were euthanized by CO_2 asphyxiation, blood (50 µL) was collected from each mouse on the final day and necropsy was performed on all animals. Serum samples were analyzed for lactate dehydrogenase (LDH) activity using the IDToxTM lactate dehydrogenase enzyme assay kit (ID Labs Inc.). Upon euthanasia of the mice on day 14, whole liver, spleen and both the kidneys were removed from each animal. The tissues were washed in ice cold saline to remove blood and immediately fixed in 10% neutral buffered formalin and processed, embedded in paraffin, sectioned, and stained with hematoxylin and eosin (H&E). (A) There was no change in the body weights (n=3, reported as mean ± S.D.) of mice injected with either saline (black circles) or UHRA 10 at doses of 100 (red squares) or 200 mg/kg (blue triangles). (B) Serum lactate dehydrogenase (LDH) levels in mice injected with saline or with 100 or 200 mg/kg UHRA 10 were all within the normal ranges for serum LDH in mice, which are typically below 400 U/mL. (C) Histopathological analysis (H&E staining) on tissue sections after administration of 200 mg/kg UHRA-10 also did not show any toxicity effects such as tissue damage, cell necrosis or inflammation. There was also no evidence of abnormalities in the necropsy analysis, further confirming the non-toxic nature of UHRA 10 *in vivo*. Data from the Kizhakkedathu lab, figure preparation by Richard Travers.

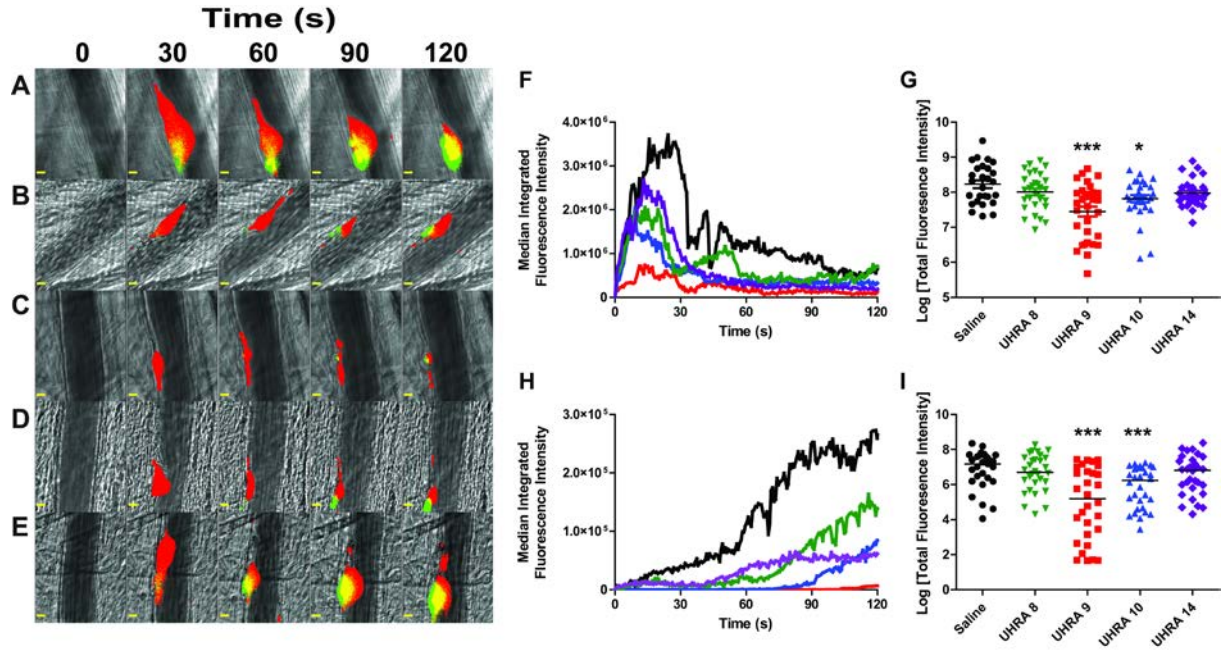

Figure 6.6 UHRA compounds inhibit thrombus formation in mouse cremaster arterioles. (A-E) Binarized images from one representative injury each showing the accumulation of platelets (red) and fibrin (green) 120 seconds after laser-induced injury to the vessel wall in mice administered either (A) saline or the following UHRA compounds at 40 mg/kg: (B) UHRA 8, (C) UHRA 9, (D) UHRA 10, or (E) UHRA 14. Scale bars: 10 µm. (F-I) Statistical analyses of the effect of administering UHRA compound on thrombus formation; data are from 27-30 injuries to 5 mice for each condition. Median integrated fluorescence intensities (non-binarized) were plotted versus time for accumulation of (F) platelets and (H) fibrin. In addition, the area under the curve (total fluorescence intensity) was plotted for accumulation of (G) platelets and (I) fibrin (each point representing one injury, plotted as log values). When median values were evaluated by Mann-Whitney test, both UHRA 9 and 10 significantly reduced total accumulation of platelets and fibrin compared to control. *$P < 0.05$, ***$P < 0.0005$. Brightfield and fluorescent images of arterioles were acquired with a Zeiss Axioplan microscope equipped with a Lumencore 4-LED light engine, a 20X water immersion lens (Zeiss W-Plan APOCHROMAT 20x/1.0 NA), and a Rolera em-c2 EMCCD Camera (Q-Imaging). Endothelial injury to the vascular wall of 50-70 µm diameter arterioles that resulted in thrombus formation was effected by the use of a 532 nm pulsed-laser system integrated with the image capture and analysis software (VIVO Imaging System with Ablate! Photomanipulation Module, Intelligent Imaging Innovations). Fluorescence images were acquired continuously, platelet fluorescence was imaged with a Cy-5 filter and 15 ms exposure, and fibrin was imaged with a fluorescein filter set and 10 ms exposure. Brightfield images were captured with a 10 ms exposure periodically (1 image every 100 captures).

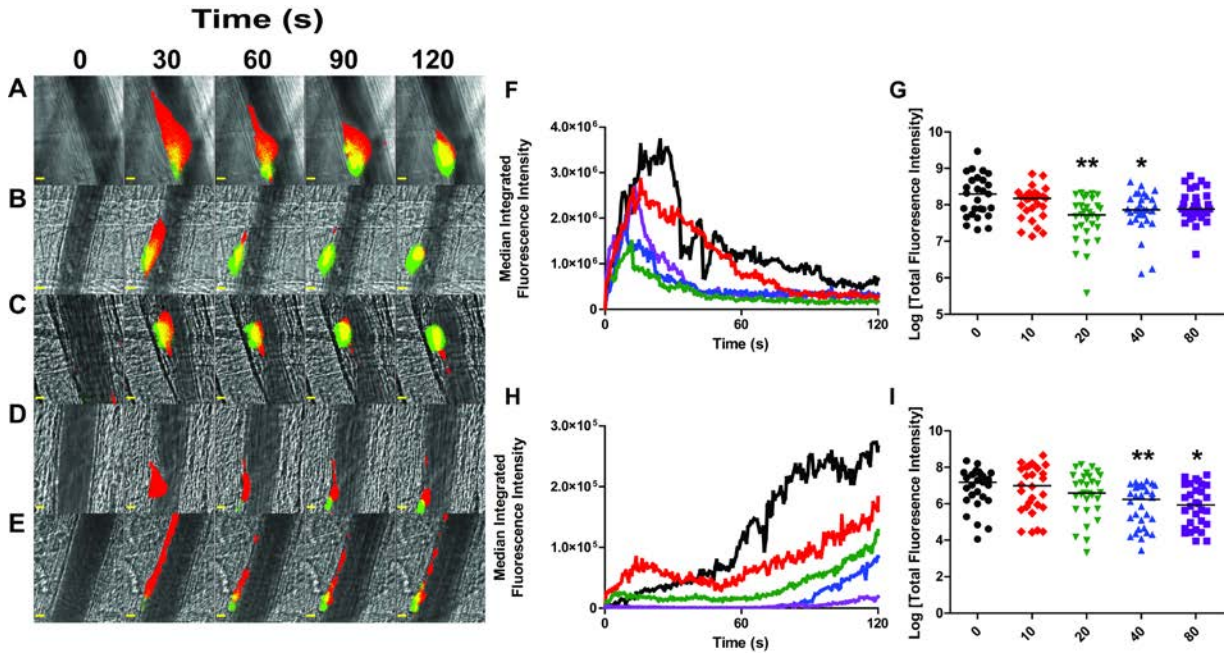

Figure 6.7 UHRA 10 inhibits thrombus formation in mouse cremaster arterioles in a dose-dependent manner. (A-E) Binarized images from one representative injury each showing the effects on accumulation of platelets (red) and fibrin (green) 120 seconds after laser-induced injury to the vessel wall in mice administered either (A) saline or UHRA 10 at (B) 10 mg/kg, (C) 20 mg/kg, (D) 40 mg/kg, or (E) 80 mg/kg. Scale bars: 10 µm. (F-I) Statistical analyses of the dose-dependent attenuation of thrombus formation by UHRA 10; data are from 27-30 injuries to 5 mice for each condition. Median integrated fluorescence intensities (non-binarized) were plotted versus time for accumulation of (F) platelets and (H) fibrin. In addition, the area under the curve (total fluorescent intensity) for each individual injury was plotted for accumulation of (G) platelets and (I) fibrin (each point represents one injury, plotted as log values). (Note: data for saline control and UHRA at 40 mg/kg are in common with the data from Figure 4.5 and are therefore repeated here in panels A and D, and the blue lines and data points in panels F-I. Median values were compared to saline control for statistical significance by Mann-Whitney test. UHRA 10 significantly reduced platelet accumulation at doses of 20 and 40 mg/kg, and significantly reduced fibrin accumulation at doses of 40 and 80 mg/kg. *P < 0.05, **P < 0.005, ***P < 0.0005. Data were captured an analyzed as in Figure 6.6.

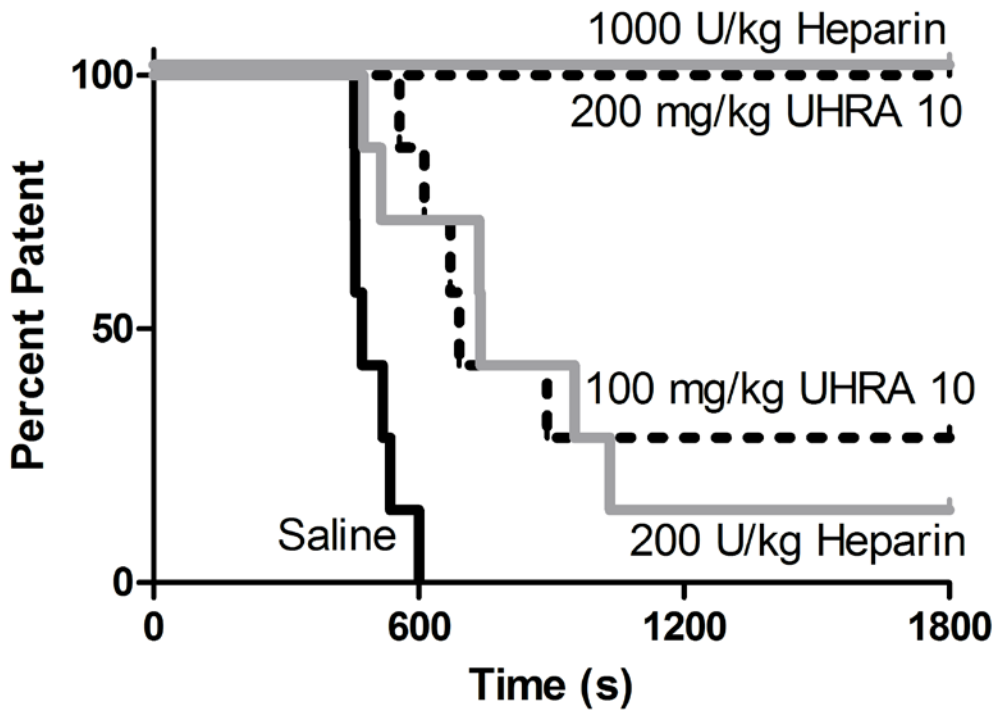

Figure 6.8 UHRA 10 delays time to occlusion in a mouse carotid artery model of thrombosis. Artery patency was monitored by Doppler flow probe following induction of FeCl3-mediated injury, and plotted here versus time in black for saline control, orange for unfractionated heparin and blue for UHRA 10. Both heparin and UHRA 10 significantly delayed median time to occlusion in a dose-dependent manner ($P < 0.0001$). Heparin at 200 U/kg was not significantly more effective than UHRA 10 at 100 mg/kg at maintaining artery patency ($P = 0.85$), while both treatment conditions significantly increased median patency time versus saline control ($P = 0.0004$ for UHRA 10 and $P = 0.007$ for heparin). UHRA 10 at 200 mg/kg or heparin at 1000 U/kg resulted in 100% patency over the 30 minutes period for all mice ($n = 7$ for all conditions). Statistical significance was assessed by log-rank analysis.

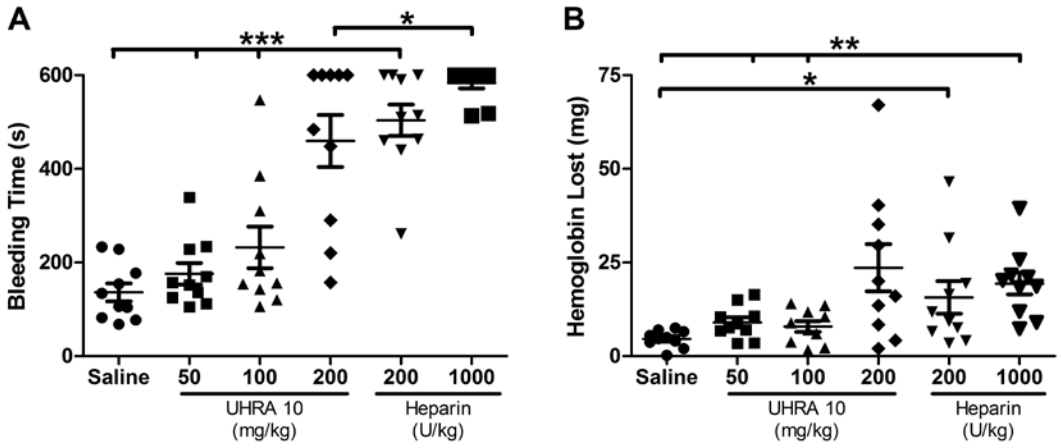

Figure 6.9 Antithrombotic doses of UHRA 10 caused less bleeding than did unfractionated heparin in a mouse tail bleeding model. (A) Bleeding times. Mice treated with 200 U/kg unfractionated heparin had significantly longer tail bleeding times than did either saline control mice or mice treated with 50 or 100 mg/kg UHRA 10. Similarly, mice treated with 1000 U/kg heparin had significantly longer bleeding times than did mice treated with 200 mg/kg UHRA 10. (B) Blood loss (quantified as mg hemoglobin collected during 30 min). Mice treated with either 200 or 1000 U/kg heparin had significantly higher hemoglobin loss than did mice treated with saline. Mice treated with 1000 U/kg heparin had significantly more hemoglobin loss than did mice treated with 50 or 100 mg/kg UHRA 10. Mice treated with 1000 U/kg heparin had no significant difference in hemoglobin loss compared to mice treated with 200 mg/kg UHRA 10. Statistical significance was assessed by individual Student's t-tests; *$P < 0.05$, **$P < 0.005$, ***$P < 0.0005$.

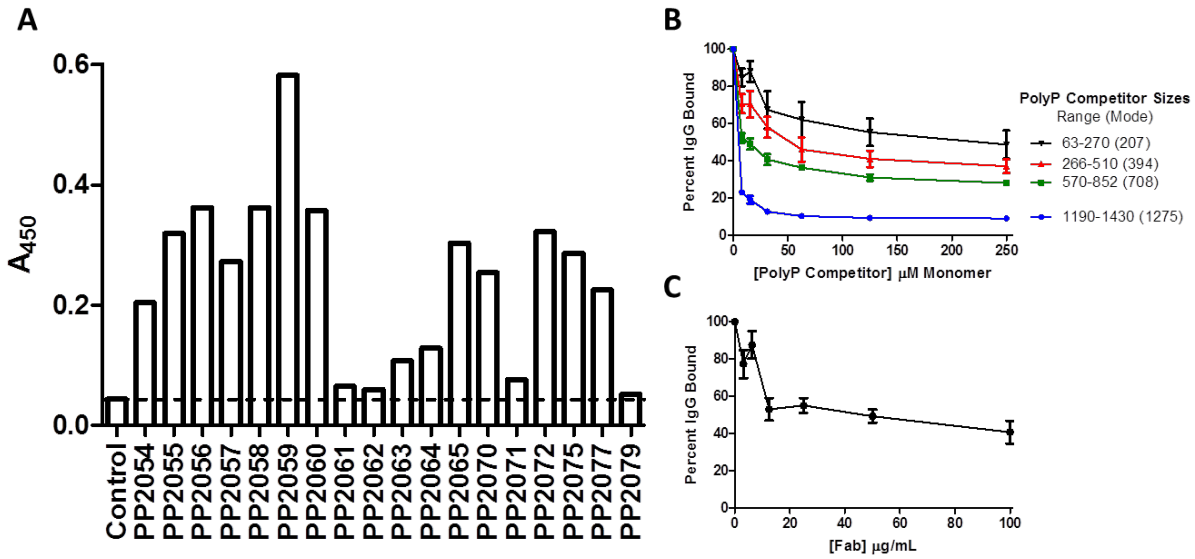

Figure 7.1 PolyP antibodies bind to long-chain polyP. (A) Screening of various monoclonal antibodies purified from hybridomas generated from NZBWF1/J mice showed differing abilities to bind to biotinylated polyP compared to an isotype control (dotted line represents no antibody control). (B) In competition assays between immobilized biotinylated long-chain polyP (200-2000 phosphates long, mode of 1090 phosphates) and free unlabeled polyP separated into size fractions by preparative PAGE, PP2059 preferentially binds to long chain polyP. (C) Fab fragments created from PP2059 cannot fully compete with intact PP2059 in binding to long-chain polyP (5 µg/mL PP2059 IgG, note that Fab fragments are ~33% of the MW of an intact IgG). Error bars for B and C are mean ± SD, n=3. Data for 5.1A from Rachel Breitenfeld, other data and figure preparation by Richard Travers.

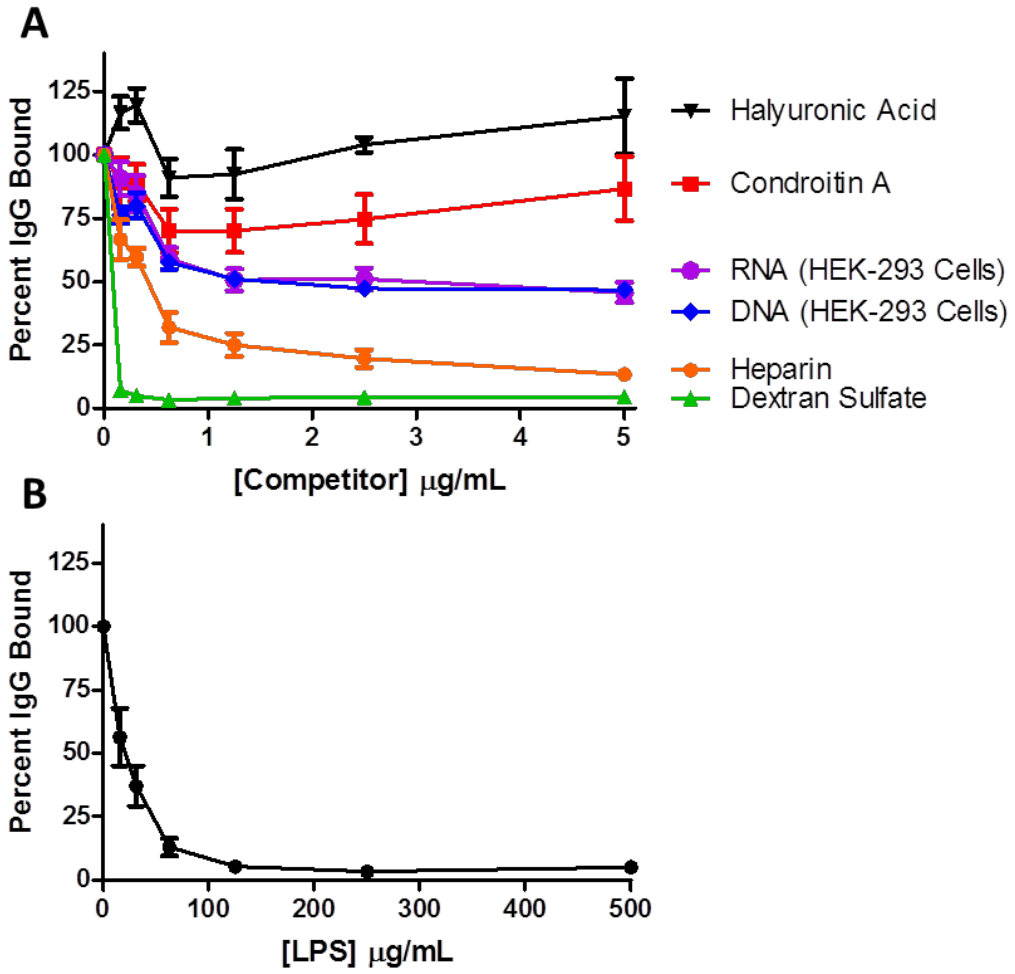

Figure 7.2 PP2059 specificity for polyP versus other anionic polymers and LPS. (A) The ability of various anionic polymers to inhibit PP2059 binding (final concentration of 5 μg/mL antibody) to immobilized biotinylated polyP was studied via an *in vitro* competition assay. Total genomic DNA and total RNA were isolated from HEK-293 cells via DNeasy and RNeasy kits (Qiagen) respectively; all other competitors were purchased from Sigma Aldrich. (B) High concentrations of LPS also compete with polyP for binding to PP2059. Error bars are mean ± SD for n=3 for all experiments.

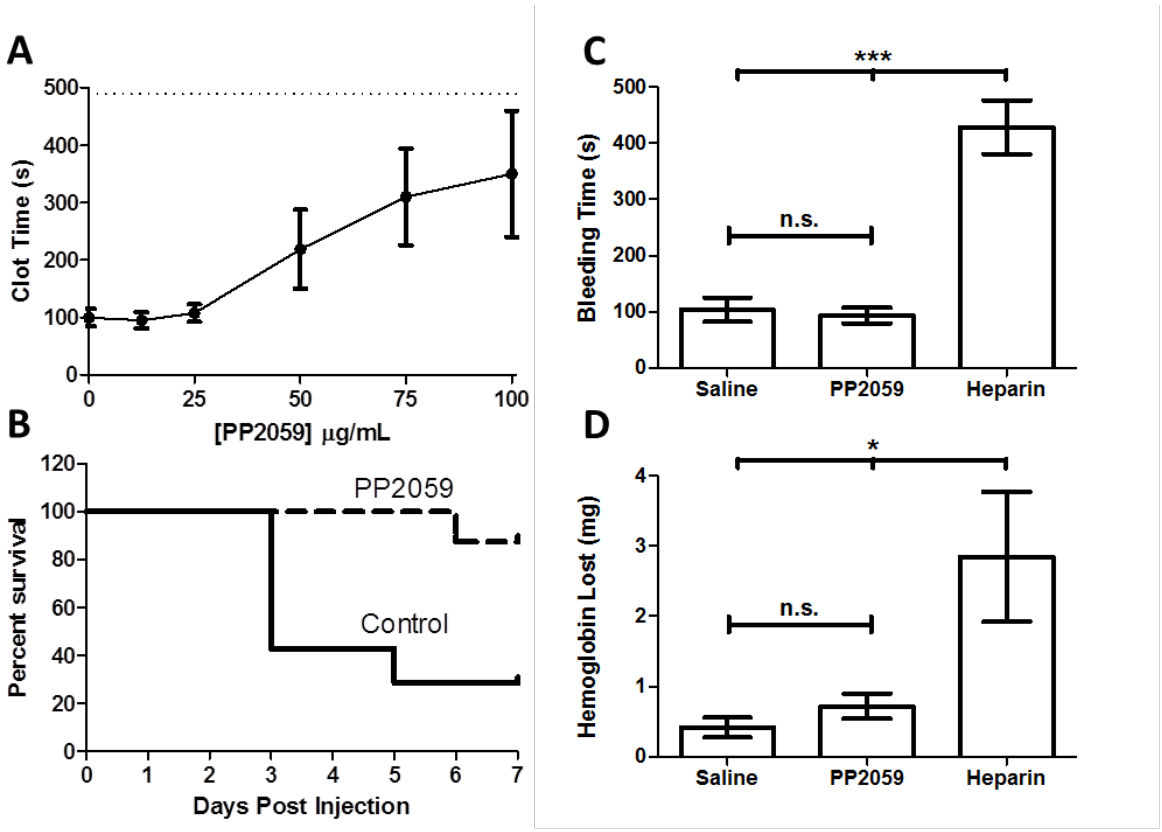

Figure 7.3 PP2059 inhibits polyP *in vitro* and improves survival during LPS challenge without impairing hemostasis. (A) PP2059 causes a dose-dependent increase in clot time in a modified aPTT assay where clotting is initiated with long-chain polyP (dotted line indicates clotting time in the absence of polyP, n=5, error bars are mean ± SD). (B) A dose of 20 mg/kg PP2059 increases survival in mice challenged with 10 mg/kg LPS. In a mouse tail bleeding assay however, a dose of 20 mg/kg PP2059 causes no significant increase in bleeding time (C) or amount of hemoglobin lost (D) compared to saline treated mice. Error bars are mean ± SEM. *P < 0.05, ***P < 0.0005. Data from figure 5.3B from the Esmon Laboratory, other data and figure preparation by Richard Travers.

REFERENCES

1. Morrissey JH. Tissue factor: an enzyme cofactor and a true receptor. Thrombosis and haemostasis. 2001;86(1):66-74.
2. Nossel HL. Differential consumption of coagulation factors resulting from activation of the extrinsic (tissue thromboplastin) or the intrinsic (foreign surface contact) pathways. Blood. 1967;29(3):331-40.
3. Renne T. The procoagulant and proinflammatory plasma contact system. Seminars in immunopathology. 2012;34(1):31-41.
4. Morrissey JH, Fakhrai H, Edgington TS. Molecular cloning of the cDNA for tissue factor, the cellular receptor for the initiation of the coagulation protease cascade. Cell. 1987;50(1):129-35.
5. Scarpati EM, Wen D, Broze GJ, Jr., Miletich JP, Flandermeyer RR, Siegel NR, Sadler JE. Human tissue factor: cDNA sequence and chromosome localization of the gene. Biochemistry. 1987;26(17):5234-8.
6. Spicer EK, Horton R, Bloem L, Bach R, Williams KR, Guha A, Kraus J, Lin TC, Nemerson Y, Konigsberg WH. Isolation of cDNA clones coding for human tissue factor: primary structure of the protein and cDNA. Proc Natl Acad Sci U S A. 1987;84(15):5148-52.
7. Paborsky LR, Caras IW, Fisher KL, Gorman CM. Lipid association, but not the transmembrane domain, is required for tissue factor activity. Substitution of the transmembrane domain with a phosphatidylinositol anchor. The Journal of biological chemistry. 1991;266(32):21911-6.
8. Drake TA, Morrissey JH, Edgington TS. Selective cellular expression of tissue factor in human tissues. Implications for disorders of hemostasis and thrombosis. The American journal of pathology. 1989;134(5):1087-97.
9. Wilcox JN, Smith KM, Schwartz SM, Gordon D. Localization of tissue factor in the normal vessel wall and in the atherosclerotic plaque. Proc Natl Acad Sci U S A. 1989;86(8):2839-43.
10. Fleck RA, Rao LV, Rapaport SI, Varki N. Localization of human tissue factor antigen by immunostaining with monospecific, polyclonal anti-human tissue factor antibody. Thrombosis research. 1990;59(2):421-37.
11. Geczy CL. Cellular mechanisms for the activation of blood coagulation. Int Rev Cytol. 1994;152:49-108.
12. Camerer E, Kolsto AB, Prydz H. Cell biology of tissue factor, the principal initiator of blood coagulation. Thrombosis research. 1996;81(1):1-41.
13. Yan SF, Mackman N, Kisiel W, Stern DM, Pinsky DJ. Hypoxia/Hypoxemia-Induced activation of the procoagulant pathways and the pathogenesis of ischemia-associated thrombosis. Arteriosclerosis, thrombosis, and vascular biology. 1999;19(9):2029-35.
14. Camera M, Brambilla M, Facchinetti L, Canzano P, Spirito R, Rossetti L, Saccu C, Di Minno MN, Tremoli E. Tissue factor and atherosclerosis: not only vessel wall-derived TF, but also platelet-associated TF. Thrombosis research. 2012;129(3):279-84.
15. Moosbauer C, Morgenstern E, Cuvelier SL, Manukyan D, Bidzhekov K, Albrecht S, Lohse P, Patel KD, Engelmann B. Eosinophils are a major intravascular location for tissue factor storage and exposure. Blood. 2007;109(3):995-1002.
16. Todoroki H, Higure A, Okamoto K, Okazaki K, Nagafuchi Y, Takeda S, Katoh H, Itoh H, Ohsato K, Nakamura S. Possible role of platelet-activating factor in the in vivo expression of tissue factor in neutrophils. The Journal of surgical research. 1998;80(2):149-55.
17. Giesen PL, Rauch U, Bohrmann B, Kling D, Roque M, Fallon JT, Badimon JJ, Himber J, Riederer MA, Nemerson Y. Blood-borne tissue factor: another view of thrombosis. Proc Natl Acad Sci U S A. 1999;96(5):2311-5.
18. Osterud B. Tissue factor/TFPI and blood cells. Thrombosis research. 2012;129(3):274-8.
19. Bogdanov VY, Balasubramanian V, Hathcock J, Vele O, Lieb M, Nemerson Y. Alternatively spliced human tissue factor: a circulating, soluble, thrombogenic protein. Nat Med. 2003;9(4):458-62.

20. Sabatier F, Roux V, Anfosso F, Camoin L, Sampol J, Dignat-George F. Interaction of endothelial microparticles with monocytic cells in vitro induces tissue factor-dependent procoagulant activity. Blood. 2002;99(11):3962-70.
21. Radcliffe R, Nemerson Y. Activation and control of factor VII by activated factor X and thrombin. Isolation and characterization of a single chain form of factor VII. The Journal of biological chemistry. 1975;250(2):388-95.
22. Kisiel W, Davie EW. Isolation and characterization of bovine factor VII. Biochemistry. 1975;14(22):4928-34.
23. Broze GJ, Jr., Majerus PW. Purification and properties of human coagulation factor VII. The Journal of biological chemistry. 1980;255(4):1242-7.
24. Fair DS. Quantitation of factor VII in the plasma of normal and warfarin-treated individuals by radioimmunoassay. Blood. 1983;62(4):784-91.
25. Neuenschwander PF, Fiore MM, Morrissey JH. Factor VII autoactivation proceeds via interaction of distinct protease-cofactor and zymogen-cofactor complexes. Implications of a two-dimensional enzyme kinetic mechanism. The Journal of biological chemistry. 1993;268(29):21489-92.
26. Tavoosi N, Smith SA, Davis-Harrison RL, Morrissey JH. Factor VII and protein C are phosphatidic acid-binding proteins. Biochemistry. 2013;52(33):5545-52.
27. Kondo S, Kisiel W. Regulation of factor VIIa activity in plasma: evidence that antithrombin III is the sole plasma protease inhibitor of human factor VIIa. Thrombosis research. 1987;46(2):325-35.
28. Seligsohn U, Kasper CK, Osterud B, Rapaport SI. Activated factor VII: presence in factor IX concentrates and persistence in the circulation after infusion. Blood. 1979;53(5):828-37.
29. Morrissey JH, Macik BG, Neuenschwander PF, Comp PC. Quantitation of activated factor VII levels in plasma using a tissue factor mutant selectively deficient in promoting factor VII activation. Blood. 1993;81(3):734-44.
30. Kisiel W, Fujikawa K, Davie EW. Activation of bovine factor VII (proconvertin) by factor XIIa (activated Hageman factor). Biochemistry. 1977;16(19):4189-94.
31. Masys DR, Bajaj SP, Rapaport SI. Activation of human factor VII by activated factors IX and X. Blood. 1982;60(5):1143-50.
32. Nemerson Y, Repke D. Tissue factor accelerates the activation of coagulation factor VII: the role of a bifunctional coagulation cofactor. Thrombosis research. 1985;40(3):351-8.
33. Rao LV, Rapaport SI. Activation of factor VII bound to tissue factor: a key early step in the tissue factor pathway of blood coagulation. Proc Natl Acad Sci U S A. 1988;85(18):6687-91.
34. Romisch J. Factor VII activating protease (FSAP): a novel protease in hemostasis. Biological chemistry. 2002;383(7-8):1119-24.
35. Seligsohn U, Osterud B, Brown SF, Griffin JH, Rapaport SI. Activation of human factor VII in plasma and in purified systems: roles of activated factor IX, kallikrein, and activated factor XII. The Journal of clinical investigation. 1979;64(4):1056-65.
36. Tsujioka H, Suehiro A, Kakishita E. Activation of coagulation factor VII by tissue-type plasminogen activator. American journal of hematology. 1999;61(1):34-9.
37. Yamamoto M, Nakagaki T, Kisiel W. Tissue factor-dependent autoactivation of human blood coagulation factor VII. The Journal of biological chemistry. 1992;267(27):19089-94.
38. Wildgoose P, Nemerson Y, Hansen LL, Nielsen FE, Glazer S, Hedner U. Measurement of basal levels of factor VIIa in hemophilia A and B patients. Blood. 1992;80(1):25-8.
39. Miller GJ. Postprandial lipaemia and haemostatic factors. Atherosclerosis. 1998;141 Suppl 1:S47-51.
40. Lefevre M, Kris-Etherton PM, Zhao G, Tracy RP. Dietary fatty acids, hemostasis, and cardiovascular disease risk. J Am Diet Assoc. 2004;104(3):410-9; quiz 92.
41. Nemerson Y, Gentry R. An ordered addition, essential activation model of the tissue factor pathway of coagulation: evidence for a conformational cage. Biochemistry. 1986;25(14):4020-33.

42. Bom VJ, Bertina RM. The contributions of Ca2+, phospholipids and tissue-factor apoprotein to the activation of human blood-coagulation factor X by activated factor VII. The Biochemical journal. 1990;265(2):327-36.
43. Komiyama Y, Pedersen AH, Kisiel W. Proteolytic activation of human factors IX and X by recombinant human factor VIIa: effects of calcium, phospholipids, and tissue factor. Biochemistry. 1990;29(40):9418-25.
44. Maynard JR, Dreyer BE, Stemerman MB, Pitlick FA. Tissue-factor coagulant activity of cultured human endothelial and smooth muscle cells and fibroblasts. Blood. 1977;50(3):387-96.
45. Drake TA, Ruf W, Morrissey JH, Edgington TS. Functional tissue factor is entirely cell surface expressed on lipopolysaccharide-stimulated human blood monocytes and a constitutively tissue factor-producing neoplastic cell line. The Journal of cell biology. 1989;109(1):389-95.
46. Bach R, Rifkin DB. Expression of tissue factor procoagulant activity: regulation by cytosolic calcium. Proc Natl Acad Sci U S A. 1990;87(18):6995-9.
47. Sevinsky JR, Rao LV, Ruf W. Ligand-induced protease receptor translocation into caveolae: a mechanism for regulating cell surface proteolysis of the tissue factor-dependent coagulation pathway. The Journal of cell biology. 1996;133(2):293-304.
48. Mulder AB, Smit JW, Bom VJ, Blom NR, Ruiters MH, Halie MR, van der Meer J. Association of smooth muscle cell tissue factor with caveolae. Blood. 1996;88(4):1306-13.
49. Bach RR, Moldow CF. Mechanism of tissue factor activation on HL-60 cells. Blood. 1997;89(9):3270-6.
50. Ahamed J, Versteeg HH, Kerver M, Chen VM, Mueller BM, Hogg PJ, Ruf W. Disulfide isomerization switches tissue factor from coagulation to cell signaling. Proc Natl Acad Sci U S A. 2006;103(38):13932-7.
51. Versteeg HH, Ruf W. Thiol pathways in the regulation of tissue factor prothrombotic activity. Curr Opin Hematol. 2011;18(5):343-8.
52. Piro O, Broze GJ, Jr. Comparison of cell-surface TFPIalpha and beta. Journal of thrombosis and haemostasis : JTH. 2005;3(12):2677-83.
53. Girard TJ, Warren LA, Novotny WF, Likert KM, Brown SG, Miletich JP, Broze GJ, Jr. Functional significance of the Kunitz-type inhibitory domains of lipoprotein-associated coagulation inhibitor. Nature. 1989;338(6215):518-20.
54. Bajaj MS, Kuppuswamy MN, Manepalli AN, Bajaj SP. Transcriptional expression of tissue factor pathway inhibitor, thrombomodulin and von Willebrand factor in normal human tissues. Thrombosis and haemostasis. 1999;82(3):1047-52.
55. Novotny WF, Girard TJ, Miletich JP, Broze GJ, Jr. Purification and characterization of the lipoprotein-associated coagulation inhibitor from human plasma. The Journal of biological chemistry. 1989;264(31):18832-7.
56. Sandset PM, Lund H, Norseth J, Abildgaard U, Ose L. Treatment with hydroxymethylglutaryl-coenzyme A reductase inhibitors in hypercholesterolemia induces changes in the components of the extrinsic coagulation system. Arteriosclerosis and thrombosis : a journal of vascular biology / American Heart Association. 1991;11(1):138-45.
57. Hansen JB, Huseby NE, Sandset PM, Svensson B, Lyngmo V, Nordoy A. Tissue-factor pathway inhibitor and lipoproteins. Evidence for association with and regulation by LDL in human plasma. Arteriosclerosis and thrombosis : a journal of vascular biology / American Heart Association. 1994;14(2):223-9.
58. Maroney SA, Haberichter SL, Friese P, Collins ML, Ferrel JP, Dale GL, Mast AE. Active tissue factor pathway inhibitor is expressed on the surface of coated platelets. Blood. 2007;109(5):1931-7.
59. Lupu C, Lupu F, Dennehy U, Kakkar VV, Scully MF. Thrombin induces the redistribution and acute release of tissue factor pathway inhibitor from specific granules within human endothelial cells in culture. Arteriosclerosis, thrombosis, and vascular biology. 1995;15(11):2055-62.

60. Lupu C, Poulsen E, Roquefeuil S, Westmuckett AD, Kakkar VV, Lupu F. Cellular effects of heparin on the production and release of tissue factor pathway inhibitor in human endothelial cells in culture. Arteriosclerosis, thrombosis, and vascular biology. 1999;19(9):2251-62.
61. Hansen JB, Svensson B, Olsen R, Ezban M, Osterud B, Paulssen RH. Heparin induces synthesis and secretion of tissue factor pathway inhibitor from endothelial cells in vitro. Thrombosis and haemostasis. 2000;83(6):937-43.
62. Grabowski EF, Zuckerman DB, Nemerson Y. The functional expression of tissue factor by fibroblasts and endothelial cells under flow conditions. Blood. 1993;81(12):3265-70.
63. Westmuckett AD, Lupu C, Roquefeuil S, Krausz T, Kakkar VV, Lupu F. Fluid flow induces upregulation of synthesis and release of tissue factor pathway inhibitor in vitro. Arteriosclerosis, thrombosis, and vascular biology. 2000;20(11):2474-82.
64. Zhang J, Piro O, Lu L, Broze GJ, Jr. Glycosyl phosphatidylinositol anchorage of tissue factor pathway inhibitor. Circulation. 2003;108(5):623-7.
65. Piro O, Broze GJ, Jr. Role for the Kunitz-3 domain of tissue factor pathway inhibitor-alpha in cell surface binding. Circulation. 2004;110(23):3567-72.
66. Chouhan VD, Comerota AJ, Sun L, Harada R, Gaughan JP, Rao AK. Inhibition of tissue factor pathway during intermittent pneumatic compression: A possible mechanism for antithrombotic effect. Arteriosclerosis, thrombosis, and vascular biology. 1999;19(11):2812-7.
67. Sandset PM, Abildgaard U, Larsen ML. Heparin induces release of extrinsic coagulation pathway inhibitor (EPI). Thrombosis research. 1988;50(6):803-13.
68. Novotny WF, Brown SG, Miletich JP, Rader DJ, Broze GJ, Jr. Plasma antigen levels of the lipoprotein-associated coagulation inhibitor in patient samples. Blood. 1991;78(2):387-93.
69. Walenga JM, Jeske WP, Samama MM, Frapaise FX, Bick RL, Fareed J. Fondaparinux: a synthetic heparin pentasaccharide as a new antithrombotic agent. Expert opinion on investigational drugs. 2002;11(3):397-407.
70. Naumnik B, Rydzewska-Rosolowska A, Mysliwiec M. Different effects of enoxaparin, nadroparin, and dalteparin on plasma TFPI during hemodialysis: a prospective crossover randomized study. Clinical and applied thrombosis/hemostasis : official journal of the International Academy of Clinical and Applied Thrombosis/Hemostasis. 2011;17(5):480-6.
71. Chang JY, Monroe DM, Oliver JA, Roberts HR. TFPIbeta, a second product from the mouse tissue factor pathway inhibitor (TFPI) gene. Thrombosis and haemostasis. 1999;81(1):45-9.
72. Hackeng TM, Sere KM, Tans G, Rosing J. Protein S stimulates inhibition of the tissue factor pathway by tissue factor pathway inhibitor. Proc Natl Acad Sci U S A. 2006;103(9):3106-11.
73. Huang ZF, Wun TC, Broze GJ, Jr. Kinetics of factor Xa inhibition by tissue factor pathway inhibitor. The Journal of biological chemistry. 1993;268(36):26950-5.
74. Wesselschmidt R, Likert K, Huang Z, MacPhail L, Broze GJ, Jr. Structural requirements for tissue factor pathway inhibitor interactions with factor Xa and heparin. Blood coagulation & fibrinolysis : an international journal in haemostasis and thrombosis. 1993;4(5):661-9.
75. Huang ZF, Higuchi D, Lasky N, Broze GJ, Jr. Tissue factor pathway inhibitor gene disruption produces intrauterine lethality in mice. Blood. 1997;90(3):944-51.
76. Chan JC, Carmeliet P, Moons L, Rosen ED, Huang ZF, Broze GJ, Jr., Collen D, Castellino FJ. Factor VII deficiency rescues the intrauterine lethality in mice associated with a tissue factor pathway inhibitor deficit. The Journal of clinical investigation. 1999;103(4):475-82.
77. Pedersen B, Holscher T, Sato Y, Pawlinski R, Mackman N. A balance between tissue factor and tissue factor pathway inhibitor is required for embryonic development and hemostasis in adult mice. Blood. 2005;105(7):2777-82.
78. Rao LV, Rapaport SI, Hoang AD. Binding of factor VIIa to tissue factor permits rapid antithrombin III/heparin inhibition of factor VIIa. Blood. 1993;81(10):2600-7.

79. Lawson JH, Butenas S, Ribarik N, Mann KG. Complex-dependent inhibition of factor VIIa by antithrombin III and heparin. The Journal of biological chemistry. 1993;268(2):767-70.
80. Tipping PG, Malliaros J, Holdsworth SR. Procoagulant activity expression by macrophages from atheromatous vascular plaques. Atherosclerosis. 1989;79(2-3):237-43.
81. Ichikawa K, Nakagawa K, Hirano K, Sueishi K. The localization of tissue factor and apolipoprotein(a) in atherosclerotic lesions of the human aorta and their relation to fibrinogen-fibrin transition. Pathology, research and practice. 1996;192(3):224-32.
82. Marmur JD, Thiruvikraman SV, Fyfe BS, Guha A, Sharma SK, Ambrose JA, Fallon JT, Nemerson Y, Taubman MB. Identification of active tissue factor in human coronary atheroma. Circulation. 1996;94(6):1226-32.
83. Thiruvikraman SV, Guha A, Roboz J, Taubman MB, Nemerson Y, Fallon JT. In situ localization of tissue factor in human atherosclerotic plaques by binding of digoxigenin-labeled factors VIIa and X. Laboratory investigation; a journal of technical methods and pathology. 1996;75(4):451-61.
84. Forrester JS, Litvack F, Grundfest W, Hickey A. A perspective of coronary disease seen through the arteries of living man. Circulation. 1987;75(3):505-13.
85. Thaler J, Ay C, Mackman N, Bertina RM, Kaider A, Marosi C, Key NS, Barcel DA, Scheithauer W, Kornek G, Zielinski C, Pabinger I. Microparticle-associated tissue factor activity, venous thromboembolism and mortality in pancreatic, gastric, colorectal and brain cancer patients. Journal of thrombosis and haemostasis : JTH. 2012;10(7):1363-70.
86. Drake TA, Cheng J, Chang A, Taylor FB, Jr. Expression of tissue factor, thrombomodulin, and E-selectin in baboons with lethal Escherichia coli sepsis. The American journal of pathology. 1993;142(5):1458-70.
87. Taylor FB, Jr. Role of tissue factor and factor VIIa in the coagulant and inflammatory response to LD100 Escherichia coli in the baboon. Haemostasis. 1996;26 Suppl 1:83-91.
88. Taylor FB, Jr., Chang A, Ruf W, Morrissey JH, Hinshaw L, Catlett R, Blick K, Edgington TS. Lethal E. coli septic shock is prevented by blocking tissue factor with monoclonal antibody. Circulatory shock. 1991;33(3):127-34.
89. Meade TW, Mellows S, Brozovic M, Miller GJ, Chakrabarti RR, North WR, Haines AP, Stirling Y, Imeson JD, Thompson SG. Haemostatic function and ischaemic heart disease: principal results of the Northwick Park Heart Study. Lancet. 1986;2(8506):533-7.
90. Balleisen L, Schulte H, Assmann G, Epping PH, van de Loo J. Coagulation factors and the progress of coronary heart disease. Lancet. 1987;2(8556):461.
91. Ruddock V, Meade TW. Factor-VII activity and ischaemic heart disease: fatal and non-fatal events. QJM : monthly journal of the Association of Physicians. 1994;87(7):403-6.
92. Broadhurst P, Kelleher C, Hughes L, Imeson JD, Raftery EB. Fibrinogen, factor VII clotting activity and coronary artery disease severity. Atherosclerosis. 1990;85(2-3):169-73.
93. Carvalho de Sousa J, Azevedo J, Soria C, Barros F, Ribeiro C, Parreira F, Caen JP. Factor VII hyperactivity in acute myocardial thrombosis. A relation to the coagulation activation. Thrombosis research. 1988;51(2):165-73.
94. Cortellaro M, Boschetti C, Cofrancesco E, Zanussi C, Catalano M, de Gaetano G, Gabrielli L, Lombardi B, Specchia G, Tavazzi L, et al. The PLAT Study: hemostatic function in relation to atherothrombotic ischemic events in vascular disease patients. Principal results. PLAT Study Group. Progetto Lombardo Atero-Trombosi (PLAT) Study Group. Arteriosclerosis and thrombosis : a journal of vascular biology / American Heart Association. 1992;12(9):1063-70.
95. Hoffman C, Shah A, Sodums M, Hultin MB. Factor VII activity state in coronary artery disease. The Journal of laboratory and clinical medicine. 1988;111(4):475-81.
96. Hoffman CJ, Miller RH, Lawson WE, Hultin MB. Elevation of factor VII activity and mass in young adults at risk of ischemic heart disease. Journal of the American College of Cardiology. 1989;14(4):941-6.

97. Kario K, Sakata T, Matsuo T, Miyata T. Factor VII in non-insulin-dependent diabetic patients with microalbuminuria. Lancet. 1993;342(8886-8887):1552.
98. Kario K, Matsuo T, Sakata T, Miyata T. Factor VII hyperactivity and ischaemic heart disease. Lancet. 1994;343(8891):233.
99. Kario K, Matsuo T, Matsuo M, Koide M, Yamada T, Nakamura S, Sakata T, Kato H, Miyata T. Marked increase of activated factor VII in uremic patients. Thrombosis and haemostasis. 1995;73(5):763-7.
100. Orlando M, Leri O, Macioce G, Mattia G, Ferri GM. Factor VII in subjects at risk for thromboembolism: activation or increased synthesis? Haemostasis. 1987;17(6):340-3.
101. Suzuki T, Yamauchi K, Matsushita T, Furumichi T, Furui H, Tsuzuki J, Saito H. Elevation of factor VII activity and mass in coronary artery disease of varying severity. Clinical cardiology. 1991;14(9):731-6.
102. Hultin MB. Fibrinogen and factor VII as risk factors in vascular disease. Progress in hemostasis and thrombosis. 1991;10:215-41.
103. Grant PJ. The genetics of atherothrombotic disorders: a clinician's view. Journal of thrombosis and haemostasis : JTH. 2003;1(7):1381-90.
104. Folsom AR, Wu KK, Shahar E, Davis CE. Association of hemostatic variables with prevalent cardiovascular disease and asymptomatic carotid artery atherosclerosis. The Atherosclerosis Risk in Communities (ARIC) Study Investigators. Arteriosclerosis and thrombosis : a journal of vascular biology / American Heart Association. 1993;13(12):1829-36.
105. Moor E, Silveira A, van't Hooft F, Suontaka AM, Eriksson P, Blomback M, Hamsten A. Coagulation factor VII mass and activity in young men with myocardial infarction at a young age. Role of plasma lipoproteins and factor VII genotype. Arteriosclerosis, thrombosis, and vascular biology. 1995;15(5):655-64.
106. Koster T, Rosendaal FR, Reitsma PH, van der Velden PA, Briet E, Vandenbroucke JP. Factor VII and fibrinogen levels as risk factors for venous thrombosis. A case-control study of plasma levels and DNA polymorphisms--the Leiden Thrombophilia Study (LETS). Thrombosis and haemostasis. 1994;71(6):719-22.
107. Sosef MN, Bosch JG, van Oostayen J, Visser T, Reiber JH, Rosendaal FR. Relation of plasma coagulation factor VII and fibrinogen to carotid artery intima-media thickness. Thrombosis and haemostasis. 1994;72(2):250-4.
108. Vaziri ND, Kennedy SC, Kennedy D, Gonzales E. Coagulation, fibrinolytic, and inhibitory proteins in acute myocardial infarction and angina pectoris. The American journal of medicine. 1992;93(6):651-7.
109. Kalaria VG, Zareba W, Moss AJ, Pancio G, Marder VJ, Morrissey JH, Weiss HJ, Sparks CE, Greenberg H, Dwyer E, Goldstein R, Watelet LF. Gender-related differences in thrombogenic factors predicting recurrent cardiac events in patients after acute myocardial infarction. The THROMBO Investigators. The American journal of cardiology. 2000;85(12):1401-8.
110. Danielsen R, Onundarson PT, Thors H, Vidarsson B, Morrissey JH. Activated and total coagulation factor VII, and fibrinogen in coronary artery disease. Scandinavian cardiovascular journal : SCJ. 1998;32(2):87-95.
111. Cooper JA, Miller GJ, Bauer KA, Morrissey JH, Meade TW, Howarth DJ, Barzegar S, Mitchell JP, Rosenberg RD. Comparison of novel hemostatic factors and conventional risk factors for prediction of coronary heart disease. Circulation. 2000;102(23):2816-22.
112. Silverberg M, Dunn JT, Garen L, Kaplan AP. Autoactivation of human Hageman factor. Demonstration utilizing a synthetic substrate. The Journal of biological chemistry. 1980;255(15):7281-6.
113. Tankersley DL, Finlayson JS. Kinetics of activation and autoactivation of human factor XII. Biochemistry. 1984;23(2):273-9.
114. Muller F, Gailani D, Renne T. Factor XI and XII as antithrombotic targets. Curr Opin Hematol. 2011;18(5):349-55.

115. Renne T, Schmaier AH, Nickel KF, Blomback M, Maas C. In vivo roles of factor XII. Blood. 2012;120(22):4296-303.
116. Mandle R, Jr., Kaplan AP. Hageman factor substrates. Human plasma prekallikrein: mechanism of activation by Hageman factor and participation in hageman factor-dependent fibrinolysis. The Journal of biological chemistry. 1977;252(17):6097-104.
117. Griffin JH, Cochrane CG. Mechanisms for the involvement of high molecular weight kininogen in surface-dependent reactions of Hageman factor. Proc Natl Acad Sci U S A. 1976;73(8):2554-8.
118. Larsson M, Rayzman V, Nolte MW, Nickel KF, Bjorkqvist J, Jamsa A, Hardy MP, Fries M, Schmidbauer S, Hedenqvist P, Broome M, Pragst I, Dickneite G, Wilson MJ, Nash AD, Panousis C, Renne T. A factor XIIa inhibitory antibody provides thromboprotection in extracorporeal circulation without increasing bleeding risk. Science translational medicine. 2014;6(222):222ra17.
119. Schmaier AH. Assembly, activation, and physiologic influence of the plasma kallikrein/kinin system. International Immunopharmacology. 2008;8(2):161-5.
120. Kannemeier C, Shibamiya A, Nakazawa F, Trusheim H, Ruppert C, Markart P, Song Y, Tzima E, Kennerknecht E, Niepmann M, von Bruehl ML, Sedding D, Massberg S, Gunther A, Engelmann B, Preissner KT. Extracellular RNA constitutes a natural procoagulant cofactor in blood coagulation. Proc Natl Acad Sci U S A. 2007;104(15):6388-93.
121. Muller F, Mutch NJ, Schenk WA, Smith SA, Esterl L, Spronk HM, Schmidbauer S, Gahl WA, Morrissey JH, Renne T. Platelet polyphosphates are proinflammatory and procoagulant mediators in vivo. Cell. 2009;139(6):1143-56. Epub 2009/12/17.
122. Maas C, Govers-Riemslag JW, Bouma B, Schiks B, Hazenberg BP, Lokhorst HM, Hammarstrom P, ten Cate H, de Groot PG, Bouma BN, Gebbink MF. Misfolded proteins activate factor XII in humans, leading to kallikrein formation without initiating coagulation. The Journal of clinical investigation. 2008;118(9):3208-18.
123. Brunnee T, Reddigari SR, Shibayama Y, Kaplan AP, Silverberg M. Mast cell derived heparin activates the contact system: a link to kinin generation in allergic reactions. Clinical and experimental allergy : journal of the British Society for Allergy and Clinical Immunology. 1997;27(6):653-63.
124. Hojima Y, Cochrane CG, Wiggins RC, Austen KF, Stevens RL. In vitro activation of the contact (Hageman factor) system of plasma by heparin and chondroitin sulfate E. Blood. 1984;63(6):1453-9.
125. Herwald H, Morgelin M, Olsen A, Rhen M, Dahlback B, Muller-Esterl W, Bjorck L. Activation of the contact-phase system on bacterial surfaces--a clue to serious complications in infectious diseases. Nat Med. 1998;4(3):298-302.
126. Nickel KF, Renne T. Crosstalk of the plasma contact system with bacteria. Thrombosis research. 2012;130 Suppl 1:S78-83.
127. Joseph K, Ghebrehiwet B, Kaplan AP. Activation of the kinin-forming cascade on the surface of endothelial cells. Biological chemistry. 2001;382(1):71-5.
128. Kaplan AP, Ghebrehiwet B. The plasma bradykinin-forming pathways and its interrelationships with complement. Molecular immunology. 2010;47(13):2161-9.
129. Martinod K, Wagner DD. Thrombosis: tangled up in NETs. Blood. 2014;123(18):2768-76.
130. Geddings JE, Mackman N. New players in haemostasis and thrombosis. Thrombosis and haemostasis. 2014;111(4):570-4.
131. Ault-Riche D, Fraley CD, Tzeng CM, Kornberg A. Novel assay reveals multiple pathways regulating stress-induced accumulations of inorganic polyphosphate in Escherichia coli. Journal of bacteriology. 1998;180(7):1841-7.
132. Brown MR, Kornberg A. Inorganic polyphosphate in the origin and survival of species. Proc Natl Acad Sci U S A. 2004;101(46):16085-7.
133. Docampo R, Moreno SN. Acidocalcisomes. Cell calcium. 2011;50(2):113-9.

134. Kornberg A, Rao NN, Ault-Riche D. Inorganic polyphosphate: a molecule of many functions. Annu Rev Biochem. 1999;68:89-125.
135. Ruiz FA, Lea CR, Oldfield E, Docampo R. Human platelet dense granules contain polyphosphate and are similar to acidocalcisomes of bacteria and unicellular eukaryotes. The Journal of biological chemistry. 2004;279(43):44250-7.
136. Moreno-Sanchez D, Hernandez-Ruiz L, Ruiz FA, Docampo R. Polyphosphate is a novel pro-inflammatory regulator of mast cells and is located in acidocalcisomes. The Journal of biological chemistry. 2012;287(34):28435-44.
137. Pisoni RL, Lindley ER. Incorporation of [32P]orthophosphate into long chains of inorganic polyphosphate within lysosomes of human fibroblasts. The Journal of biological chemistry. 1992;267(6):3626-31.
138. Kumble KD, Kornberg A. Inorganic polyphosphate in mammalian cells and tissues. The Journal of biological chemistry. 1995;270(11):5818-22.
139. Smith SA, Mutch NJ, Baskar D, Rohloff P, Docampo R, Morrissey JH. Polyphosphate modulates blood coagulation and fibrinolysis. Proc Natl Acad Sci U S A. 2006;103(4):903-8. Epub 2006/01/18.
140. Choi SH, Collins JN, Smith SA, Davis-Harrison RL, Rienstra CM, Morrissey JH. Phosphoramidate end labeling of inorganic polyphosphates: facile manipulation of polyphosphate for investigating and modulating its biological activities. Biochemistry. 2010;49(45):9935-41. Epub 2010/10/21.
141. Smith SA, Choi SH, Davis-Harrison R, Huyck J, Boettcher J, Rienstra CM, Morrissey JH. Polyphosphate exerts differential effects on blood clotting, depending on polymer size. Blood. 2010;116(20):4353-9. Epub 2010/08/17.
142. Smith SA, Choi SH, Collins JN, Travers RJ, Cooley BC, Morrissey JH. Inhibition of polyphosphate as a novel strategy for preventing thrombosis and inflammation. Blood. 2012;120(26):5103-10.
143. Shibayama Y, Joseph K, Nakazawa Y, Ghebreihiwet B, Peerschke EI, Kaplan AP. Zinc-dependent activation of the plasma kinin-forming cascade by aggregated beta amyloid protein. Clinical immunology. 1999;90(1):89-99.
144. Bergamaschini L, Donarini C, Foddi C, Gobbo G, Parnetti L, Agostoni A. The region 1-11 of Alzheimer amyloid-beta is critical for activation of contact-kinin system. Neurobiology of aging. 2001;22(1):63-9.
145. Bergamaschini L, Parnetti L, Pareyson D, Canziani S, Cugno M, Agostoni A. Activation of the contact system in cerebrospinal fluid of patients with Alzheimer disease. Alzheimer Dis Assoc Disord. 1998;12(2):102-8.
146. Silverberg M, Diehl SV. The autoactivation of factor XII (Hageman factor) induced by low-Mr heparin and dextran sulphate. The effect of the Mr of the activating polyanion. The Biochemical journal. 1987;248(3):715-20.
147. Noga O, Brunnee T, Schaper C, Kunkel G. Heparin, derived from the mast cells of human lungs is responsible for the generation of kinins in allergic reactions due to the activation of the contact system. International archives of allergy and immunology. 1999;120(4):310-6.
148. Kishimoto TK, Viswanathan K, Ganguly T, Elankumaran S, Smith S, Pelzer K, Lansing JC, Sriranganathan N, Zhao G, Galcheva-Gargova Z, Al-Hakim A, Bailey GS, Fraser B, Roy S, Rogers-Cotrone T, Buhse L, Whary M, Fox J, Nasr M, Dal Pan GJ, Shriver Z, Langer RS, Venkataraman G, Austen KF, Woodcock J, Sasisekharan R. Contaminated heparin associated with adverse clinical events and activation of the contact system. The New England journal of medicine. 2008;358(23):2457-67.
149. Sala-Cunill A, Bjorkqvist J, Senter R, Guilarte M, Cardona V, Labrador M, Nickel KF, Butler L, Luengo O, Kumar P, Labberton L, Long A, Di Gennaro A, Kenne E, Jamsa A, Krieger T, Schluter H, Fuchs T, Flohr S, Hassiepen U, Cumin F, McCrae K, Maas C, Stavrou E, Renne T. Plasma contact system activation drives anaphylaxis in severe mast cell-mediated allergic reactions. The Journal of allergy and clinical immunology. 2015;135(4):1031-43 e6.

150. Zeerleder S. C1-inhibitor: more than a serine protease inhibitor. Seminars in thrombosis and hemostasis. 2011;37(4):362-74.
151. Walford HH, Zuraw BL. Current update on cellular and molecular mechanisms of hereditary angioedema. Annals of allergy, asthma & immunology : official publication of the American College of Allergy, Asthma, & Immunology. 2014;112(5):413-8.
152. Karlsrud TS, Buo L, Aasen AO, Johansen HT. Bradykinin release from high molecular weight kininogen in surgical ICU patients. Immunopharmacology. 1996;33(1-3):365-8.
153. Karlsrud TS, Buo L, Aasen AO, Johansen HT. Cleavage of plasma high molecular weight kininogen in surgical ICU patients. Intensive care medicine. 1996;22(8):760-5.
154. Kaufman N, Page JD, Pixley RA, Schein R, Schmaier AH, Colman RW. Alpha 2-macroglobulin-kallikrein complexes detect contact system activation in hereditary angioedema and human sepsis. Blood. 1991;77(12):2660-7.
155. Gailani D, Renne T. Intrinsic pathway of coagulation and arterial thrombosis. Arteriosclerosis, thrombosis, and vascular biology. 2007;27(12):2507-13.
156. Muller F, Renné T. Novel roles for factor XII-driven plasma contact activation system. Current Opinion in Hematology. 2008;15(5):516-21.
157. Grundt H, Nilsen DW, Hetland O, Valente E, Fagertun HE. Activated factor 12 (FXIIa) predicts recurrent coronary events after an acute myocardial infarction. American heart journal. 2004;147(2):260-6.
158. Doggen CJ, Rosendaal FR, Meijers JC. Levels of intrinsic coagulation factors and the risk of myocardial infarction among men: Opposite and synergistic effects of factors XI and XII. Blood. 2006;108(13):4045-51.
159. Salomon O, Steinberg DM, Koren-Morag N, Tanne D, Seligsohn U. Reduced incidence of ischemic stroke in patients with severe factor XI deficiency. Blood. 2008;111(8):4113-7.
160. Renne T, Pozgajova M, Gruner S, Schuh K, Pauer HU, Burfeind P, Gailani D, Nieswandt B. Defective thrombus formation in mice lacking coagulation factor XII. The Journal of experimental medicine. 2005;202(2):271-81.
161. Kleinschnitz C, Stoll G, Bendszus M, Schuh K, Pauer HU, Burfeind P, Renne C, Gailani D, Nieswandt B, Renne T. Targeting coagulation factor XII provides protection from pathological thrombosis in cerebral ischemia without interfering with hemostasis. The Journal of experimental medicine. 2006;203(3):513-8.
162. Jain S, Pitoc GA, Holl EK, Zhang Y, Borst L, Leong KW, Lee J, Sullenger BA. Nucleic acid scavengers inhibit thrombosis without increasing bleeding. Proc Natl Acad Sci U S A. 2012;109(32):12938-43. Epub 2012/07/28.
163. Travers RJ, Shenoi RA, Kalathottukaren MT, Kizhakkedathu JN, Morrissey JH. Nontoxic polyphosphate inhibitors reduce thrombosis while sparing hemostasis. Blood. 2014;124(22):3183-90.
164. Bussey H, Francis JL, Heparin Consensus G. Heparin overview and issues. Pharmacotherapy. 2004;24(8 Pt 2):103S-7S.
165. Alban S. Adverse effects of heparin. Handbook of experimental pharmacology. 2012(207):211-63.
166. Chudasama SL, Espinasse B, Hwang F, Qi R, Joglekar M, Afonina G, Wiesner MR, Welsby IJ, Ortel TL, Arepally GM. Heparin modifies the immunogenicity of positively charged proteins. Blood. 2010;116(26):6046-53.
167. Dasararaju R, Singh N, Mehta A. Heparin induced thrombocytopenia: review. Expert review of hematology. 2013;6(4):419-28.
168. Weitz JI. Low-molecular-weight heparins. The New England journal of medicine. 1997;337(10):688-98.
169. van Veen JJ, Maclean RM, Hampton KK, Laidlaw S, Kitchen S, Toth P, Makris M. Protamine reversal of low molecular weight heparin: clinically effective? Blood coagulation & fibrinolysis : an international journal in haemostasis and thrombosis. 2011;22(7):565-70.

170. Elliott MJ, Zimmerman D, Holden RM. Warfarin anticoagulation in hemodialysis patients: a systematic review of bleeding rates. American journal of kidney diseases : the official journal of the National Kidney Foundation. 2007;50(3):433-40.
171. Neidecker M, Patel AA, Nelson WW, Reardon G. Use of warfarin in long-term care: a systematic review. BMC Geriatr. 2012;12:14.
172. Kuruvilla M, Gurk-Turner C. A review of warfarin dosing and monitoring. Proc (Bayl Univ Med Cent). 2001;14(3):305-6.
173. Adam SS, McDuffie JR, Ortel TL, Williams JW, Jr. Comparative effectiveness of warfarin and new oral anticoagulants for the management of atrial fibrillation and venous thromboembolism: a systematic review. Annals of internal medicine. 2012;157(11):796-807.
174. Goy J, Crowther M. Approaches to diagnosing and managing anticoagulant-related bleeding. Seminars in thrombosis and hemostasis. 2012;38(7):702-10.
175. Yau JW, Liao P, Fredenburgh JC, Stafford AR, Revenko AS, Monia BP, Weitz JI. Selective depletion of factor XI or factor XII with antisense oligonucleotides attenuates catheter thrombosis in rabbits. Blood. 2014;123(13):2102-7.
176. Crosby JR, Marzec U, Revenko AS, Zhao C, Gao D, Matafonov A, Gailani D, MacLeod AR, Tucker EI, Gruber A, Hanson SR, Monia BP. Antithrombotic effect of antisense factor XI oligonucleotide treatment in primates. Arteriosclerosis, thrombosis, and vascular biology. 2013;33(7):1670-8.
177. Buller HR, Bethune C, Bhanot S, Gailani D, Monia BP, Raskob GE, Segers A, Verhamme P, Weitz JI, Investigators F-AT. Factor XI antisense oligonucleotide for prevention of venous thrombosis. The New England journal of medicine. 2015;372(3):232-40.
178. Docampo R, Moreno SN. The acidocalcisome. Molecular and biochemical parasitology. 2001;114(2):151-9.
179. Kornberg A. Inorganic polyphosphate: toward making a forgotten polymer unforgettable. Journal of bacteriology. 1995;177(3):491-6.
180. Moreno SN, Docampo R. Polyphosphate and its diverse functions in host cells and pathogens. PLoS pathogens. 2013;9(5):e1003230.
181. Rao NN, Gomez-Garcia MR, Kornberg A. Inorganic Polyphosphate: Essential for Growth and Survival. Annual Review of Biochemistry. 2009;78:605-47.
182. Freimoser FM, Hurlimann HC, Jakob CA, Werner TP, Amrhein N. Systematic screening of polyphosphate (poly P) levels in yeast mutant cells reveals strong interdependence with primary metabolism. Genome Biology. 2006;7(11).
183. Keasling JD. Regulation of intracellular toxic metals and other cations by hydrolysis of polyphosphate. Annals of the New York Academy of Sciences. 1997;829:242-9.
184. Andreeva N, Ryazanova L, Dmitriev V, Kulakovskaya T, Kulaev I. Cytoplasmic inorganic polyphosphate participates in the heavy metal tolerance of Cryptococcus humicola. Folia microbiologica. 2014;59(5):381-9.
185. Gray MJ, Wholey WY, Wagner NO, Cremers CM, Mueller-Schickert A, Hock NT, Krieger AG, Smith EM, Bender RA, Bardwell JC, Jakob U. Polyphosphate is a primordial chaperone. Molecular cell. 2014;53(5):689-99.
186. Rashid MH, Rumbaugh K, Passador L, Davies DG, Hamood AN, Iglewski BH, Kornberg A. Polyphosphate kinase is essential for biofilm development, quorum sensing, and virulence of Pseudomonas aeruginosa. Proc Natl Acad Sci U S A. 2000;97(17):9636-41.
187. Tunpiboonsak S, Mongkolrob R, Kitudomsub K, Thanwatanaying P, Kiettipirodom W, Tungboontina Y, Tungpradabkul S. Role of a Burkholderia pseudomallei polyphosphate kinase in an oxidative stress response, motilities, and biofilm formation. Journal of microbiology. 2010;48(1):63-70.

188. Peng L, Luo WY, Zhao T, Wan CS, Jiang Y, Chi F, Zhao W, Cao H, Huang SH. Polyphosphate kinase 1 is required for the pathogenesis process of meningitic Escherichia coli K1 (RS218). Future microbiology. 2012;7(3):411-23.
189. Pavlov E, Aschar-Sobbi R, Campanella M, Turner RJ, Gomez-Garcia MR, Abramov AY. Inorganic polyphosphate and energy metabolism in mammalian cells. The Journal of biological chemistry. 2010;285(13):9420-8.
190. Wang X, Schroder HC, Feng Q, Diehl-Seifert B, Grebenjuk VA, Muller WE. Isoquercitrin and polyphosphate co-enhance mineralization of human osteoblast-like SaOS-2 cells via separate activation of two RUNX2 cofactors AFT6 and Ets1. Biochemical pharmacology. 2014;89(3):413-21.
191. Hernandez-Ruiz L, Gonzalez-Garcia I, Castro C, Brieva JA, Ruiz FA. Inorganic polyphosphate and specific induction of apoptosis in human plasma cells. Haematologica-the Hematology Journal. 2006;91(9):1180-6.
192. Ghosh S, Shukla D, Suman K, Lakshmi BJ, Manorama R, Kumar S, Bhandari R. Inositol hexakisphosphate kinase 1 maintains hemostasis in mice by regulating platelet polyphosphate levels. Blood. 2013;122(8):1478-86.
193. Kretz CA, Vaezzadeh N, Gross PL. Tissue Factor and Thrombosis Models. Arteriosclerosis Thrombosis and Vascular Biology. 2010;30(5):900-8.
194. Colman RW, Schmaier AH. Contact system: a vascular biology modulator with anticoagulant, profibrinolytic, antiadhesive, and proinflammatory attributes. Blood. 1997;90(10):3819-43. Epub 1997/11/14.
195. Oehmcke S, Morgelin M, Herwald H. Activation of the human contact system on neutrophil extracellular traps. Journal of innate immunity. 2009;1(3):225-30.
196. Gansler J, Jaax M, Leiting S, Appel B, Greinacher A, Fischer S, Preissner KT. Structural requirements for the procoagulant activity of nucleic acids. PLoS One. 2012;7(11):e50399.
197. Brenner B, Laor A, Lupo H, Zivelin A, Lanir N, Seligsohn U. Bleeding predictors in factor-XI-deficient patients. Blood coagulation & fibrinolysis : an international journal in haemostasis and thrombosis. 1997;8(8):511-5.
198. Gailani D, Broze GJ, Jr. Factor XI activation in a revised model of blood coagulation. Science. 1991;253(5022):909-12.
199. Choi SH, Smith SA, Morrissey JH. Polyphosphate is a cofactor for the activation of factor XI by thrombin. Blood. 2011;118(26):6963-70.
200. Choi SH, Smith SA, Morrissey JH. Polyphosphate accelerates factor V activation by factor XIa. Thrombosis and haemostasis. 2014;113(2).
201. Smith SA, Morrissey JH. Polyphosphate as a general procoagulant agent. Journal of Thrombosis and Haemostasis. 2008;6(10):1750-6.
202. Smith SA, Morrissey JH. Polyphosphate enhances fibrin clot structure. Blood. 2008;112(7):2810-6. Epub 2008/06/12.
203. Mutch NJ, Engel R, de Willige SU, Philippou H, Ariens RAS. Polyphosphate modifies the fibrin network and down-regulates fibrinolysis by attenuating binding of tPA and plasminogen to fibrin. Blood. 2010;115(19):3980-8.
204. McFadyen JD, Jackson SP. Differentiating haemostasis from thrombosis for therapeutic benefit. Thrombosis and haemostasis. 2013;110(5):859-67. Epub 2013/08/16.
205. Stalker TJ, Traxler EA, Wu J, Wannemacher KM, Cermignano SL, Voronov R, Diamond SL, Brass LF. Hierarchical organization in the hemostatic response and its relationship to the platelet-signaling network. Blood. 2013;121(10):1875-85.
206. Bae JS, Lee W, Rezaie AR. Polyphosphate elicits pro-inflammatory responses that are counteracted by activated protein C in both cellular and animal models. Journal of thrombosis and haemostasis : JTH. 2012;10(6):1145-51.

207. Semeraro F, Ammollo CT, Morrissey JH, Dale GL, Friese P, Esmon NL, Esmon CT. Extracellular histones promote thrombin generation through platelet-dependent mechanisms: involvement of platelet TLR2 and TLR4. Blood. 2011;118(7):1952-61. Epub 2011/06/16.
208. Koupenova M, Freedman JE. Platelets: the unsung hero of the immune response. Journal of thrombosis and haemostasis : JTH. 2015;13(2):268-70.
209. Duerschmied D, Bode C, Ahrens I. Immune functions of platelets. Thrombosis and haemostasis. 2014;112(4):678-91.
210. Garraud O, Hamzeh-Cognasse H, Pozzetto B, Cavaillon JM, Cognasse F. Bench-to-bedside review: Platelets and active immune functions - new clues for immunopathology? Critical care. 2013;17(4).
211. Martin P, Van Mooy BA. Fluorometric quantification of polyphosphate in environmental plankton samples: extraction protocols, matrix effects, and nucleic acid interference. Appl Environ Microbiol. 2013;79(1):273-81.
212. Wang J, Dore S. Inflammation after intracerebral hemorrhage. Journal of cerebral blood flow and metabolism : official journal of the International Society of Cerebral Blood Flow and Metabolism. 2007;27(5):894-908.
213. Kudela D, Smith SA, May-Masnou A, Braun GB, Pallaoro A, Nguyen CK, Chuong TT, Nownes S, Allen R, Parker NR, Rashidi HH, Morrissey JH, Stucky GD. Clotting Activity of Polyphosphate-Functionalized Silica Nanoparticles. Angewandte Chemie. 2015.
214. Morrissey JH. Polyphosphate: a link between platelets, coagulation and inflammation. International journal of hematology. 2012;95(4):346-52. Epub 2012/04/06.
215. Werner TP, Amrhein N, Freimoser FM. Specific localization of inorganic polyphosphate (poly P) in fungal cell walls by selective extraction and immunohistochemistry. Fungal genetics and biology : FG & B. 2007;44(9):845-52. Epub 2007/02/27.
216. Rangarajan ES, Nadeau G, Li Y, Wagner J, Hung MN, Schrag JD, Cygler M, Matte A. The structure of the exopolyphosphatase (PPX) from Escherichia coli O157:H7 suggests a binding mode for long polyphosphate chains. J Mol Biol. 2006;359(5):1249-60.
217. Kerbiriou-Nabias D. Platelet polyphosphates: new mediators linking thrombosis with inflammation. M S-Medecine Sciences. 2010;26(4):343-6.
218. Merkulov S, Zhang WM, Komar AA, Schmaier AH, Barnes E, Zhou Y, Lu X, Iwaki T, Castellino FJ, Luo G, McCrae KR. Deletion of murine kininogen gene 1 (mKng1) causes loss of plasma kininogen and delays thrombosis. Blood. 2008;111(3):1274-81.
219. Hagedorn I, Schmidbauer S, Pleines I, Kleinschnitz C, Kronthaler U, Stoll G, Dickneite G, Nieswandt B. Factor XIIa inhibitor recombinant human albumin Infestin-4 abolishes occlusive arterial thrombus formation without affecting bleeding. Circulation. 2010;121(13):1510-7.
220. Smith SA, Morrissey JH. Rapid and efficient incorporation of tissue factor into liposomes. Journal of thrombosis and haemostasis : JTH. 2004;2(7):1155-62.
221. Cooley BC. In vivo fluorescence imaging of large-vessel thrombosis in mice. Arteriosclerosis, thrombosis, and vascular biology. 2011;31(6):1351-6.
222. Mutch NJ, Myles T, Leung LLK, Morrissey JH. Polyphosphate binds with high affinity to exosite II of thrombin. Journal of Thrombosis and Haemostasis. 2010;8(3):548-55.
223. Schuksz M, Fuster MM, Brown JR, Crawford BE, Ditto DP, Lawrence R, Glass CA, Wang L, Tor Y, Esko JD. Surfen, a small molecule antagonist of heparan sulfate. Proc Natl Acad Sci U S A. 2008;105(35):13075-80.
224. Saito K, Ohtomo R, Kuga-Uetake Y, Aono T, Saito M. Direct labeling of polyphosphate at the ultrastructural level in Saccharomyces cerevisiae by using the affinity of the polyphosphate binding domain of Escherichia coli exopolyphosphatase. Appl Environ Microbiol. 2005;71(10):5692-701.

225. Rotteveel RC, Roozendaal KJ, Weijers RN, Eijsman L. Influence of heparin, protamine and polybrene on the time integral of thrombin generation (endogenous thrombin potential). Haemostasis. 1996;26(1):1-10.
226. Kim KS, Rao NN, Fraley CD, Kornberg A. Inorganic polyphosphate is essential for long-term survival and virulence factors in Shigella and Salmonella spp. Proc Natl Acad Sci U S A. 2002;99(11):7675-80.
227. Michalski R, Lane DA, Pepper DS, Kakkar VV. Neutralization of heparin in plasma by platelet factor 4 and protamine sulphate. British journal of haematology. 1978;38(4):561-71.
228. Boas U, Heegaard PM. Dendrimers in drug research. Chem Soc Rev. 2004;33(1):43-63.
229. Morrissey JH. Tissue factor: a key molecule in hemostatic and nonhemostatic systems. International journal of hematology. 2004;79(2):103-8.
230. Chu AJ, Wang ZG, Raicu M, Beydoun S, Ramos N. Protamine inhibits tissue factor-initiated extrinsic coagulation. British journal of haematology. 2001;115(2):392-9.
231. Corona-de-la-Pena N, Uribe-Carvajal S, Barrientos-Rios R, Matias-Aguilar L, Montiel-Manzano G, Majluf-Cruz A. Polyamines inhibit both platelet aggregation and glycoprotein IIb/IIIa activation. Journal of cardiovascular pharmacology. 2005;46(2):216-21.
232. Via LD, Francesconi M, Mazzucato M, Pradella P, De Marco L, Vecchia FD, Rascio N, Deana R. On the mechanism of the spermine-exerted inhibition on alpha-thrombin-induced platelet activation. Thrombosis research. 2000;98(1):59-71.
233. Pakala R. Effect of polyamines on in vitro platelet aggregation and in vivo thrombus formation. Cardiovasc Radiat Med. 2002;3(3-4):213-20.
234. Joseph S, Krishnamurthi S, Kakkar VV. Effect of the polyamine-spermine on agonist-induced human platelet activation--specific inhibition of "aggregation-independent" events induced by thrombin, but not by collagen, thromboxane mimetic, phorbol ester or calcium ionophore. Thrombosis and haemostasis. 1987;57(2):191-5.
235. Mendez JD, Zarzoza E. Inhibition of platelet aggregation by L-arginine and polyamines in alloxan treated rats. Biochemistry and molecular biology international. 1997;43(2):311-8.
236. Agam G, Gartner TK, Livne A. Inhibition of platelet aggregation and endogenous lectin activity by oligoamines. Thrombosis research. 1984;33(3):245-57.
237. de la Pena NC, Sosa-Melgarejo JA, Ramos RR, Mendez JD. Inhibition of platelet aggregation by putrescine, spermidine, and spermine in hypercholesterolemic rabbits. Archives of medical research. 2000;31(6):546-50.
238. Pakala R. Inhibition of arterial thrombosis by polyamines in a canine coronary artery injury model. Thrombosis research. 2003;110(1):47-51.
239. Zhang M, Wang H, Tracey KJ. Regulation of macrophage activation and inflammation by spermine: a new chapter in an old story. Critical care medicine. 2000;28(4 Suppl):N60-6.
240. Clarkson AN, Liu H, Pearson L, Kapoor M, Harrison JC, Sammut IA, Jackson DM, Appleton I. Neuroprotective effects of spermine following hypoxic-ischemic-induced brain damage: a mechanistic study. FASEB journal : official publication of the Federation of American Societies for Experimental Biology. 2004;18(10):1114-6.
241. Mackman N. Triggers, targets and treatments for thrombosis. Nature. 2008;451(7181):914-8.
242. Francis CW. Clinical practice. Prophylaxis for thromboembolism in hospitalized medical patients. The New England journal of medicine. 2007;356(14):1438-44.
243. Brenner B, Hoffman R. Emerging options in the treatment of deep vein thrombosis and pulmonary embolism. Blood reviews. 2011;25(5):215-21.
244. De Caterina R, Husted S, Wallentin L, Agnelli G, Bachmann F, Baigent C, Jespersen J, Kristensen SD, Montalescot G, Siegbahn A, Verheugt FW, Weitz J. Anticoagulants in heart disease: current status and perspectives. European heart journal. 2007;28(7):880-913.

245. Hirsh J, Warkentin TE, Raschke R, Granger C, Ohman EM, Dalen JE. Heparin and low-molecular-weight heparin: mechanisms of action, pharmacokinetics, dosing considerations, monitoring, efficacy, and safety. Chest. 1998;114(5 Suppl):489S-510S.
246. Vincentelli A, Jude B, Belisle S. Antithrombotic therapy in cardiac surgery. Canadian journal of anaesthesia = Journal canadien d'anesthesie. 2006;53(6 Suppl):S89-102.
247. Suranyi M, Chow JS. Review: anticoagulation for haemodialysis. Nephrology. 2010;15(4):386-92.
248. Blossom DB, Kallen AJ, Patel PR, Elward A, Robinson L, Gao G, Langer R, Perkins KM, Jaeger JL, Kurkjian KM, Jones M, Schillie SF, Shehab N, Ketterer D, Venkataraman G, Kishimoto TK, Shriver Z, McMahon AW, Austen KF, Kozlowski S, Srinivasan A, Turabelidze G, Gould CV, Arduino MJ, Sasisekharan R. Outbreak of adverse reactions associated with contaminated heparin. The New England journal of medicine. 2008;359(25):2674-84.
249. Nagler M, Haslauer M, Wuillemin WA. Fondaparinux - data on efficacy and safety in special situations. Thrombosis research. 2012;129(4):407-17.
250. Schulman S, Beyth RJ, Kearon C, Levine MN, American College of Chest P. Hemorrhagic complications of anticoagulant and thrombolytic treatment: American College of Chest Physicians Evidence-Based Clinical Practice Guidelines (8th Edition). Chest. 2008;133(6 Suppl):257S-98S.
251. Schiele F, Meneveau N, Seronde MF, Descotes-Genon V, Dutheil J, Chopard R, Ecarnot F, Bassand JP, Reseau de Cardiologie de Franche C. Routine use of fondaparinux in acute coronary syndromes: a 2-year multicenter experience. American heart journal. 2010;159(2):190-8.
252. Melnikova I. The anticoagulants market. Nat Rev Drug Discov. 2009;8(5):353-4.
253. Crowther MA, Warkentin TE. Bleeding risk and the management of bleeding complications in patients undergoing anticoagulant therapy: focus on new anticoagulant agents. Blood. 2008;111(10):4871-9.
254. Pai M, Crowther MA. Neutralization of heparin activity. Handbook of experimental pharmacology. 2012(207):265-77.
255. Nybo M, Madsen JS. Serious anaphylactic reactions due to protamine sulfate: a systematic literature review. Basic & clinical pharmacology & toxicology. 2008;103(2):192-6.
256. Bakchoul T, Zollner H, Amiral J, Panzer S, Selleng S, Kohlmann T, Brandt S, Delcea M, Warkentin TE, Sachs UJ, Greinacher A. Anti-protamine-heparin antibodies: incidence, clinical relevance, and pathogenesis. Blood. 2013;121(15):2821-7.
257. Lee GM, Welsby IJ, Phillips-Bute B, Ortel TL, Arepally GM. High incidence of antibodies to protamine and protamine/heparin complexes in patients undergoing cardiopulmonary bypass. Blood. 2013;121(15):2828-35.
258. Singla A, Sullivan MJ, Lee G, Bartholomew J, Kapadia S, Aster RH, Curtis BR. Protamine-induced immune thrombocytopenia. Transfusion. 2013;53(10):2158-63.
259. Weitz JI, Hirsh J, Samama MM, American College of Chest P. New antithrombotic drugs: American College of Chest Physicians Evidence-Based Clinical Practice Guidelines (8th Edition). Chest. 2008;133(6 Suppl):234S-56S.
260. Fifth Organization to Assess Strategies in Acute Ischemic Syndromes I, Yusuf S, Mehta SR, Chrolavicius S, Afzal R, Pogue J, Granger CB, Budaj A, Peters RJ, Bassand JP, Wallentin L, Joyner C, Fox KA. Comparison of fondaparinux and enoxaparin in acute coronary syndromes. The New England journal of medicine. 2006;354(14):1464-76.
261. Schick BP, Maslow D, Moshinski A, San Antonio JD. Novel concatameric heparin-binding peptides reverse heparin and low-molecular-weight heparin anticoagulant activities in patient plasma in vitro and in rats in vivo. Blood. 2004;103(4):1356-63.
262. Rodrigo AC, Barnard A, Cooper J, Smith DK. Self-assembling ligands for multivalent nanoscale heparin binding. Angewandte Chemie. 2011;50(20):4675-9.

263. Choi S, Clements DJ, Pophristic V, Ivanov I, Vemparala S, Bennett JS, Klein ML, Winkler JD, DeGrado WF. The design and evaluation of heparin-binding foldamers. Angewandte Chemie. 2005;44(41):6685-9.
264. Moreau E, Domurado M, Chapon P, Vert M, Domurad D. Biocompatibility of polycations: in vitro agglutination and lysis of red blood cells and in vivo toxicity. J Drug Target. 2002;10(2):161-73.
265. Howes JL, Smith RS, Helmer SD, Taylor SM. Complications of recombinant activated human coagulation factor VII. American journal of surgery. 2009;198(6):895-9.
266. Jones GR, Hashim R, Power DM. A comparison of the strength of binding of antithrombin III, protamine and poly(L-lysine) to heparin samples of different anticoagulant activities. Biochimica et biophysica acta. 1986;883(1):69-76.
267. Imran ul-haq M, Lai BF, Chapanian R, Kizhakkedathu JN. Influence of architecture of high molecular weight linear and branched polyglycerols on their biocompatibility and biodistribution. Biomaterials. 2012;33(35):9135-47.
268. Kizhakkedathu JN, Creagh AL, Shenoi RA, Rossi NA, Brooks DE, Chan T, Lam J, Dandepally SR, Haynes CA. High molecular weight polyglycerol-based multivalent mannose conjugates. Biomacromolecules. 2010;11(10):2567-75.
269. Olsson TS, Ladbury JE, Pitt WR, Williams MA. Extent of enthalpy-entropy compensation in protein-ligand interactions. Protein Sci. 2011;20(9):1607-18.
270. Agnelli G, George DJ, Kakkar AK, Fisher W, Lassen MR, Mismetti P, Mouret P, Chaudhari U, Lawson F, Turpie AG, Investigators S-O. Semuloparin for thromboprophylaxis in patients receiving chemotherapy for cancer. The New England journal of medicine. 2012;366(7):601-9.
271. Hemker HC, Giesen P, Al Dieri R, Regnault V, de Smedt E, Wagenvoord R, Lecompte T, Beguin S. Calibrated automated thrombin generation measurement in clotting plasma. Pathophysiology of haemostasis and thrombosis. 2003;33(1):4-15.
272. Bolliger D, Seeberger MD, Tanaka KA. Principles and practice of thromboelastography in clinical coagulation management and transfusion practice. Transfusion medicine reviews. 2012;26(1):1-13.
273. Malik N, Wiwattanapatapee R, Klopsch R, Lorenz K, Frey H, Weener JW, Meijer EW, Paulus W, Duncan R. Dendrimers: relationship between structure and biocompatibility in vitro, and preliminary studies on the biodistribution of 125I-labelled polyamidoamine dendrimers in vivo. Journal of controlled release : official journal of the Controlled Release Society. 2000;65(1-2):133-48.
274. de Kort M, Buijsman RC, van Boeckel CA. Synthetic heparin derivatives as new anticoagulant drugs. Drug Discov Today. 2005;10(11):769-79.
275. Kizilay E, Kayitmazer AB, Dubin PL. Complexation and coacervation of polyelectrolytes with oppositely charged colloids. Adv Colloid Interface Sci. 2011;167(1-2):24-37.
276. van der Gucht J, Spruijt E, Lemmers M, Cohen Stuart MA. Polyelectrolyte complexes: bulk phases and colloidal systems. Journal of colloid and interface science. 2011;361(2):407-22.
277. Reagan-Shaw S, Nihal M, Ahmad N. Dose translation from animal to human studies revisited. FASEB journal : official publication of the Federation of American Societies for Experimental Biology. 2008;22(3):659-61.
278. Lee J, Sohn JW, Zhang Y, Leong KW, Pisetsky D, Sullenger BA. Nucleic acid-binding polymers as anti-inflammatory agents. Proc Natl Acad Sci U S A. 2011;108(34):14055-60.
279. Deng C, Tian H, Zhang P, Sun J, Chen X, Jing X. Synthesis and characterization of RGD peptide grafted poly(ethylene glycol)-b-poly(L-lactide)-b-poly(L-glutamic acid) triblock copolymer. Biomacromolecules. 2006;7(2):590-6.
280. Jain K, Kesharwani P, Gupta U, Jain NK. Dendrimer toxicity: Let's meet the challenge. International journal of pharmaceutics. 2010;394(1-2):122-42. Epub 2010/05/04.
281. Jones CF, Campbell RA, Brooks AE, Assemi S, Tadjiki S, Thiagarajan G, Mulcock C, Weyrich AS, Brooks BD, Ghandehari H, Grainger DW. Cationic PAMAM dendrimers aggressively initiate blood clot formation. ACS nano. 2012;6(11):9900-10. Epub 2012/10/16.

282. Shenoi RA, Kalathottukaren MT, Travers RJ, Lai BF, Creagh AL, Lange D, Yu K, Weinhart M, Chew BH, Du C, Brooks DE, Carter CJ, Morrissey JH, Haynes CA, Kizhakkedathu JN. Affinity-based design of a synthetic universal reversal agent for heparin anticoagulants. Science translational medicine. 2014;6(260):260ra150.
283. Jasuja R, Passam FH, Kennedy DR, Kim SH, van Hessem L, Lin L, Bowley SR, Joshi SS, Dilks JR, Furie B, Furie BC, Flaumenhaft R. Protein disulfide isomerase inhibitors constitute a new class of antithrombotic agents. The Journal of clinical investigation. 2012;122(6):2104-13. Epub 2012/05/09.
284. Sweet DM, Kolhatkar RB, Ray A, Swaan P, Ghandehari H. Transepithelial transport of PEGylated anionic poly(amidoamine) dendrimers: implications for oral drug delivery. Journal of controlled release : official journal of the Controlled Release Society. 2009;138(1):78-85.
285. Wang X, Xu L. An optimized murine model of ferric chloride-induced arterial thrombosis for thrombosis research. Thrombosis research. 2005;115(1-2):95-100. Epub 2004/11/30.
286. Furie B, Furie BC. In vivo thrombus formation. Journal of thrombosis and haemostasis : JTH. 2007;5 Suppl 1:12-7. Epub 2007/08/01.
287. Keirstead ND, Wagoner MP, Bentley P, Blais M, Brown C, Cheatham L, Ciaccio P, Dragan Y, Ferguson D, Fikes J, Galvin M, Gupta A, Hale M, Johnson N, Luo W, McGrath F, Pietras M, Price S, Sathe AG, Sasaki JC, Snow D, Walsky RL, Kern G. Early prediction of polymyxin-induced nephrotoxicity with next-generation urinary kidney injury biomarkers. Toxicological sciences : an official journal of the Society of Toxicology. 2014;137(2):278-91.
288. Nielsen VG. Protamine enhances fibrinolysis by decreasing clot strength: role of tissue factor-initiated thrombin generation. The Annals of thoracic surgery. 2006;81(5):1720-7. Epub 2006/04/25.
289. Von Kaulla KN. Intravenous protein-free pyrogen; a powerful fibrinolytic agent in man. Circulation. 1958;17(2):187-98. Epub 1958/02/01.
290. Stewart GJ, Niewiarowski S. Nonenzymatic polymerization of fibrinogen by protamine sulfate. An electron microscope study. Biochimica et biophysica acta. 1969;194(2):462-9. Epub 1969/12/23.
291. Jennewein C, Paulus P, Zacharowski K. Linking inflammation and coagulation: novel drug targets to treat organ ischemia. Current opinion in anaesthesiology. 2011;24(4):375-80.
292. Gurbuz HA, Durukan AB, Sevim H, Ergin E, Gurpinar A, Yorgancioglu C. Heparin toxicity in cell culture: a critical link in translation of basic science to clinical practice. Blood coagulation & fibrinolysis : an international journal in haemostasis and thrombosis. 2013;24(7):742-5. Epub 2013/09/26.
293. Fuchs TA, Brill A, Duerschmied D, Schatzberg D, Monestier M, Myers DD, Wrobleski SK, Wakefield TW, Hartwig JH, Wagner DD. Extracellular DNA traps promote thrombosis. Proceedings of the National Academy of Sciences of the United States of America. 2010;107(36):15880-5.
294. Yun TH, Morrissey JH. Polyphosphate and omptins: novel bacterial procoagulant agents. Journal of Cellular and Molecular Medicine. 2009;13(10):4146-53.
295. Effeney DJ, Blaisdell FW, McIntyre KE, Graziano CJ. The relationship between sepsis and disseminated intravascular coagulation. The Journal of trauma. 1978;18(10):689-95.
296. Bone RC. Gram-positive organisms and sepsis. Archives of internal medicine. 1994;154(1):26-34.
297. Kotsaki A, Giamarellos-Bourboulis EJ. Emerging drugs for the treatment of sepsis. Expert opinion on emerging drugs. 2012;17(3):379-91.
298. Berkower I. The promise and pitfalls of monoclonal antibody therapeutics. Curr Opin Biotechnol. 1996;7(6):622-8.
299. Kellermann SA, Green LL. Antibody discovery: the use of transgenic mice to generate human monoclonal antibodies for therapeutics. Curr Opin Biotechnol. 2002;13(6):593-7.
300. Reichert JM, Valge-Archer VE. Development trends for monoclonal antibody cancer therapeutics. Nat Rev Drug Discov. 2007;6(5):349-56.

301. Merino R, Iwamoto M, Fossati L, Izui S. Polyclonal B cell activation arises from different mechanisms in lupus-prone (NZB x NZW)F1 and MRL/MpJ-lpr/lpr mice. Journal of immunology. 1993;151(11):6509-16.
302. Hubbard WJ, Choudhry M, Schwacha MG, Kerby JD, Rue LW, 3rd, Bland KI, Chaudry IH. Cecal ligation and puncture. Shock. 2005;24 Suppl 1:52-7.